Hydrogen Production from Supercritical Water Gasification of Lignin, Cellulose, and Other Biomass Residues

A Thesis Submitted to the College of Graduate Studies & Research

in Partial Fulfillment of the Requirements

for the Degree of

Doctor of Philosophy

in the Division of Environmental Engineering,

University of Saskatchewan

Saskatoon, SK, Canada

By
KANG KANG

Permission to Use

I grant that the libraries of the University of Saskatchewan may make this thesis available for inspection for free. I also grant that permission for using this thesis in any form for scholarly purposes may be granted by Dr. Ajay Dalai and Dr. Hui Wang, who are the supervisors during my PhD study. In the case of their absence, the use of this thesis could be granted by Head of the Division of Environmental Engineering or the Dean of the College of Engineering.

Any other use of the thesis for financial gain without the University of Saskatchewan and author's permission is prohibited. Also, due recognition shall be given to me and the University of Saskatchewan for any use.

The requests for permission to copy, or use any content in this thesis should be sent to:

Head, Division of Environmental Engineering
57 Campus Drive
Saskatoon, Saskatchewan
Canada S7N 5A9

Abstract

Hydrogen production from biomass is an attractive alternative for clean energy generation. This thesis presents the results from four research phases which were carried out to maximize the hydrogen yield from various biomass via supercritical water gasification (SCWG).

In the first step, non-catalytic SCWG of lignin was optimized to achieve high hydrogen yield using Central Composite Design (CCD) method. The parameters that were optimized include temperature (400−650 °C), water to biomass mass ratio (3-8), and pressure (23−29 MPa). To achieve higher hydrogen production, higher temperature was desirable. The change of pressure does not show a significant effect on hydrogen yield. According to the response surface model, the highest hydrogen yield was predicted as 1.60 mmol/g. The optimum reaction conditions for highest hydrogen yield were predicted as temperature = 651 °C, water to biomass ratio = 3.9, and pressure = 25 MPa.

In the second phase, Ni based catalysts were screened and modified for hydrogen production from lignin SCWG. The activity of Ni based catalysts using different supports follows the order of MgO < activated carbon (AC) < ZrO_2 < TiO_2 < Al_2O_3. The activity of the Ni based catalysts with different metal promoters follows the order of Cu < Co < Ce. The 20Ni-0.36Ce/Al_2O_3 catalyst showed highest hydrogen yield of 2.15 mmol/g at 650 ºC, 26 MPa, and water to biomass ratio of 5.

In the third phase, two types of novel catalysts were prepared and tested, including Ni-Co/Mg-Al bimetallic catalysts and TiO_2 supported Ni catalysts. For Ni-Co/Mg-Al bimetallic catalyst system, the hydrogen yield was well correlated to the quantity of strong acidic sites measured by NH_3-TPD within the temperature range of 400-600 °C. Catalysts prepared by precipitation showed higher hydrogen yield than those prepared by impregnation. For Ni/TiO_2 catalysts, 5 wt% Ni loading in the range of 0–20 wt% was the best for hydrogen production. However, improvement of hydrogen yield was not observed when Co, Ru, Ce or Mg was added to the 5Ni/TiO_2 catalyst as promoters. A detailed mechanism for catalytic SCWG of lignin was proposed to address the role of different components of the catalyst in this process. The best catalysts found in this phase are

Cop.2.6Ni-5.2Co/2.6Mg and 5Ni/TiO_2, which showed hydrogen yield of 2.36 and 1.82 mmol/g, respectively.

The last phase focuses on real biomass. K_2CO_3 and 20Ni-0.36Ce/Al_2O_3 catalyst were identified as the promising homogeneous and heterogeneous catalysts. The results from Taguchi optimization study indicate that the order of relative importance of the parameters was: biomass type < catalyst type < catalyst loading < temperature. Using different real biomass as hydrogen precursor, the order of hydrogen yield from various biomass was timothy grass < wheat straw < canola meal. The highest hydrogen yield of 3.31mmol/g was observed at 650 ºC, 26MPa, using K_2CO_3 as the catalyst at a loading of 100% and using canola meal as feedstock.

During this study, the best composition of heterogeneous catalysts and better preparation methods were determined targeting higher hydrogen yield for the SCWG of biomass. The relative importance of different operating parameters was assessed using statistical methods. Also, the detailed mechanism of catalytic lignin SCWG was proposed to facilitate further understanding of the role of different catalyst building blocks in the process. The results presented in this work can lead to better understanding of the non-catalytic/catalytic SCWG processes, and provide a valuable reference for future study in the similar area.

Acknowledgements

I want to express my great appreciation to every person who kindly helped me during my Ph.D. research. Firstly, I deeply appreciate my supervisors, Dr. Ajay Dalai, and Dr. Hui Wang. They provided patient guidance and support throughout my Ph.D. work. Especially, I am thankful to them for offering me this precious opportunity to get oversea education and experience, and also for providing valuable guidance for my decisions so I could focus on my work.

My deep appreciation and thanks to my Ph.D. advisory committee, Dr. Bob Tyler, Dr. Catherine Niu, Dr. Venkatesh Meda, and Dr. Ramaswami Sammynaiken. They showed great patience and kindness in supporting my academic work. I would like to thank post-doctoral follow Dr. Ramin Azargohar for his guidance. Dr Ramin helped me with every phase of my research work with his accuracy and profession in chemical engineering research.

Also, I sincerely appreciate all the technical support and suggestions from Ms. Heli Eunike, Mr. Rlee, and Mr. Richard B. Prokopishyn. I would also like to express my appreciation to the colleagues in catalysis and chemical reaction engineering laboratories at the University of Saskatchewan. Special thanks to Mr. Asish Somidi, Dr. Sandeep Badoga, Mr. Vahid Vosoughi, Ms. Prachee Misra for their friendship and sharing of knowledge.

My sincere gratitude to the financial supporters of my research including China Scholarship Council, BioFuelNet Canada, Natural Science and Engineering Research Council of Canada, and the University of Saskatchewan.

Dedication

Dedicated to:

My dear parents and sister, Chonglin Gao, Zuowen Kang, and Fang Kang, who have been loving and encouraging me. I could not have gone this far on my academic journey without their support.

My wonderful wife, Fengmei Zhang, who has gone through all the happy and sad moments together with me.

My lovely daughter, Jiayi Kang, who came to my family like an angel and magically boosted my research progress.

Table of Contents

List of Tables

List of Figures

Nomenclature

Abbreviations

AC: Activated carbon

BET: Brunauer-Emmett-Teller method

CCD: Central composite design

CM: Canola meal

Cop: Coprecipitation

FID: Flame ionization detector

FTIR: Fourier transform infrared spectroscopy

HHV: Higher heating value

Imp: Impregnation

RSM: Response surface methodology

R-squared: Coefficient of determination

SCW: Supercritical water

SCWG: Supercritical water gasification

STDV: Standard deviation

TCD: Thermal conductivity detector

TG: Timothy grass

TG/DTG: Thermogravimetry/derivative thermogravimetry

TPD: Temperature-programmed desorption

TPR: Temperature-programmed reduction

WS: Wheat straw

XRD: X-ray diffraction

Symbols

C_i: Concentration of the gas species i (mol%)

L_{metal}: Specific metal loading of a catalyst (wt%)

$L_{reactor}$: Length of reactor (cm)

MB_{total}: Total mass balance (%)

m_{cat}: Mass of catalyst to be prepared (g)

M_i: Molecular weight of species i in gas phase product (g/mol)

m_i: Mass of species i in gas phase product (g)

M_{metal}: Atomic weight of metal used in catalysts (g/mol)

$MM_{precursor}$: Molecular weight of metal precursors used in catalysts (g/mol)

$mM_{precursor}$: Mass of metal precursors used in catalysts (g)

mp_i: Mass of product phase i (g)

$MP_{precursor}$: Molecular weight of promoter precursors used in catalysts (g/mol)

$mP_{precursor}$: Mass of promoter precursors used in catalysts (g)

$M_{promoter}$: Atomic weight of promoters used in catalysts (g/mol)

MP_{purity}: Purity of metal precursors been used (wt%)

m_{Total}: Total mass of reactant (g)

n_i: Mole number of species i in gas phase product (mol)

n_{N_2}: Mole number of N_2 in gas phase (mol)

P_{N_2}: Initial pressure of N_2 (atm)

PP_{purity}: Purity of promoter precursor used in catalysts (wt%)

R_A: The gas constant (0.082 L·atm/(mol·K))

$R_{P/M}$: Atom ratio of promoter to metal in catalysts (mol/mol)

$R_{W/B}$: Ratio of water to biomass (g/g)

V_{sealed}: Sealed reaction volume (cm^3)

Y_i: Yield of product phase i (wt%)

Y_{Gas}: Yield of gas (wt%)

Yg_i: Yield of species i in gas phase product (mmol/g)

Y_{total}: Total yield of the SCWG (wt%)

η_{H_2}: Hydrogen selectivity (%)

Chapter 1 Introduction

1.1 Background of research project

The human race is now facing two emerging problems: first, the predictable depletion of fossil fuels and the increasingly severe energy crisis, second, global environmental challenges caused by increased utilization of fossil fuels. Thus, the field of renewables becomes increasingly attractive for research. According to Guo et al. (2010), for decades, many kinds of renewable energies were explored such as solar power, wind energy, hydropower, geothermal energy. However, renewable resources still make a limited contribution to the world's energy need. Thus, it is evident that more efforts should be made to increase the usage of renewables.

There are several reasons to consider biomass as potential source of renewable energy: i) Easy availability throughout the world (Castello and Fiori 2011); ii) Large capacity as energy provider and stability of energy storage: via photosynthesis, solar energy is converted into the chemical buildup of the biomass, and thus energy is stabilized; iii) Use of biomass reduces carbon emission by maintaining the CO_2 concentration in the atmosphere at the same level, because CO_2 is consumed and converted to energy which is accumulated in biomass. Lignin is of particular importance and interest as a biomass model compound. Lignin is the most abundant polymeric material available in nature (Ragauskas, Beckham, Biddy, Chandra, et al. 2014). However, lignin conversion is yet a severe challenge because of its highly cross-linked aromatic structure.

Hydrogen (H_2) is considered as a clean, renewable energy carrier as the only product it releases during its consumption is H_2O. Future areas for application of hydrogen might include portable charging devices for electronics, fuel cell, and pilot scale power plant (Dahmen, Dinjus, and Kruse 2009). Gasification refers to the conversion of the feedstock into gaseous products using thermochemical method (Basu 2010). To conquer the drawbacks of traditional biomass gasification technologies Supercritical Water Gasification (SCWG) was developed and progress has been made in the last two decades. However, temporarily, SCWG is still not a commercial biomass conversion technology as there are several technical aspects still developing. Catalysis is considered the fundamental solution to the SCWG technology, especially when considering the use of lignin as the feedstock (Zakzeski et al. 2010). In SCWG, the high temperature and the pressure demand for achieveing supercritical condition of water significantly increases the cost of the process. Therefore, it is crucial to develop catalysts that could be used to enable the reactions

at a lower temperature (Azadi, Afif, et al. 2012, Elliott 2008). The other challenge is the relatively low gasification efficiency due to the conplex structure of biomass. Therefore, to enhance H_2 yield and selectivity, development of active catalyst with high hydrogen selectivity is crucial (Lu, Li, and Guo 2014).

1.2 Project overview and research strategy

The core objective of this Ph.D. project is to maximize the hydrogen yield in the process of SCWG of lignin and other lignocellulosic biomass as hydrogen precursors. To achieve the goal in step by step manner, this project has been divided into four phases with the main objective of each phase described in Figure 1.1.

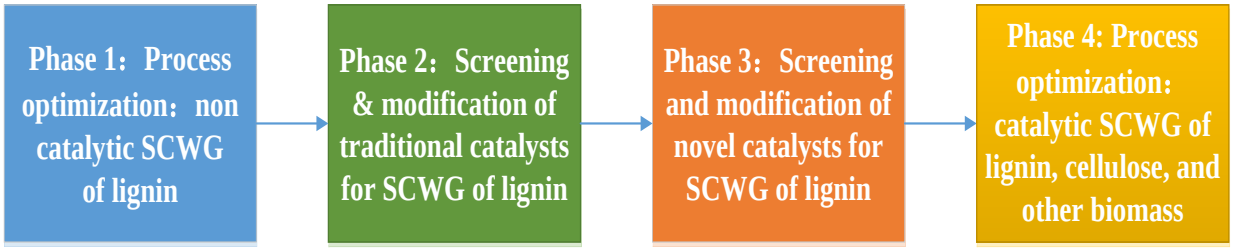

Figure 1.1 Research phases and primary objectives

This PhD project is divided into four research phases. Phase one begins with the optimization of the non-catalytic SCWG process using lignin as feedstock. In phase two, the focus is on the evaluation and screening of traditional Ni based catalysts. In the third phase of this research, an exploration into novel catalysts was carried out. In phase four, the overall optimization study of the catalytic process, including performance comparison of best catalysts and hydrogen production, from various real biomass residues was conducted.

The research strategy applied through this project is summarized in Figure 1.2. Based on the literature review, decisions on the initial investigation for this study were made. This included the selection of recepies for catalyst preparation, critical parameters as well as a potential biomass feedstock. The catalysts that showed promising hydrogen yield in previous studies from other biomass precursors (e.g., glucose, cellulose, etc.) via SCWG process were chosen. Also, catalysts that were successfully applied in other relevant reactions (e.g., steam reforming) and showed promising properties required for SCWG process such as high coke resistance, sintering resistance, etc. were considered. The parameters and their corresponding range for optimization study were mainly chosen based on the fundamental knowledge of the process. For the non-catalytic SCWG

of lignin, the optimization study primarily covers pressure, temperature, and the mass ratio of water to biomass. For catalytic SCWG of biomass, the effect of parameters such as biomass type, catalyst type, temperature, and catalyst loading have been studied. The biomass used for this project could be divided into two categories namely model biomass and real biomass. Model biomass is mainly lignin, which is considered an excellent material for evaluating the process effectiveness and catalyst performance, as is with its structural complexity and stability under thermochemical conditions. Cellulose, which is another important biomass mother compound, was also used in this study. The real biomass was also used as feedstock to test the capability of this process and catalysts to handle biomass in its un-separated, raw state.

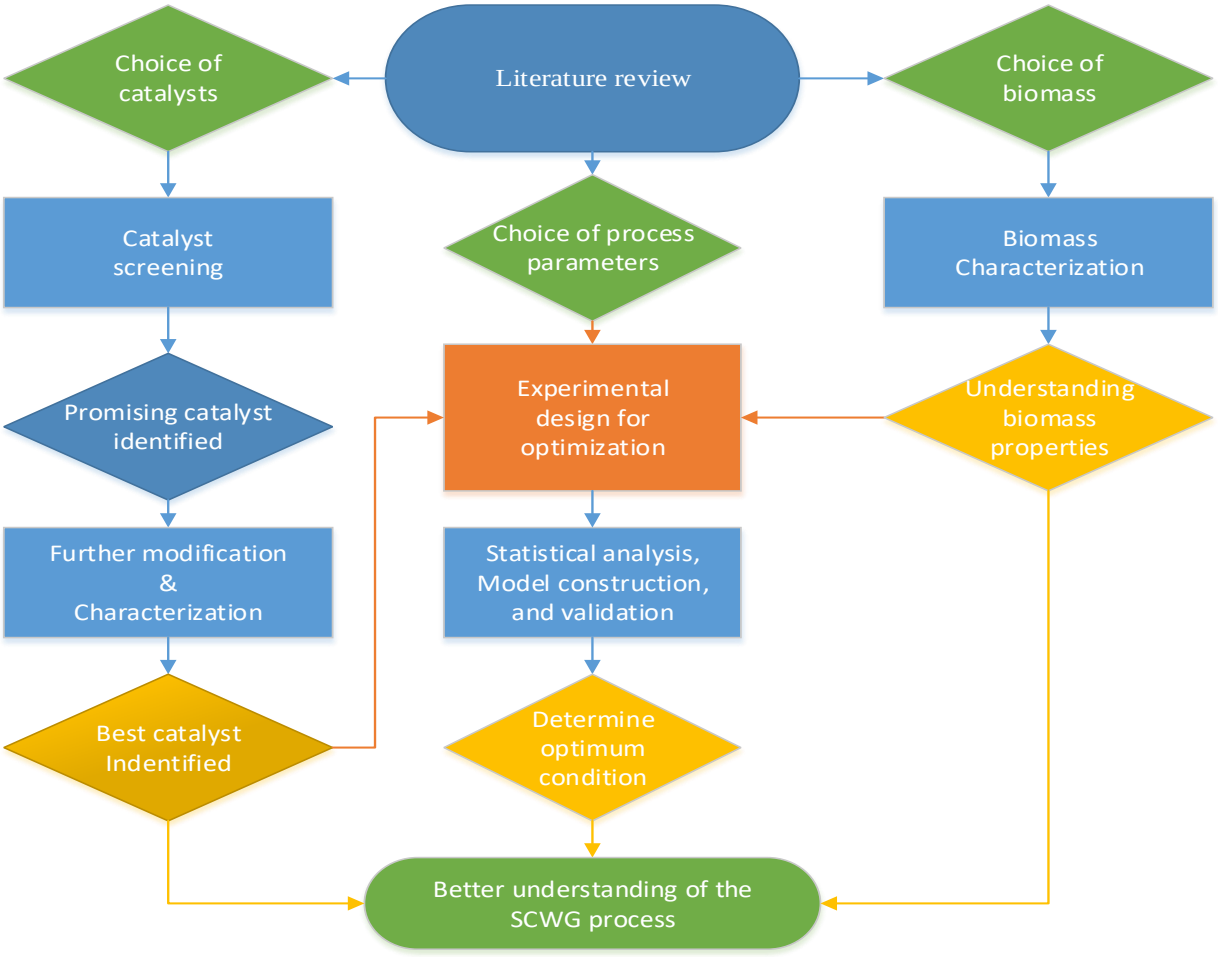

Figure 1.2 Research strategy applied for this project

The research on catalysis started with catalyst screening by testing catalyst under identical reaction conditions. Their performances are evaluated by hydrogen yield, gas yield, and hydrogen selectivity. Then the promising catalyst identified by screening may be further modified, evaluated

for the best performance possible, and characterization techniques were used to facilitate the understanding of the properties of the catalysts. As a result, the best catalyst was employed as an input to the experimental design for process optimization study. Though the research focus is to identify promising heterogeneous catalysts for the SCWG process, in the last phase of research the performance of best heterogeneous catalyst was compared with several homogeneous competitors. Also, although in the third phase the 2.6Ni-5.2Co/2.6Mg-Al catalyst prepared by coprecipitation showed slightly higher hydrogen yield than that of the 20Ni-0.36Ce/Al_2O_3 catalyst from SCWG of lignin (2.36 vs. 2.15 mmol/g), the later catalyst was considered and modified in research phase four as the preparation of the coprecipitated catalyst is a complicated process and the accurate control of catalyst composition is difficult.

For the optimization study, the procedure starts with experimental design. In this project, these optimization experiments were designed following either central composite design (CCD) or Taguchi design methodology, to reduce the workload and maintain the statistical accuracy of conception. Based on the results of statistical analysis, a model was constructed, and the prediction of optimum conditions for hydrogen production was also carried out. The optimization study ended with experimental validation of the optimum condition.

For the better understanding of the properties of different biomass and their role in the SCWG process, characterization of biomass was also performed. Based on all above, this work directs towards identifying promising catalysts, understanding the effects of operation parameters and the properties of feedstock. The results presented in this work should be valuable for future study on the SCWG technology.

1.3 Thesis style and organization

This manuscript-based thesis starts with an overview of the research background and research strategy in this chapter. Then, in Chapter 2, a more detailed literature review will be provided. Followed by that, details about the knowledge gaps, hypothesis, and objectives of each research phase, as well as the results and discussion of this project will be presented in a manuscript based format. Each chapter is written based on a published journal paper or a to-be-published journal paper, which is under review.

Specifically, Chapter 3 is written based on: Kang, K., Azargohar R., Dalai, A.K., and Wang, H. Noncatalytic Gasification of Lignin in Supercritical Water Using a Batch Reactor for Hydrogen Production: An Experimental and Modeling Study. *Energy & Fuels*. 29 (2015) 1776-84.

Chapter 4 is written based on: Kang, K., Azargohar R., Dalai, A.K., and Wang, H. Systematic screening and modification of Ni based catalysts for hydrogen generation from supercritical water gasification of lignin. *Chemical Engineering Journal*. 283 (2016) 1019-32.

Chapter 5 is written based on a manuscript which is still under review.

Chapter 6 is written based on: Kang, K., Azargohar R., Dalai, A.K., and Wang, H. Hydrogen production from lignin, cellulose and waste biomass via supercritical water gasification: Catalyst activity and process optimization study. *Energy Conversion and Management*. 117 (2016) 528-37.

The original manuscripts may have been modified for inclusion in the thesis, the introduction sections were simplified, and the discussion part was extended when necessary. The thesis ends up with a summarization chapter (Chapter 7) where conclusions and recommendations for future research were provided.

1.4 Statement of contributions

The author of this thesis is the first author of all the manuscripts used in this thesis. His contribution to these manuscripts are: (1) preparing the samples and the catalysts, (2) carrying out experimental design, (3) performing SCWG tests in the laboratory, (4) performing characterizations for gasification products and catalysts, (5) analysing the experimental results, and (6) writing the manuscript and provide responses to reviewers' comments. The postdoctoral fellow, Dr. Ramin Azargohar, provided support by reviewing the calculations for the preparation of catalysts and characterization of gasification products, experimental procedures, and reviewing the manuscripts. The supervisors, Dr. Ajay K. Dalai and Dr. Hui Wang, performed overall supervision of this research, examined the research results, oversaw the preparation of the manuscripts, and submitted the papers.

Chapter 2 Literature Review

2.1 Biomass availability and properties

2.1.1 General definitions and information

As a broad definition, biomass covers any living matter on earth and therefore abundant. Narrow down to available resources, biomass includes a wide range of materials such as different types of wood, crops, their by-products, and different types of wastes derived from these materials (Goyal, Seal, and Saxena 2008). Biomass contributes approximately 45 EJ of energy every year and for the time being, it is the dominant renewable energy source for human beings. Biomass contributes to approximately 20-30% of the total energy required by developing countries, whereas the share is decreased to around biomass 10% in developed countries (Bioenergy 2007).

For the particular interest of this study, lignocellulosic biomass refers to biomaterial which is mainly composed of three cell-wall mother compounds including cellulose, lignin, and hemicellulose (Azadi et al. 2013). In plant body, the content of the three biomass precursor varies from species to species, percentage wise, cellulose can contribute up to 44 wt% of the plant body, followed by lignin (up to 35 wt%), and hemicellulose (up to 35 wt%) (Basu 2010). Regarding chemical structure, cellulose microfibrils are assembled by β-1,4-linked glucan units (Thomas et al. 2013). Lignin structure is constructed by the polymerization of its basic unit, which is phenyl propylene (Ragauskas, Beckham, Biddy, Chandra, et al. 2014). Hemicellulose often refers to the non-cellulosic polysaccharides presents in the plant cell wall and has no particular structure (Pauly et al. 2013).

Lignin and cellulose are two crucial biomass precursors. In plant body, cellulose provides mechanical strength to the plant (Siró and Plackett 2010). Lignin holds together the lignocellulose matrix by filling the space which is not filled with other components (Zakzeski et al. 2010). As the starting material of this study, lignin is used as a model biomass compound to explore the SCWG process as well as to evaluate the catalyst performance. Therefore, more information about lignin will be reviewed here.

2.1.2 Structure of lignin

Lignin has a three-dimensional amorphous polymeric structure, which mainly contains highly cross-linked phenyl propane groups. Though the decoding of proto lignin structure is like solving

a tough jigsaw puzzle, immense efforts have facilitated progress in understanding its degradation products. Now, it is well established that there are three building blocks of lignin, namely conifers, sinapoyl, and p-country alcohol (Chakar and Ragauskas 2004). Structures, as well as a relative abundance of typical linkages between phenylpropane units existing in softwood lignin, is well summarized in a review work (Chakar and Ragauskas 2004). According to this review, the dominant linkage in softwood lignin is the β-O-4 linkage, consisting more than 50% of the linkages in lignin structure. Softwood lignin has lower methoxyl content due to the presence of only guaiacol unit, whereas hardwood lignin has higher methoxyl content as it contains both syringe and guaiacol units (Liu et al. 2008).

For lignin used in industry, structural alternation is inevitable after separation. Many aspects of the structural change of lignin during the pulping process was systematically discussed by a series of papers published together by Gellerstedt et al. back in the 1990s (Gellerstedt and Lindfors 1984a, Gellerstedt et al. 1984, Robert et al. 1984, Gellerstedt and Lindfors 1984b, Gellerstedt and Gustafsson 1987). In a later study (Lawoko, Henriksson, and Gellerstedt 2005), where lignin-carbohydrate complexes were prepared from spruce wood and its Kraft pulps and characterized after fraction into the carbohydrates. It was found that two different forms of lignin are co-existing in the forest. One type is linked to glucomannan and the other linked to xylan, and they showed various activities during pulping. Specifically, the xylan-linked type experienced large-scale degradation, whereas the glucomannan-linked type was more stable: it was partially condensation to form high molecular mass products.

By the results from comprehensive physics-chemical characterization, it was understood that Kraft pine lignin has more activated free ring positions, higher molecular weight as well as higher thermal stability than ethanol –water wild tamarind lignin and soda –anthraquinone flax lignin (Tejado et al. 2007). Based on the literature, Bjorkman Lignin, also known as milled wood lignin has the most similar structure with the lignin in the natural biomass, therefore, is suitable for analytical research (Azadi et al. 2013).

2.1.3 Source of lignin

In nature, lignin, cellulose, and hemicellulose are three mother precursors of lignocellulosic biomass (Zakzeski et al. 2010). An earlier estimation is that about 300 billion metric tons of lignin could be produced from the plants on earth, and lignin is regenerating with the rate of 20 billion

tonnes per year via plant biosynthesis (Singh et al. 2005). Softwood contains a higher amount of lignin (25 to 35 wt%) than that of hardwood (18-25 wt%). (Pandey and Kim 2011).

For industrial utilization, lignin should be pre-isolated from feedstock and undergo corresponding pre-treatments. High quality and purity of the lignin are desirable for future bio-refinery. Isolation of lignin from the lignocellulosic biomass could be achieved by various processes involving different chemical and mechanical processing. As was summarized in a recent review, biomass pre-treatment technologies for the lignocellulosic feedstock could be divided into four categories: 1) Physical pre-treatment, which focuses on the reduction of particle size by application of mechanical force. 2) Solvent fractionation, which breaks the hydrogen bonding between microfibrils and separates different components of the cell wall (Heinze and Koschella 2005). 3) Chemical pre-treatment, which uses acidic, alkaline and oxidative agents to achieve separation of different biomass components. 4) Biological treatment, which involves using of fungi (Leonardo da Costa Sousa et al. 2009), and has the advantage of low energy consumption (Lee et al. 2008).

2.1.4 Extraction of lignin

Based on the mechanism, lignin separation methods could be divided into two categories. For one category, lignin is initially fractionated into soluble fragments and then recovered by separating the solid residue from the spent liquor (Azadi et al. 2013). For another category, the process involves selective extracting of polysaccharides (cellulose, hemicellulose) of the plant body and leave most of the lignin in the solid phase residue (Ragauskas, Beckham, Biddy, Chandra, et al. 2014, Pandey and Kim 2011).

For industrial separation of lignin, currently, the Kraft pulping process plays a predominating role so is considered the most accessible source of lignin (Chakar and Ragauskas 2004). Kraft pulping process has been adopted from 1879, only limited modifications have been made for modification since then, a good description of the process could be found in a recent work here (Gierer 1980). Briefly, the pulping process starts with heating of wood pellets in the aqueous solution of sodium hydroxide and sodium sulfide. For the heating, the temperature increases from about 70 °C to 170 °C. Afterward, a 1-2 h cooking process was applied and lignin degradation occurs. Later, after removal of the extractives the liquid phase, lignin was obtained. However, it should be mentioned that in this process hemicellulose is also partially degraded and dissolved, thus, might become impurity of the final product.

2.1.5 Physical and chemical properties of lignin

As mentioned before, isolated lignin by different sources has different properties. Lignin isolation procedures always leave some carbohydrate linkages such as cellulose and hemicellulose to commercial lignin which is 2–8 wt%. These linkages play a major role in determining the chemical properties of the material (Singh et al. 2005).

Under room temperature, the commercially available Kraft lignin has dark brown color, natural wood fragrance and is in the powder form. In a recent study by Mansouri et al. (Mansouri and Salvadó 2006), results of structural characterizations of various industrial lignin including Kraft lignin, organosol lignin, soda-anthraquinone lignin, and ethanol process lignin are presented. The results cover a broad range of molecular weight distribution, functional groups analysis, and elemental analysis, etc.

Thermal stability also varies amongst different lignin samples, it was reported that during thermal degradation reactions bond fissions within lignin molecule occurs when the temperature changes between 100 °C and 900 °C (Jakab, Faix, and Till 1997), however, the major degradation finishes within a narrower temperature range of 200-700 °C (Sahoo et al. 2011). Regarding solubility, lignin is insoluble in water under ambient conditions. However, ionic liquids as a green solvent are gaining more attention for lignin separation. Specifically, it was found that ionic liquids such as CF_3SO_3, $MeSO_4$ and $MeSO_4$ could be green and efficient solutions for lignin produced from Kraft process (Pu, Jiang, and Ragauskas 2007). Also, it was reported that ionic liquid CH_3COO could selectively decrease lignin content by 40% from maple wood powder and lignin with high hydrophobicity could be precipitated from concentrated lignin solution in CH_3COO by using an excess amount of water (Lee et al. 2009).

2.2 Technologies for hydrogen production from biomass

Currently, there are mainly two routes to produce H_2 from biomass, namely, biochemical and thermochemical conversion. The thermochemical conversion provides many advantages over biochemical conversions, such as high H_2 production rate, high energy efficiency, ability to handle municipal wastes (Peterson et al. 2008). Thus, the thermochemical route seems to be more feasible and receives much attention for H_2 production in recent years.

As summarized by Levin et al.(2010) in their recent review, there are three main methods for hydrogen production from biomass via thermochemical conversion namely i) conventional

gasification ii) pyrolysis, and iii) supercritical water gasification (SCWG). Conventional gasification converts biomass into a combustible product gas with a high reaction temperature of about 800 to 900 °C (Kalinci, Hepbasli, and Dincer 2009). There are some drawbacks such as difficulty in wet biomass handling and low energy efficiency of the process (Kumar, Jones, and Hanna 2009). Supercritical gasification (SCWG) of biomass was developed to tackle some of the issues of conventional gasification; it involves gasification of biomass in water under the supercritical conditions. In the following section, the present scenario and prospects of SCWG are reviewed and discussed in detail as it is the process been used for this project.

2.3 Supercritical water gasification

2.3.1 Supercritical water and its properties

The supercritical point of water is at a temperature of 374.29 °C, and at a pressure of 22.1 MPa. When temperature and pressure go beyond this point, the water becomes supercritical. According to Guo et al. (2010), under the supercritical conditions, water has significantly different properties from either its gas or liquid phase.

By adjusting the pressure and the temperature near its critical point, the properties of SCW could be tuned to facilitate the gasification reactions (Basu 2010). Some unique properties of the SCW which is interesting for biomass gasification are listed below:

i) The solvent property: Under the supercritical condition, the dielectric constant of water declines significantly and the dissolving capacity changes. Therefore, SCW can behave as a nonpolar solvent and an ideal medium for homogeneous reactions involving organic molecules (Basu 2010).

ii) The surface tension, viscosity, and density: These properties of SCW are all lower than that of water in its liquid phase. Surface tension of water also decreases dramatically (Basu 2010). These features enable more efficient and faster reactions by enhancing the mass transfer efficiency.

iii) The ion production ability: The quantity of ion produced from the water near its critical point could be one hundred times higher than that of ordinary water (Kritzer 2004).

2.3.2 Role of supercritical water in supercritical water gasification

As mentioned above, apart from an excellent reaction media, SCW could play following roles in an SCWG reaction:

i) SCW as a reactant: SCW is a primary source of H_2 and free radicals (Park and Tomiyasu 2003). Moreover, according to Guo et al. (2010), hydrolysis in SCW environment helps the removal of sulfur in comparison with hydrolysis in ordinary water.

ii) SCW as a catalyst: SCW can produce a high concentration of H^+ and OH^-. Therefore, SCW can be a popular media for acid-base facilitated catalytic reactions. According to Boero et al. (2004), significant acceleration of Beckmann and Pinacol rearrangements can be achieved using SCW and even without the presence of any acid catalyst.

2.3.3 Advantages of supercritical water gasification process

Compared to the conventional gasification, the benefits of using SCWG for H_2 production from biomass are listed below.

i) Processing of biomass with high moisture content: Different from other conversion methods, wet biomass drying process can be eliminated in case of SCWG. Therefore, the high cost associated with biomass drying is waived by SCWG.

ii) Lower tar and char production: The intermediates which lead to tar formation are soluble in SCW, therefore can be reformed effectively in SCWG process (Basu 2010). Also, it is reported by Antal et al. (2000) that, char is produced with a minimal amount in SCWG.

iii) Higher hydrogen production efficiency: SCWG can produce gas with high H_2 content and low CO and CH_4 content within a single step and therefore downstream shift or reforming procedure are not needed.

iv) Ease of hydrogen collection and product purification: In SCWG process, H_2 is already produced with high pressure so no need for downstream compression. Also, inorganic impurities become insoluble, and heteroatoms like S, N, and halogens become soluble in SCW and hence they can be removed easily (Basu 2010).

2.4 Research progress in biomass supercritical water gasification

2.4.1 Reaction chemistry

The SCWG of biomass is a complex process. As summarized by Guo et al. (2007), the overall chemical reaction for biomass gasification to H_2 in SCWG can be represented by:

$$(2 - y)\, H_2O + CH_xO_y \rightarrow CO_2 + (2 - y + x/2)\, H_2 \quad (2.1)$$

In this equation, *x* represents H/C atomic ratio and *y* represents O/C atomic ratio of the feedstock. It is clear that the quality of the produced gas depends on both *x* and *y*. As summarized in Table 2, most of the experiments on H_2 production from biomass SCWG were conducted using model compounds rather than real biomass. Amongst three major compounds of biomass, glucose, cellulose and lignin, the conversion pathways of cellulose has been extensively investigated (Kruse and Gawlik 2002).

2.4.2 Supercritical water reactors

Literature survey reveals that (Table 2.1), so far, extensive research is carried out on different reactions using several types of reactors, starting from the micro batch reactor to bench scale pilot plant, at different reaction conditions. Most of the SCWG experiments were carried out in batch scale, autoclave or tubular reactors. Under the severe conditions of SCWG, use of tubular reactors is convenient in terms of construction, cost, and maintenance. Also, it is easy to control the reaction conditions because of its structure simplicity. Furthermore, feedstock loading problem which is usually associated with continuous reactors is automatically solved. However, in the case of batch scale reactors, due to the small volume and the simplified operation which is significantly different from that of the practical application, they are not significant to provide enough references for future applications.

Table 2.1 Information on reactor and biomass feedstock used in recent studies

Reference	Reactor type	Reactor material	Feedstock	Biomass loading Method/(rate)
Zhang et al., 2011	Bench continuous downflow tubular reactor	Inconel 625	Glucose	HPLC pump/ (1 or 2 mL/min)
Lee & Ihm, 2008	Bench continuous packed bed tubular reactor	Hastelloy C276	Glucose	High-pressure pump /(240g/h)
Osada et al., 2006	Tube bomb reactor	316 Stainless Steel	Lignin powder	-
Byrd, Pant, and Gupta, 2008	Fixed bed continuous tubular reactor	Inconel 600	Glycerol (99.5% purity)	HPLC pump/(-)
Demirbas, 2004	Autoclave	316 stainless steel	Fruit shell	-/(50g/run)
Lu et al., 2012	SCW fluidized bed	316 stainless steel	Glucose/corn cob	High pressure pump/(25.1g/min)
Hao et al, 2005	Autoclave	316 stainless steel	Cellulose and sawdust	-/(1.0g)

2.4.3 Effect of biomass feedstock

Most of the previous studies focused on biomass model compounds, including glucose and cellulose (Table 2.1). Recently, however, interest are shifting to lignin as literature reveals that H_2 yield is adversely affected by the proportion of lignin (Kruse 2009) and the mechanism of lignin decomposition in SCWG is still unclear.

Limited literature exists which dealt with real biomass, Lu et al. (2012a) studied SCWG of corn cob and fruit shells. The effect of feedstock dry matter content was examined by Kruse's group (2003). They found that when using a continuous stirred tank (CSTR) reactor, the increase in the content of dry matter caused an increase in the and gas and phenol yield. However, this phenomenon was not observed using a batch reactor at the same temperature (500 °C). Nanda et al. performed SCWG study of fructose as model compounds for fruit and vegetable wastes (Nanda et al. 2015). They found that using KOH as a catalyst could effective improve the hydrogen selectivity of the process. In another study, they performed SCWG for different food waste biomass such as banana peel, coconut shell, aloe vera rind, and sugarcane bagasse and observed highest hydrogen yield of 4.8 mmol/g when using the coconut shell as feed stock and K_2CO_3 as catalyst (Nanda et al. 2016). Moreover, in another study showed, the decrease in gasification efficiency was observed when the solid content of biomass increased in the range of 0.2–0.6 mole/L (Basu and Mettanant 2009)

2.4.4 Effects of reaction conditions

2.4.4.1 Effect of temperature

Temperature is a pivotal factor which has a significant impact on the conversion of carbon, gas yield, and the product composition of in an SCWG reactor. Within the tested temperature range between 500 °C and 700 °C in literature, higher temperature is reported to be beneficial for H_2 production. The overall carbon conversion and hydrogen yield increased with temperature while methane yield decreases (Basu 2010). The reaction conditions, catalysts as well as hydrogen yield used in recent studies are reported in Table 2.2. As can be seen, as different bases were used to report the hydrogen yield, comparison of the results is not easy.

Table 2.2 Reaction conditions, catalysts and hydrogen yield from recent studies

Reference	Temperature (°C)	Pressure (MPa)	Reaction time	Catalyst	Maximum H_2 yield
Zhang et al., 2011	600	24	-	Metals: Ru, Ni,Cu,Co; Promoters: ,Mg,Ru Na,K; Supporst:, AC, r-Al_2O_3, ZrO_2	38.4 mol/kg glucose
Lee & Ihm, 2008	575-725	28	5 h	Ni/Activated carbon (AC)	0.50 mol fractions of gas production
Osada et al., 2006	400	-	0-200 min	Metal: Ru, Pt, Ni, Support: TiO_2, Al_2O_3,AC	< 20wt% gas of yield
Byrd, Pant and Gupta, 2008	700/750/800	24.1	1-4 s	Ru/Al_2O_3 (5 wt. %)	6.1 mol/mol glycerol
Demirbas, 2004	376.85 to 476.85	23 to 48	60 min	No	15 wt% dry base
Lu et al., 2012	600	25	5 h	No	7.67 mol/kg
Hao et al., 2005	500	27	20 min	Ru/C, Pd/C, CeO_2,CeO	2-4g/100g feedstock
Nanda et al., 2016	400-600	23-25	15-45 min	NaOH, K_2CO_3	4.8 mmol/g feedstock

As per a recent survey by Lu et al. (2012a), the relative importance of different factors on H_2 yield of corn cob gasification in SCW is found as, residence time < feedstock concentration < pressure < temperature. Guo et al. (2007) suggested that for SCWG, when loaded with high concentrations, high temperature should be applied to effectively gasify the feedstock.

2.4.4.2 Effect of pressure

The effect of pressure is not clear based on available data in the literature. For example, reported by Demirbas (2004), when the reaction pressure increased from 23 to 48 MPa, the growth in H_2 yield was observed (5.9% to 12.6%). However, as reported by Guo et al. (Guo et al. 2007), pressure has no significant effect on SCWG of sawdust. Another point needs to be mentioned here is that high pressure might be favorable for char formation. As explained by Castello and Fiori (2011), high pressure tends to minimize the volume of the reaction system. Thus, with high pressure, the formation of the solid product whose specific volume is usually much lower than that of gas is favored.

2.4.4.3 Effect of heating rate

The high heating rate could increase the gas yield of SCWG. In a study by Kruse et al. (2003), a higher heating rate seems to reduce the char/coke formation in the CSTR reactor, whereas higher char/coke formation was found in their batch reactor with a low heating rate. In another study (Matsumura et al. 2006), it was found that the carbon gasification efficiency increased when the heating rate increased from 1 to 30 ºC/s.

2.4.4.4 Effect of reaction time

Reaction time has a substantial effect at the beginning of the reaction. Lu et al. (2006) observed that the yields of H_2, CO_2 and CH_4 increased with a residence time in SCWG of wood sawdust. The experiments were performed at 25 MPa and 650 °C. It was observed that for SCWG of sawdust, the yields of H_2, CO_2 and CH_4 increased with the increase in residence time from 9 to 46 second, at a pressure of 25 MPa, and temperature of 650 °C (Lu et al. 2006). Moreover, there is usually an optimum residence time, beyond which the conversion efficiency will not increase. For example, from SCWG study of 0.4 M glucose at 650 °C and 25MPa, the optimum residence time was identified as 3.6 min (Hao et al. 2005).

2.4.5 Catalysts for supercritical water gasification

The catalyst used for SCWG requires different properties compared to those used for the traditional gasification for the purpose of producing hydrogen . An important role of catalysts in SCWG is to reduce gasification temperature for a particular yield (Basu 2010). Main types of catalysts that have been used so far for SCWG are briefly discussed below.

Commonly used alkali catalysts include NaOH, KOH, Na_2CO_3, and K_2CO_3. Lu et al. (2006) suggest that the alkali catalysts are considered to be effective to enhance the H_2 production by promoting the water–gas shift reaction. Although alkali catalysts are effective in increasing high H_2 production, they may cause problems such as corrosion, plugging of the reactor. Moreover, the homogeneous are hard to recycle (Basu 2010). There is growing interest in developing of the heterogeneous catalyst due to their recyclable nature and high H_2 selectivity. The Ni-based catalyst was studied widely as it is relatively cost effective. Most of the results showed that Ni catalyst could improve the carbon conversion efficiency, but their stability is not satisfying as it involves metal sintering and deactivation via coking. According to Lee and Ihm (2008), Ni/activated charcoal catalyst showed promising H_2 yield from SCWG of glucose. However, deactivation was observed at temperatures lower than 650 °C. One reason for the deactivation was sintering of Ni particles, another is the coke deposition on the catalyst surface.

Another mostly investigated transition metal catalyst is the Ru-based catalyst. Ru/Al_2O_3 catalyst on glycerol SCWG can not only enhance biomass conversion rate and H_2 yield, but also reduce CH_4 production (Byrd, Pant, and Gupta 2008). High H_2 selectivity of Ru catalyst was shown in SCWG experiment of lignin and glucose (Elliott, Sealock Jr, and Baker 1993). Reported by Osada et al. (2006), Ru/C catalyst on lignin SCWG at 400 °C showed high gasification activity; however, activity was found to decrease gradually after reuse because due to the loses of the surface area.

The carbon-supported catalyst is also promising as it has high activity in the hydrothermal conversion of biomass. An early study by Xu et al. (1996) indicates that wood charcoal, and activated carbon produced from different biomass could promote the SCWG of organic compounds. In this study, a hydrogen-rich product gas was produced by glucose SCWG at 600 °C and 34.5 MPa. However, the carbon catalyst was deactivated after the experiment was conducted for 4h.

The development and use of bimetallic catalyst emerge as a new direction of interest only in recent studies. Guo et al. (2010) suggested that addition of trace amount of Ru could improve the activity and stability of the Ni catalyst. Zhang et al. (2011) found that the Ni/Al_2O_3 catalyst with either Mg or Ru as promoter got improved coke resistance.

Chapter 3 Process Modeling and Optimization of Non-Catalytic Supercritical Water Gasification of Lignin

This Chapter is based on: Kang, K., Azargohar, R., Dalai, A.K., Wang, H. Noncatalytic Gasification of Lignin in Supercritical Water Using a Batch Reactor for Hydrogen Production: An Experimental and Modeling Study. *Energy & Fuels*. 29 (2015) 1776-84.

Contributions of authors: KANG: (1) preparing the samples and carrying out experimental design and performing SCWG tests in the laboratory, (2) performing characterizations for gasification products, (3) analysing the experimental results and buid the statistical model (4) writing the manuscript and provide responses to reviewers' comments. Dr. Ramin Azargohar provided support by training KANG to use the SCWG reactor, reviewing the calculations for characterization of gasification products, and reviewing the manuscript. Dr. Ajay K. Dalai and Dr. Hui Wang, performed overall supervision of this research, examined the research results, oversaw the preparation of the manuscript, and submitted the paper.

3.1 Knowledge gaps, objectives, and hypothesis

3.1.1 Knowledge gaps

- The decomposition and conversion of lignin are usually studied by using model compounds rather than lignin itself (Pandey and Kim 2011), so study using lignin is needed.
- No statistical model was developed to optimize the hydrogen yield from non-catalytic SCWG of lignin.
- Discussions on interaction effects of operation parameters are missing from the literature. Also, their importance can even surpass the effect of individual parameters (Montgomery, Runger, and Hubele 2009).

3.1.2 Hypothesis

- Use of Central Composite Design (CCD) experimental design and statistical modeling helps understood the non-catalytic SCWG process with minimized workload and maximized statistical accuracy.
- Best combination of reaction parameters could be established to improve hydrogen yield from this process by using the response surface model.

3.1.3 Objectives

- To investigate the effects of important parameters on gas and hydrogen yield for non-catalytic SCWG of lignin.
- To develop a statistical model for the hydrogen yield as a function of SCWG operating parameters.
- To optimize the reaction parameters to produce hydrogen with maximum yield via non-catalytic SCWG of lignin.

3.2 Abstract

In this research phase, CCD methodology was used in experimental design, model building, and data analysis. SCWG of lignin was performed in a batch reactor without the presence of any catalysts to optimize the process for hydrogen production. By both experimental and statistical modeling, the main effects, as well as interaction effects of three parameters including temperature, pressure and water to biomass ratio, were investigated in the range of 399-651 °C, 23-29 MPa, 3-8, respectively. As a result, up to 651 °C, higher temperature is required for hydrogen production. However, change of pressure from 23 to 29 MPa did not significantly affect the hydrogen yield. The Strong interaction between temperature and water to biomass ratio was observed at a temperature higher than 525 °C, and dramatic decrease in hydrogen yield with an increase in water to biomass ratio was observed at 600 °C. According to the model, the maximum hydrogen yield will be 1.60 mmol/g of lignin. The best combination for reaction parameters for hydrogen production is: Temperature = 651 °C, Pressure = 25 MPa, Water to biomass ratio = 3.9.

3.3 Introduction

Environment and security concerns raised by the usage of fossil fuels drive the research of producing hydrogen as a clean source of energy (Cortright, Davda, and Dumesic 2002). Production of hydrogen from biomass could perfectly bridge the gap between the current fossil fuel based energy strategy and the practical water splitting in future (Navarro, Peña, and Fierro 2007). Currently, more than 80% of the biomass used to produce energy is lignocellulosic biomass such as logs, bark, wood chips, wood pellets, sawdust or other by-products (Kopetz 2013).

One of the significant barriers for of fuel production from lignocellulosic biomass is the difficulty in lignin conversion (Parsell et al. 2013). The recalcitrance of lignin comes from its complicated structure, which is amorphous and three-dimensionally cross-linked (Yong and Matsumura 2012).

Above all, finding a proper way of lignin utilization may lead to a breakthrough in bio-energy research.

Hydrogen is a very versatile fuel which can be easily used directly or transformed to other fuels. Hydrogen is also environmentally friendly as when it burns, the product is only H_2O. Currently, the industrial-scale hydrogen production is mainly dependent on electrolysis of water or steam reforming of methane (Levin, Pitt, and Love 2004). However, the production of H_2 from biomass is still in its infancy, as none of the technology is ultimately demonstrated and commercialized (Dahmen, Dinjus, and Kruse 2009).

Pointed out in a recent review by Levin and Chahine (2010), a significant problem for biochemical production of H_2 is difficulty in getting a sufficient production rate of H_2 for practical applications. On the contrary, thermochemical processing offers some advantages over biochemical methods, including a high rate of H_2 production, high energy efficiency and the ability to handle mixed feedstock like municipal wastes (Peterson et al. 2008). Thus, the thermochemical route seems to be more feasible and receives much attention for H_2 production from lignocellulosic biomass in recent years.

At supercritical conditions, both chemical and physical properties of water vary significantly compared to its liquid phase (Furusawa et al. 2007). The advantages of using SCWG lie in: first, the directly handling ability of wet biomass. Most of the biomass wastes are wet and contain up to 95% water. Before conversion in conventional gasification or liquefaction, the wet biomass needs to be pre-dried involving high costs (Kruse and Gawlik 2002). Secondly, coking problem can be solved by SCWG process. The tar-forming compounds are soluble in SCW, therefore complete reforming is possible (Basu 2010). Also, low char formation was observed in another research work (Antal et al. 2000).

The Central Composite Design (CCD) methodology is a classical experimental design especially for building response surface models (RSM). This method has been widely applied in optimization studies for different engineering processes (Wang and Shan 2007, Ibrahim et al. 2005). This method is significant to allow one to test not only the main effects of the individual parameter but more importantly, also the interrelations amongst the parameters. Also, CCD method decreases the number of experiments required for a certain research task. In this study, the CCD methodology is a reasonable choice for the purpose of providing statistical accuracy for the modeling work,

examine the possible interactions amongst parameters as well as reducing the number of experimental runs. In this study, three types of statistical tests were performed including the test of significance, the R-squared test, and the test for lack-of-fit. The test for lack-of-fit used to determine the source of differences between experimental observations and model predictions, and the result of this test indicates whether or not the data can be fitted to the model (Azargohar and Dalai 2008). The test of significance is used to check the significance level of individual parameters as well as their interaction effects. By using the test of significance, factors or interactions which have a significant effect on the response could be identified, so a simpler mathematical model and easier interpretation could be achieved (Azargohar and Dalai 2008). The R-squared test evaluates the extent to which observed results are represented by the model, as the proportion of total variation in outcomes explained by the statistical model (Minitab 2006).

Some experimental studies have been done to evaluate the effects of reaction conditions on the hydrogen yield from non-catalytic SCWG of lignin. Study on (Resende et al. 2008) lignin SCWG in the complete absence of metal catalyst in quartz reactors was reported. It was concluded that low biomass loadings should be used to maximize the hydrogen yield from lignin. For lignin decomposition in SCW, the influence of the water density was studied by Osada et al. (2006), using lignin and 4-propylphenol as lignin model compound. It was observed that the increase of water density above 0.33 g/cm^3 could improve the lignin decomposition rate in SCW. It was also pointed out that water density has no effect on gasification of low-molecular weight products of lignin decomposition with the presence of supported ruthenium catalysts. There has not been any optimization study which combines effects of all parameters considered here for non-catalytic SCWG of lignin. Also, the information on their interaction effects is missing.

Limited work can also be found in open literature about decomposition mechanism of lignin in SCW. Saisu et al. (2003), performed SCWG of lignin and lignin/phenol mixture at fixed temperature of 400 °C, and they proposed a two-stage scheme for lignin reactions under SCW conditions. It was proved by direct visual observations that phenol could be helpful to inhibit re-polymerization of the phenolic compounds in SCWG of lignin (Fang et al. 2008). The mechanism study seems focused mostly on using lignin as a source of different chemicals; however, a specific optimization study for using lignin to produce hydrogen via non-catalytic SCWG is not available.

Following the identification of relevant parameters for this process and a basic understanding of the reaction mechanism, optimization study on these parameters is in urgent need for decision making for subsequent research, such as scaled-up reactor design, process economic analysis, etc. However, there are still some gaps in the existing literature. To get a comprehensive view of the process, systematic optimization data about lignin is, of course, necessary. Secondly, although several studies have been done to investigate the optimum reaction condition for hydrogen production from different biomass or model compounds. What's more, as most of the results in this area are analyzed in a manner that studies the effect of an individual parameter sequentially while maintaining others at the same level, they are limited in a sense that most of them neglected the potential interaction effects amongst these parameters. The interactions may show significant impact on the hydrogen yield from the process, and their importance can even surpass the effect of individual parameters (Montgomery, Runger, and Hubele 2009).

The goal of this research phase is to build a statistical model for the hydrogen yield as a function of SCWG process parameters. The model could be used to optimize the parameters to produce hydrogen with maximum yield. This study has its uniqueness. First, this is the first work in this field to introduce the statistical tools in experimental design, model building and data analysis for the optimization of hydrogen yield from non-catalytic SCWG of lignin. Using this approach, the interaction effects of parameters are discussed, and the model can be utilized as a guide to obtain optimum hydrogen yield in the range of operating conditions. Second, in comparison with the previous study, a wider range of parameter combinations are investigated simultaneously. Therefore, this work may provide a more comprehensive view on the role of each parameter and their potential interactions. Third, the information contained in this study may also be a helpful reference for other optimization studies in this area with or without catalysts, and in related studies where lignin could act as a model compound such as SCWG of different biomass species.

3.4 Experimental section

3.4.1 Material

The lignin used for this study was purchased from Sigma-Aldrich Corporation (Oakville, ON, CANADA). It was provided in the form of dry amorphous powder.

3.4.2 Reaction setup

All the SCWG tests were performed in a batch SCW reactor. The schematic of the setup is given in Figure 3.1.

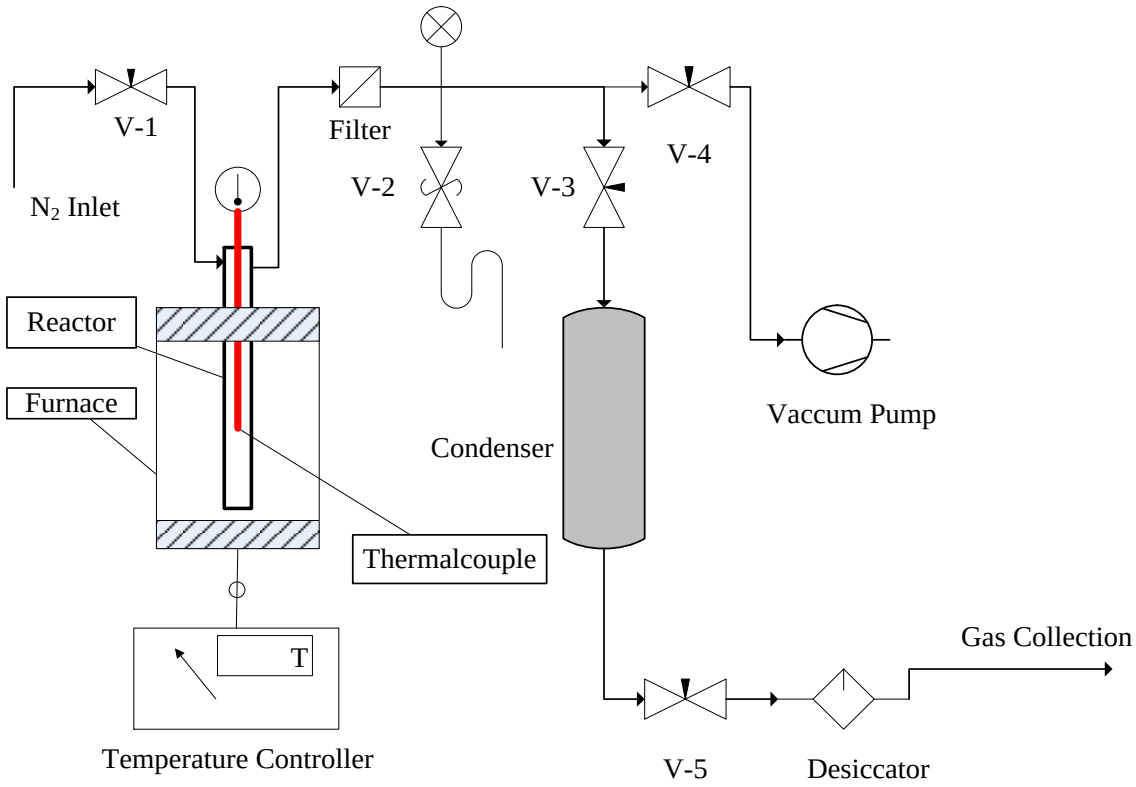

Figure 3.1 Structure of the supercritical water reactor

3.4.3 Procedure for supercritical water gasification tests

All the parts such as tubing, tube fittings, filter, and valves were bought from Swagelok (Winnipeg, MB, Canada). A furnace was connected to the reactor for heating of the SCW reactor. The furnace was manufactured by Carbolite (Hope Valley, UK). A Buchi V-700 vacuum pump was used for air removal. The pump was supplied by BUCHI Corporation (New Castle, USA). The type CN7500 temperature controller and the type K thermocouple used for the project were purchased from Omega Engineering Inc. (Stamford, USA).

For each SCWG test, 0.65g lignin was used as a biomass feedstock. Also loaded into the reactor is the amount of water, which was determined by the specific water to biomass mass ratio. After sealing of the reactor, the leak test was performed before the experiment. The pressure needed for

the experiment comes from an N_2 cylinder. Once the gas tightness of the reactor was confirmed, the second step was to establish an N_2 environment in the reactor. Vacuuming the reactor with the vacuum pump helps the removal of air. Then, a certain amount of N_2 was released into the reactor to create the required initial pressure. The third step was to start the reaction. It should be mentioned that to achieve the desired pressure for the reaction, the initial pressure was in the range of 11.03 to 13.79 MPa).

Once the SCWG test starts, the reactor is heated up by an electrical furnace at the heating rate of 30 °C/min. The typical reaction time of 50 Min was fixed. This reaction time takes into account of the time used for reactor heating. Controlling of the furnace temperature was achieved by the temperature controller and monitored/calibrated by the type K thermocouple inside the reactor. During the experiment, two asbestos insulating plates were placed on top of the furnace to prevent temperature fluctuation of the reactor.

The product collection was carried out at the end of the test. To cool the reactor down, cold water spray was applied. Before opening the reactor, the produced gas was released into the condenser. Then the vent line was opened and the stabilized product gas was collected with a Tedlar bag. The function of the desiccator in the vent line was to remove the moisture from the product gas. After the collection of the produced gas, the reactor was removed from the setup, followed by the collection of other products. The liquid phase and solid phase products were obtained using clean beakers by washing the reactor. Two types of washing agents were applied including distilled water and HPLC grade acetone. To collect the solid phase product, all the liquid phase and solid products were filtered with filter paper. For water removal from the water phase a rotary evaporator was used. Flowing N_2 was applied during the evaporation of the acetone phase. After filtration and drying in an oven for 8 hours at 100 °C, all water phase, and acetone phase products were quantified by weighing. Normally, the temperature of the evaporator was set at 80 °C. Thus, evaporation of the products with lower boiling points may occur during the separation procedure, which may lead to variance in weighing the liquid phase products.

3.4.4 Characterization of lignin sample and products from gasification

The elemental analysis of the lignin was performed using the “Elementar Vario Ⅲ” elemental analyzer. A Spectrum GX FTIR Spectrometer (PerkinElmer Inc., USA) was used to perform the

Fourier transform infrared spectroscopy (FT-IR) analysis. And the analysis of the lignin sample was conducted following KBr technique.

The solid products and the filter paper was dried in the oven at 105 °C for 3 hours in an oven then weighted. An Agilent GC 7890A gas chromatograph was used to analyze the product gas. The Gc was equipped with both thermal conductivity detectors(TCD) and flame ionization detector (FID). The gas chromatograph is also equipped with one capillary column and five pack columns. The peak normalization method was applied for calculation of the gas composition.

3.4.5 Statistical design of experiments

In this study, reaction parameters including reaction pressure (P) and temperature (T), as well as the mass ratio of water to biomass ($R_{W/B}$) were used to develop the experimental design. They varied in the ranges of 23-29 MPa, 399-651 °C, and 3-8, respectively. To develop the model for optimum operating conditions for hydrogen yield from non-catalytic SCWG of lignin. The definitions of gas, hydrogen yield, and hydrogen selectivity in this project are provided as bellow:

$$\text{Gas yield (wt \%)} = \frac{\text{Milligrams of gas produced per run}}{\text{Milligrams of lignin sample used per run}} \quad \text{.....(3.1)}$$

$$\text{Hydrogen yield (mmol/g)} = \frac{\text{Millimoles of hydrogen produced per run}}{\text{Grams of lignin sample used per run}} \quad \text{.....(3.2)}$$

$$\text{Hydrogen selectivity} = \frac{\text{Hydrogen yield}}{2\times\text{Methane yield}} \quad \text{.....(3.3)}$$

Central Composite Design methodology (CCD) was followed to conduct the experimental design. The CCD methodology is very popular in building second-order response surface models (RSM)(Montgomery, Runger, and Hubele 2009). The method enables the optimization with fewer experiments. The method also allows the investigation of the interaction effects of different operating conditions. The design was conducted using Minitab software. The list of main reaction parameters is shown in Table 3.1 and other parameters used in this set of experiments are residence time: 50 min and heating rate: 30 °C /min. The CCD design contains three types of runs namely, axial runs (2·k), factorial runs (2^k), and center runs, where k is the number of parameters (Lazic 2004).

In this study there are three parameters, and six center runs. Therefore, the total number of experiments needed to be performed for the current study is:

$N=2\cdot k+2^k+6=2\cdot 3+2^3+6=20$……(3.4)

Based upon the range of different parameters, the design matrix of experiments required for this study is shown in Table 3.1. As shown in Table 3.1, to estimate the residual error, the conditions of the center point were repeated for six times. The center runs have all parameters set at their mid-level. In this CCD design, each parameter's level is coded to (-1, +1) by their range. In Table 3.1, the -1 represents a low level of the parameter, and +1 represents the high level of the parameter.

Table 3.1 The design matrix of the experiment in coded variables

Experiment Number	Temperature （T）	Pressure （P）	Water to biomass ratio （$R_{W/B}$）
1	1	1	-1
2	-1	1	-1
3	1	-1	1
4	- a	0	0
5	a	0	0
6	0	0	0
7	0	0	0
8	0	0	0
9	-1	-1	1
10	0	0	0
11	0	0	0
12	0	0	- a
13	1	-1	-1
14	1	1	1
15	0	- a	0
16	0	a	0
17	-1	-1	-1
18	0	0	a
19	-1	1	1
20	0	0	0

These center points were added to protect against curvature on the response surface (Montgomery, Runger, and Hubele 2009). Each parameter has five different levels based on the type of the point. Specifically, ±1 were assigned to the factorial points, the ±a were assigned to the axial points, and 0 was assigned to the center points. The "a" is the distance between the center point and the axial point,which was calculated as $(2^{k})^{0.25}$ (Azargohar and Dalai 2008), which is 1.68 in this case. What also need to be mentioned here is that to minimize the possible influence brought by differences in time of each run, the run sequence is randomized.

3.5 Results and discussion

3.5.1 Characterization of lignin sample

Since there are many different types of lignin available, and the procedures of manufacturing the products might vary, a solid understanding of the lignin sample which was used in this study was obtained by characterization. The lignin sample in this study was categorized as "Kraft lignin". Kraft lignin is produced from black liquor which is generated by the Kraft pulping process. The result from elemental analysis shows that the composition of the lignin sample, in terms of weight percentage is N: 0.07 ± 0.01, C: 48.19 ± 0.0, S: 4.57 ± 0.89, H: 4.57 ± 0.09, O: 42.60 ± 1.00, where the oxygen content was determined by difference. Compared to lignin in the biomass, it should be pointed out that the manufacturing process introduced a small amount of sulfur.

Figure 3.2 shows the FT-IR spectrum of the lignin sample. The bands appearing at 1429, 1464, 1509 and 1601 cm^{-1} are the characteristic peaks of C—H and aromatic rings in the lignin sample (Liu et al. 2008). The bands observed around 1270 cm^{-1} indicates the existence of guaiacyl group in the sample. However, the absence of bands at 1330-1375 cm^{-1} shows the lack of syringyl group in the sample (Liu et al. 2008). The peak at 2935 cm^{-1} can be assigned to the C—H vibration of aliphatic carbon. Furthermore, the stretching O—H bonds in the methyl groups was evident by the presence of the band at 3419 cm^{-1} (Crouch and Skoog 2007). Moreover, the bands appear around 1000 and 1400 cm^{-1} are caused by C—O or C—H in the sample. According to the spectrum, the lignin sample used in this study share similar structure with lignin extracted from fir and birch (Liu et al. 2008), so the sample can be considered as a representation of lignin structure existing in real biomass.

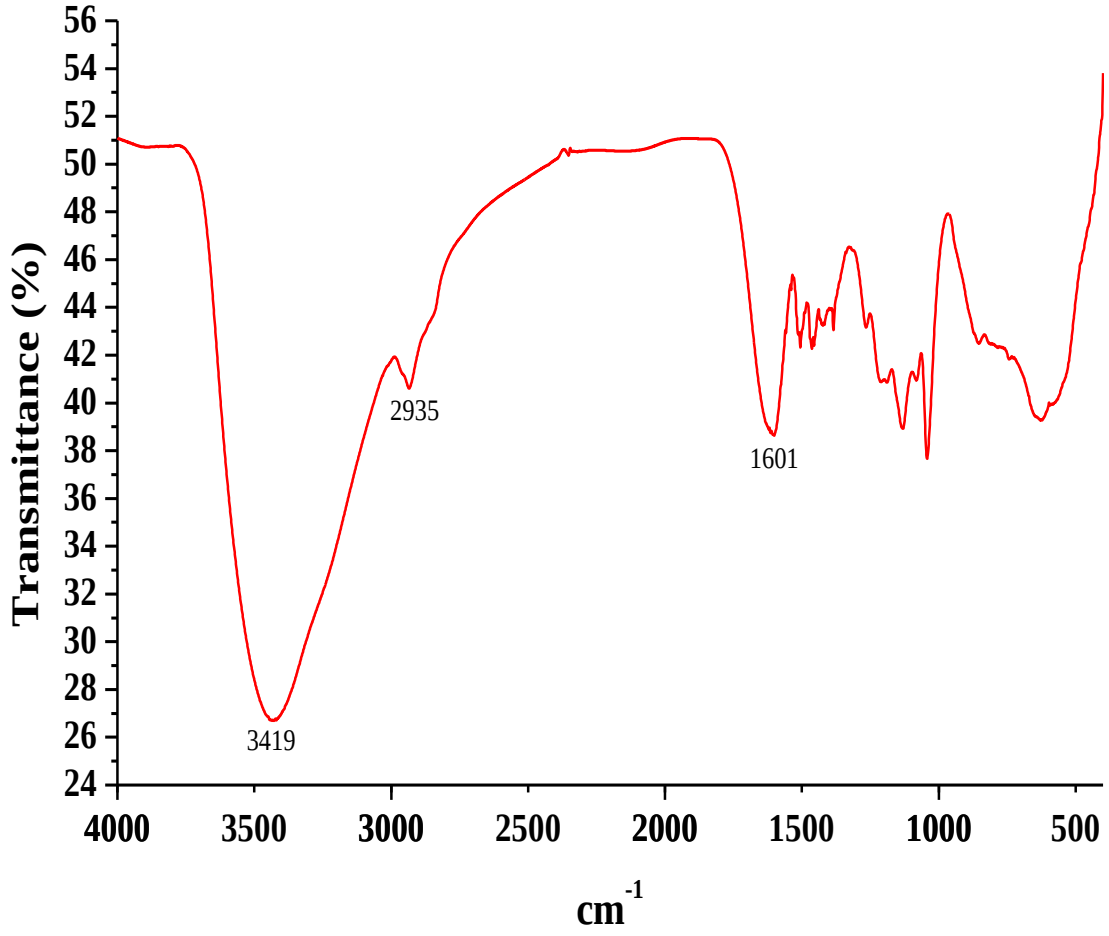

Figure 3.2 FT-IR spectrum of the lignin sample

3.5.2 Results of gasification experiments

CCD methodology was applied to the experimental design. 20 runs were performed as required by the experimental design, with six runs repeated under similar operation conditions (runs No. 6, 7, 8, 10, 11 & 20 in Table 3.2. These repeated runs were all performed under process conditions of 26 MPa, 525 °C, with the water to biomass mass ratio of five. The results of the statistical analysis showed that the variation in experimental results was within ±2% for hydrogen yield.

Table 2 reports the reaction conditions, gas yield, H_2 yield as well as mass balance for each run. A general trend of increasing in both gas and H_2 yield with temperature is evident. The mass balance obtained from the experiments ranges between 85.9% and 93.5%. The product collection procedure introduces the loss in mass due to loss of some low boiling point contents.

Table 3.2 Reaction conditions, yield and mass balance result of gasification experiments

Experiment Number	Temperature (°C)	Pressure (MPa)	Water to biomass ratio (g/g)	Gas Yield (wt%)	H_2 yield (mmol/g)	Total mass balance (wt%)
1	600	28	3	13.0	0.99	90.0
2	450	28	3	8.0	0.13	86.5
3	600	24	7	3.1	0.16	92.8
4	399	26	5	3.5	0.02	96.0
5	651	26	5	16.1	1.59	94.5
6	525	26	5	7.6	0.16	92.0
7	525	26	5	9.9	0.16	92.3
8	525	26	5	8.6	0.16	92.4
9	450	24	7	10.2	0.02	92.3
10	525	26	5	10.3	0.16	92.8
11	525	26	5	8.1	0.16	92.5
12	525	26	2	4.8	0.12	87.3
13	600	24	3	11.4	1.01	88.8
14	600	28	7	2.9	0.11	92.2
15	525	23	5	1.2	0.08	88.9
16	525	29	5	6.7	0.13	92.5
17	450	24	3	7.2	0.03	85.9
18	525	26	8	2.4	0.04	92.6
19	450	28	7	4.5	0.07	93.5
20	525	26	5	8.1	0.16	92.4

As shown in Table 2, the maximum gas yield of 16.1 wt% and H_2 yield 1.59 mmol/g were obtained at 651 °C, 26 MPa and ratio 5 (Run 5), which was significantly higher than the amount obtained at 399 °C (Run 4) with other parameters kept at the same level with the gas yield of 3.5 wt% and H_2 yield 0.02 mmol/g. Also, the low H_2 production at 399 °C indicates that the temperature is not high enough for high hydrogen production from lignin SCWG. Other than temperature, however, the effects of pressure and water to biomass ratio are complicated. Thus, the more detailed statistical analysis is needed for accurate interpretations. The result of the statistical analysis was performed on these data, and the results are discussed in the following section.

3.5.3 Improve data normality

Before building the model, the normality of data is tested. When the data are perfectly normal, the data points on the probability plot will form a straight line (Minitab 2006).

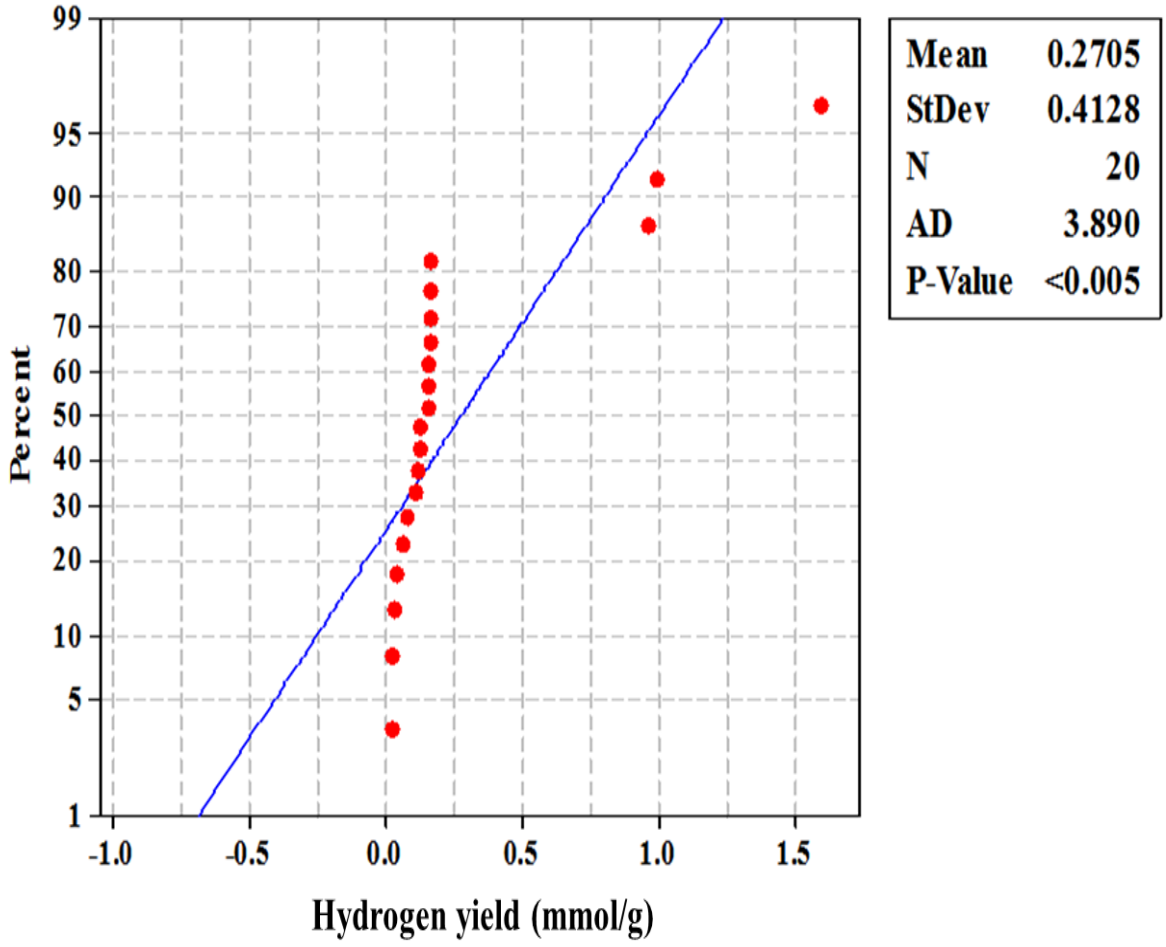

Figure 3.3 The probability plot of hydrogen yield data

However, the probability plot of H_2 yield data (Figure 3.3) shows that the points do not fall reasonably close to the reference line. Also, the P-value is less than 0.005, indicating that the data do not follow a normal distribution (Minitab 2006). When the maximum response is ten times higher than the minimum response, a transformation of the response should be performed. In our study, the ratio between the maximum and minimum response was 79.5; this indicates that the transformation is needed. Firstly, Box-Cox transformation is applied to the H_2 yield data to correct the non-normality (Minitab 2006).

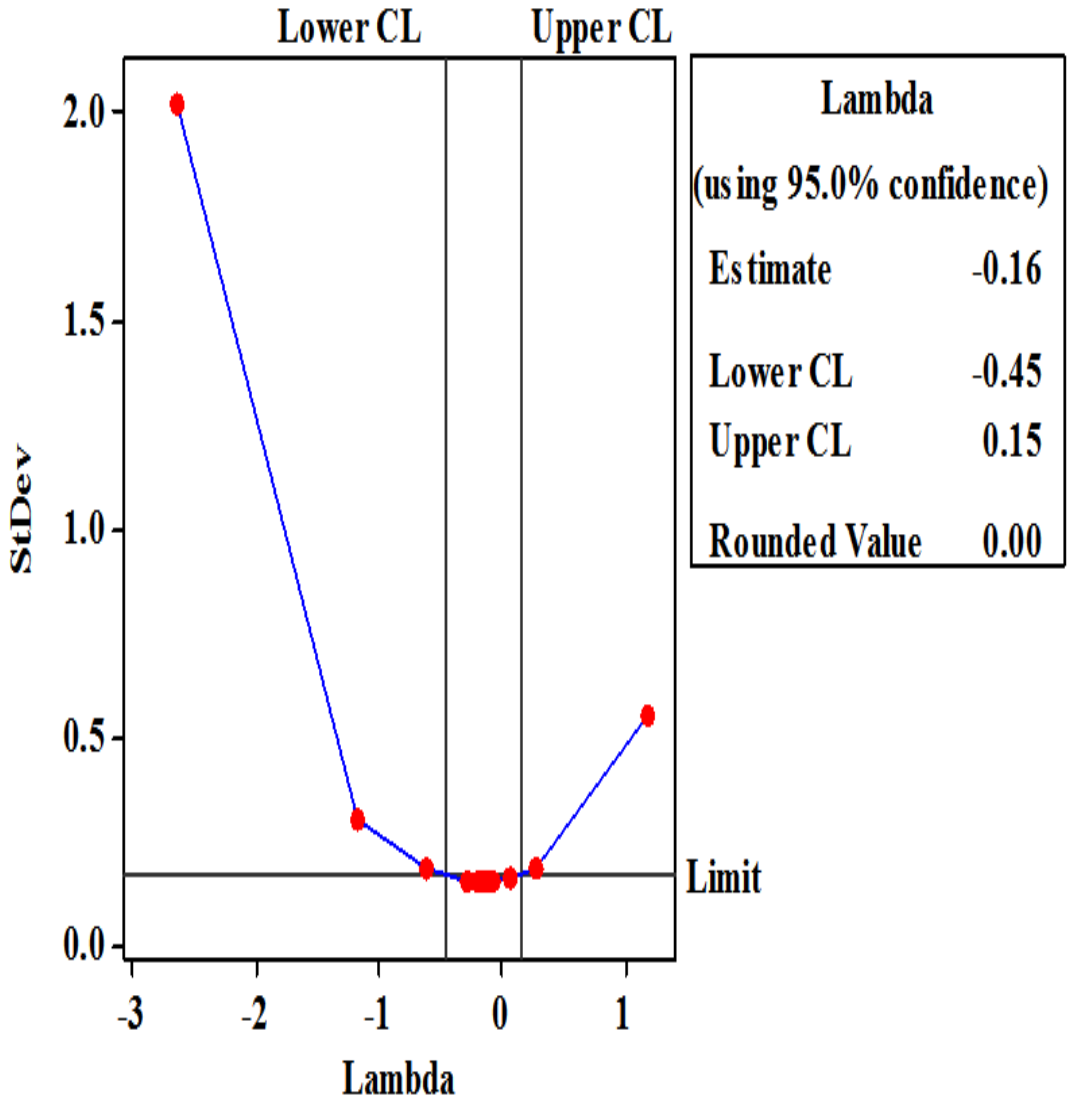

Figure 3.4 Box-Cox plot of hydrogen yield data

As shown in the Box-Cox plot (Figure 3.4) for the H_2 yield data, the rounded value for lambda is 0.00. The lambda value of zero means that the natural logarithmic value of the response is located in the desired region for the transformation. Therefore, a conversion of "Transformed H_2 yield" = Ln (H_2 yield) is applied to the data. As shown in the probability plot of transformed H_2 yield (Figure 3.5), it can be seen that in the plot of the transformed H_2 yield, data points fall reasonably close to the reference line, so the normality of the data are now improved. As the P-value is now 0.01, the normality of the data is now satisfied (Minitab 2006).

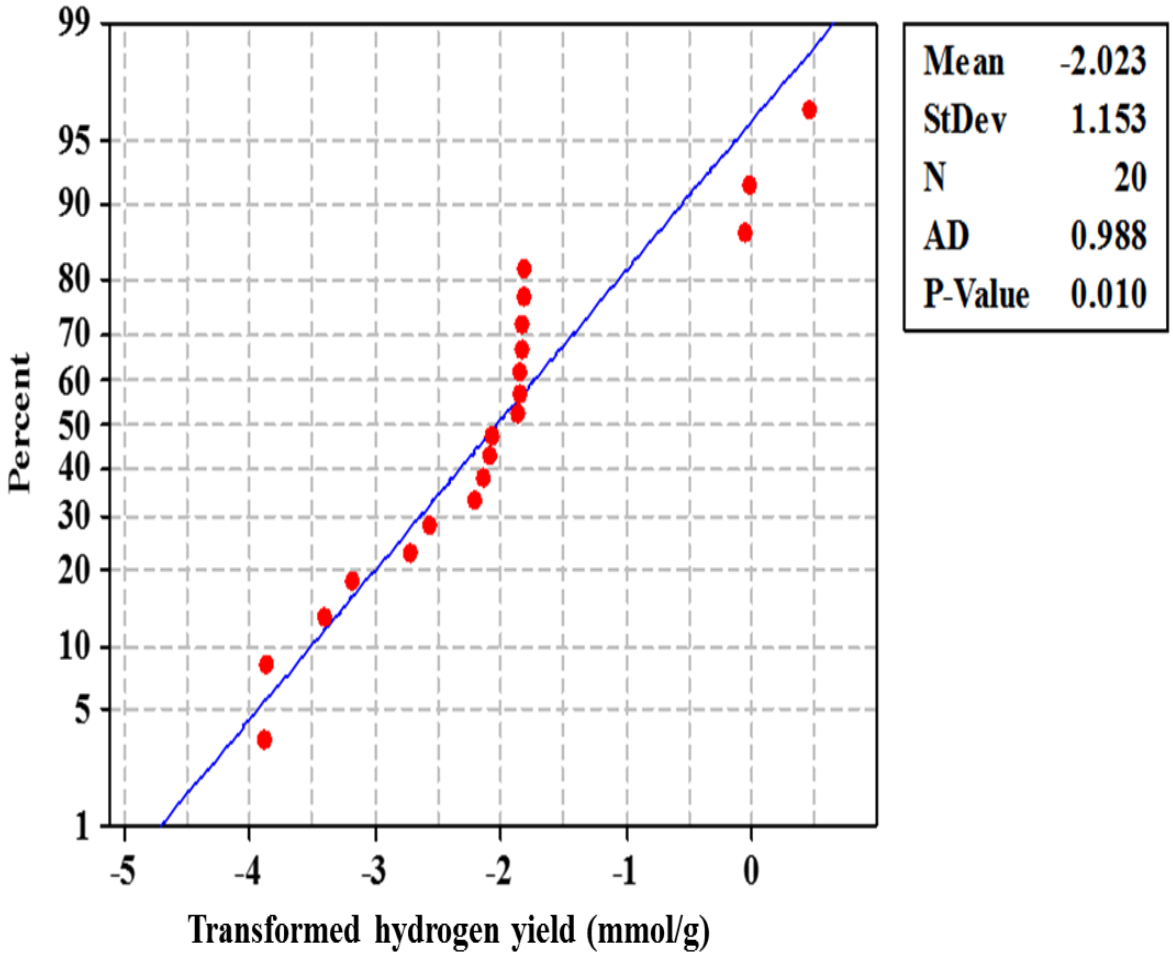

Figure 3.5 The probability plot of transformed hydrogen yield data

3.5.4 Statistical analysis and model construction

After improvement of the normality, three trials were used to find the appropriate model for the data. The statistics used in each trial including lack-of-fit test and R-squared statistics are shown in Table 3.3. As mentioned before, the test of lack-of-fit can be used for judging the correctness of the model, while the value of R-squared statistics reflects the proportion of total variability of observations explained by the model (Minitab 2006). These statistics should be first examined before any further discussion based on the model. If the p-value for the lack-of-fit test is smaller than 0.05, the fit of the model insufficient at the confidence level of 95%. It further means that the data cannot be properly interpreted by the model. In the 3rd trial, the p-value for the lack-of-fit test was 0.139, which means the model is adequate to explain the data.

Table 3.3 Lack-of- fit and R-squared statistics for different models fitted to the data

Model No.	Terms in Model	Eliminated Effects	P value for Lack-of-Fit	R-squared	Adjusted R-squared
1	T,P,$R_{W/B}$,T^2,P^2, $R_{W/B}^2$,TP,T $R_{W/B}$,$PR_{W/B}$		0.000	96.6%	93.5%
2	T,P, $R_{W/B}$, $R_{W/B}^2$,TP,T $R_{W/B}$,	P^2,P,$R_{W/B}$,T^2	0.000	94.9%	92.5%
3	T, $R_{W/B}$, $R_{W/B}^2$,T^2,	P^2,P $R_{W/B}$,T $R_{W/B}$,P,TP	0.139	85.1%	81.1%

T=Temperature (°C)； P=Pressure (MPa)； $R_{W/B}$=Ratio of water to biomass (g/g)

R-squared statistics (R^2) have a value range of 0-1, in the case of a model, a large R^2 indicates that the model is successful in interpreting the variability in the response(Montgomery, Runger, and Hubele 2009). In this case, R^2 for the third trial is 85.1%, indicates that this model could explain 85.1% of the variation been observed in hydrogen yield. Also, the value of 81.1% for the adjusted R^2 should be reported because this value has been adjusted based on the number of parameters included in the model (Azargohar and Dalai 2008).

Table 3.4 gives the results of the test of significance. The result covers all three factors and interactions which were included in each model of the three trails. If the p-value of one factor is larger than 0.05, change in this factor will not significantly affect the response at the 95% confidence level, so this factor should be excluded from the model (Minitab 2006). Therefore, after each trial, the insignificant factors were eliminated in the next trial. Specifically, as in trial 1, the squared effects of pressure and temperature, and the interaction effect between pressure and water to biomass ratio were found to be insignificant. Thus they were eliminated for the 2nd trial. Although in the 2nd trial, the interaction between temperature and pressure was not insignificant, it was deleted for the 3rd trial as the main effect of pressure is eliminated to satisfy the lack of fit test.

Table 3.4 Results of analysis of variance of factors and interactions for different models

Factor/ Interactions	P value for Model No. 1	P value for Model No. 2	P value for Model No. 3
T	0.000	0.000	0.000
P	0.021	0.024	Eliminated
$R_{W/B}$	0.000	0.000	0.002
T*T	0.229	Eliminated	0.411
P*P	0.148	Eliminated	Eliminated
$R_{W/B}$*$R_{W/B}$	0.011	0.012	0.102
T*P	0.007	0.007	Eliminated
T*$R_{W/B}$	0.007	0.007	Eliminated
P*$R_{W/B}$	0.502	Eliminated	Eliminated

Based on the results of the final trial, the remaining effects are the individual effects of temperature (T) and water to biomass mass ratio ($R_{W/B}$). For a full quadratic model of a response surface with three factors, the universal equation is:

$$\bar{y}=\beta_0+\beta_1 \cdot x_1+\beta_2 \cdot x_2+\beta_3 \cdot x_3+\beta_{12} \cdot x_1 \cdot x_2+\beta_{13} \cdot x_1 \cdot x_3+\beta_{23} \cdot x_2 \cdot x_3+\beta_{11} \cdot x_1^2+\beta_{22} \cdot x_2^2+\beta_{33} \cdot x_3^2 \quad (3.5)$$

Thus, based on the coefficients given by model 3. The relationship of data obtained by this set of experiment could be written as：

$$\text{Transformed } H_2 \text{ yield} = -4.51-0.01 \times T+0.32 \times R_{W/B}+1.97 \times 10^{-5} \times T^2-0.06 \times R_{W/B}^2 \quad (3.6)$$

where:

$$\text{Transformed } H_2 \text{ yield} = \text{Ln}(H_2 \text{ yield}) \quad (3.7)$$

So the gross parameter-response relationship could be written as:

$$H_2 \text{ yield} = e^{(-4.51-0.01 \times T+0.32 \times R_{W/B}+1.97 \times 10^{-5} \times T^2-0.06 \times R_{W/B}^2)} \quad (3.8)$$

3.5.5 Effects of different process parameters and interaction

3.5.5.1 Effect of reaction temperature

Rough ideas about best operation conditions can be obtained from the plots of the response surface. Figure 3.6 is the three-dimensional surface plot of H_2 yield which shows the effect of both temperature and water to biomass ratio when the pressure was held at 26 MPa. The plot indicates that the decomposition of lignin in SCW is an overall endothermic process as there is a general trend that when the temperature increases, the hydrogen yield increased.

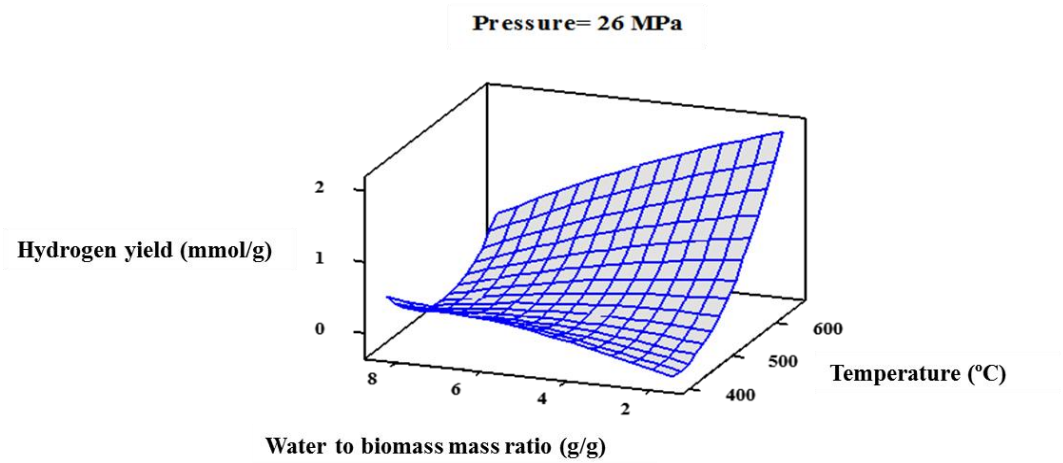

Figure 3.6 Three-dimensional surface plot of hydrogen yield

More detailed information is in the main effects plot for hydrogen yield (Figure 3.7). This plot indicates that change in temperature will significantly affect the hydrogen yield from lignin SCWG. Specifically, a significant increase in hydrogen yield from 0.02 mmol/g to 1.59 mmol/g was found with an increase in temperature from 399 to 651 °C. This trend is also confirmed by the results of another study (Resende et al. 2008). Also, when the temperature goes above 525 °C, the increase in H_2 production becomes much more dramatic than under lower temperature. This is similar to the work of Boukis et al.(2003), who witnessed a dramatic 5 times jump in hydrogen yield when temperature increased from 600 °C to 725 °C in non-catalytic SCWG of lignin.

3.5.5.2 Effect of reaction pressure

As is shown in Figure 3.7, no clear effect of pressure on hydrogen yield was observed when the reaction pressure was changing from 23 to 29 MPa. High pressure is argued to be helpful for improving the hydrogen yield. When pressure increases, the ion reactions will be boosted and free-radical reaction will slow down for glucose SCWG (Lu et al. 2006). However, as reported by Guo et al. (2007), change of pressure showed no significant effect in sawdust gasification, and a decrease in the rate of decomposition reaction rate was observed.

The effect of reaction pressure on hydrogen yield is complicated. On one hand, high-pressure help to enhance the fluid density in the system, hence reduce the formation of char or coke by decrease the rate of carbonization reaction (Fang 2014). On the other hand, based on the Le Châtelier's law, high pressure seems to promote the methanation reaction which consumes hydrogen to produce methane. In our case, lignin has a more complicated molecular structure. Thus the decomposition reaction is more important than other reactions. Therefore, the pressure change in our study did not bring significant change in the hydrogen yield.

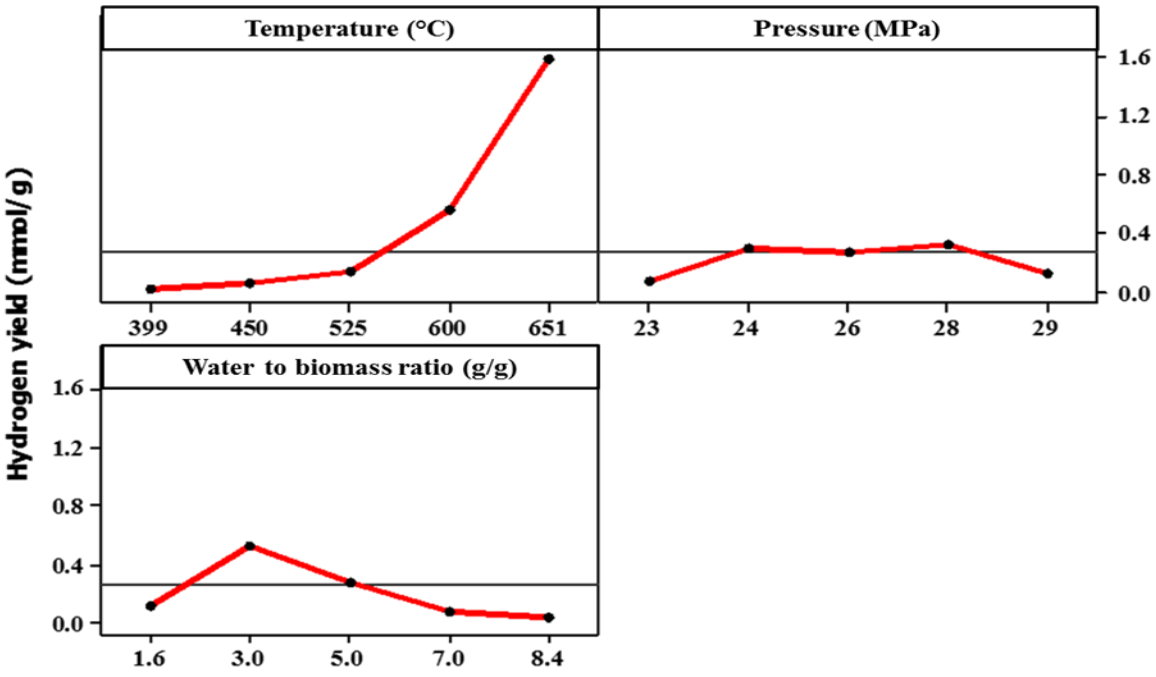

Figure 3.7 Main effects plot for hydrogen yield

3.5.5.3 Effect of water to biomass mass ratio

For the water to biomass mass ratio, the best-observed value for hydrogen yield is around three in this set of the experiment. The H_2 yield decreased when the ratio goes beyond three, which is different from Ding's work on SCWG of cellulose and pinewood (2014). In Ding's work, when the ratio rises from 3 to 7, the H_2 yield was increased by 44%. The explanation is that H_2O can boost the hydrolysis of the glycosidic bonds contained in cellulose which is polar and could be easily hydrolyzed. However, in our case, lignin has highly cross-linked polymeric structure, which may not be easily broken by a simple increase of water amount.

As deduced from the work of Osada et al.(Osada, Sato, Watanabe, et al. 2006), the low hydrogen yield under low water to biomass ratio (water density $<0.2 g/cm^3$) can be due to the polymerization of lignin caused by poor contact pattern between SCW and the feedstock. Also, they found that although the when the water density increases the gas yield also increased, the composition is independent of it. At high water to biomass ratio, overloaded water may form a cage as a physical barrier for the chemical reactions in SCWG. Specifically, diffusion of the solution will be interrupted because the solvent will form a cage to surround the solved molecules. This effect will hinder the decomposition reactions in SCWG by detaining emerging products within this cage. The cage can also decrease the reaction rate via isolation of the solved molecules and prevent the reactions amongst different solutes. The cage effect will become more dramatic when the water density increases, therefore, may lead to poor decomposition of lignin in SCW, which in turn leads to low hydrogen yield (Sricharoenchaikul 2009).

3.5.5.4 Effect of parameter interaction

Other than individual parameters, the statistical model also allows investigating the interaction effects amongst parameters. As shown in Figure 3.6, the curvature accompanying the change in water to biomass ratio indicates that the change of the ratio has a different effect in different temperature zone. To be more specific, as shown in Figure 3.8, when the temperature is below 525 °C, the interaction between temperature and water to biomass ratio is weak, which means that the change in the water to biomass ratio at a certain temperature will not lead to a dramatic change in the hydrogen yield. However, when the temperature increases, the interaction becomes significant. Specifically, at a temperature higher than 525 °C (in this case 600 °C, 651 °C), the increase in water to biomass ratio may lead to a decrease in hydrogen yield.

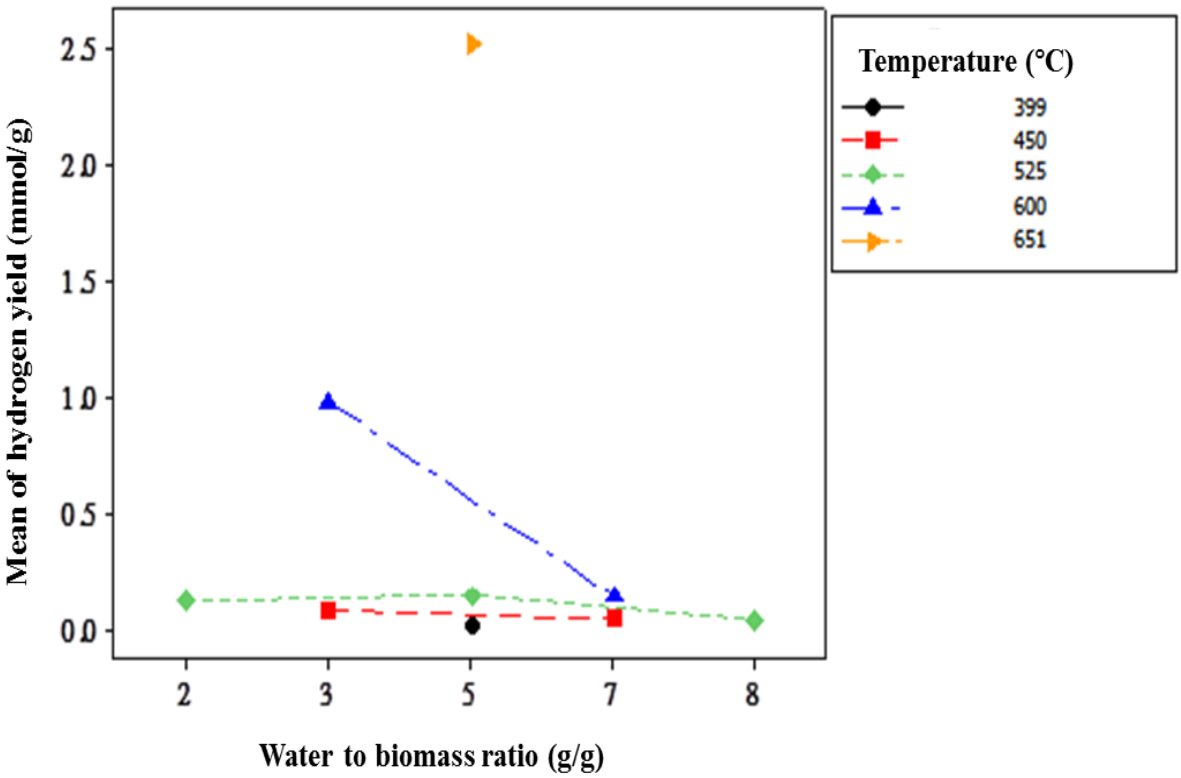

Figure 3.8 Interaction plot for hydrogen yield: temperature vs. water to biomass ratio

The interaction observed here could be because of that at low temperatures, water is needed as a desirable reaction media, which will enhance the hydrolysis of lignin. Whereas at high reaction temperatures, decomposition of lignin is already complete, and the cage effect of water become more significant when overloaded.

What's more, as shown in Figure 3.9, the interaction between temperature and pressure is not significant in this study, which means at a certain temperature, the change in the reaction pressure showed no significant effect on the yield of hydrogen. Therefore, the dramatic decrease in hydrogen yield (from run 14 (0.11 mmol/g) to run 13 (1.01 mmol/g)), can be attributed to the strong interaction between water to biomass ratio and temperature. Whilst the dramatic increase of hydrogen yield (from run 14 to run 5 (1.59 mmol/g)) can be attributed to two reasons: first, the decrease of water to biomass ratio from 7 to 5; second, the increase in temperature by 51 °C, and the increased positive effect of temperature at high temperature zone (above 525 °C).

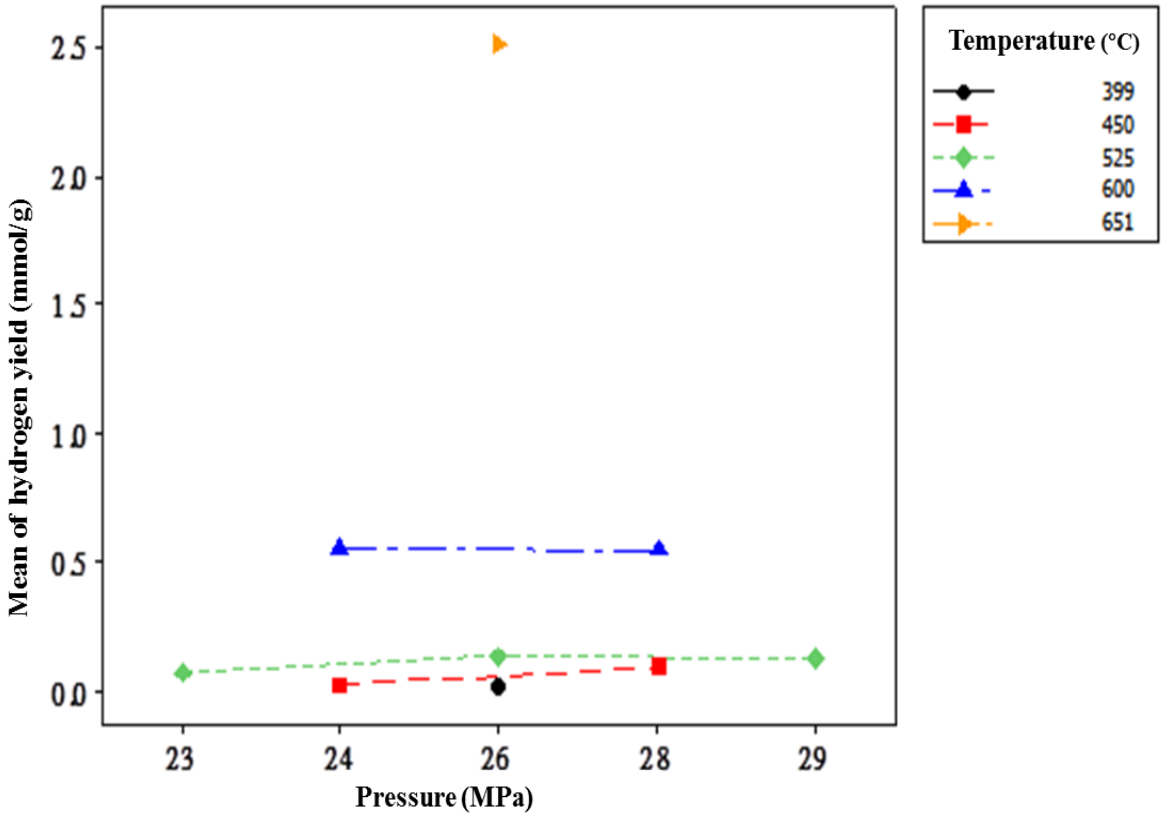

Figure 3.9 Interaction plot for hydrogen yield: temperature vs. pressure

3.5.6 Optimization of operation conditions

The objective of optimizing the reaction condition for non-catalytic gasification of lignin in SCW could be achieved by using the model. To start with, the contour plot (Figure 3.10) can be used to roughly locate the best combination of reaction parameters. The plot indicates that when water to biomass ratio is less than 4 and the temperature is above 620 °C, H_2 yield could be higher than 1.5 mmol/g biomass.

Then, the response optimizer in Minitab software was used to optimize the H_2 yield in a certain range of the reaction parameters. In this case, the following constraints are applied to obtain the best condition for H_2 production: H_2 yield $\geqq$ 1.5 mmol/g. The solution for the operation conditions obtained from the model is as follow: pressure = 25.1 Mpa, temperature = 651.1 °C, and water to biomass ratio = 3.9. To test the validity of the solution, one test run was performed at the predicted operating conditions. As a result, the hydrogen yield was 1.48 mmol/g. As the predicted maximum

hydrogen yield from the model is 1.60 mmol/g, the difference between the experimental result and the model prediction is less than 8%.

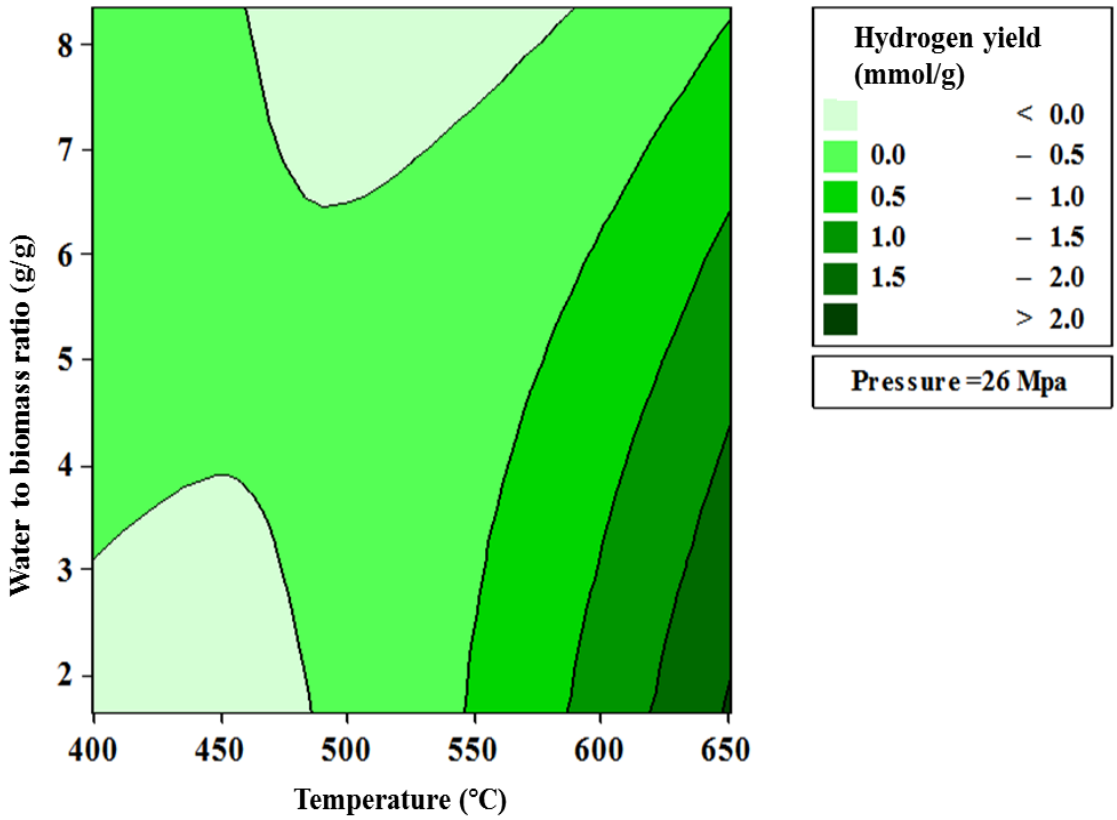

Figure 3.10 Contour plot of hydrogen yield vs. temperature and water to biomass ratio

3.6 Conclusions

In this phase of research, non-catalytic SCWG of lignin was investigated. A batch reactor was used and three parameters were optimized including temperature, pressure and water to biomass ratio. The parameters varied in the range of 399 -651 °C, 23-29 MPa, 3-8, respectively. Subsequently, a statistical model was built using the SCWG test results to determine the optimum operation condition for hydrogen yield. Results from the statistical tests including the R-squared statistics, the test of significance, and the lack-of-fit indicate that the model can be used to explain the experimental data with sufficient accuracy. The main effects of various reaction parameters, as well as the interaction effects amongst parameters, were investigated. The results obtained without the presence of the catalyst will be used as a reference for the following catalytic work in this project.

Chapter 4 Screening and Modification of Ni Based Catalysts for Hydrogen Production from Supercritical Water Gasification of Lignin

This Chapter is based on: Kang, K., Azargohar, R., Dalai, A.K., Wang, H. Systematic screening and modification of Ni based catalysts for hydrogen generation from supercritical water gasification of lignin. *Chemical Engineering Journal*. 283 (2016) 1019-32.

Contributions of authors: KANG: (1) preparing the samples and catalysts (2) performing SCWG tests, (3) performing characterizations for products and catalysts and analysing the experimental data (4) writing the manuscript and provide responses to reviewers' comments. Dr. Ramin Azargohar: (1) reviewing the experimental results, (2) revising the manuscript. Dr. Ajay K. Dalai and Dr. Hui Wang, provided overall supervision of this study, examined the experimental results, oversaw the preparation of the manuscripts, and submitted the paper.

4.1 Knowledge gaps, objectives, and hypothesis

4.1.1 Knowledge gaps

- Systematic comparison and screening Ni based catalysts with different supports and promoters for hydrogen production from SCWG of lignin are missing from the literature.
- Catalyst modification study based on screening work mentioned above will also be important, however, no such work could be found in the literature.

4.1.2 Hypothesis

- Appropriate catalyst components including support and metal promoter for the Ni based catalyst could be identified by catalyst screening.
- Further modification of the catalyst composition, including metal loading and promoter/metal molar ratio could improve the hydrogen yield.

4.1.3 Objectives

- To screen five supports for Ni-based catalysts including Al_2O_3, activated carbon (AC), TiO_2, ZrO_2, and MgO.
- To Screen of three promoters for Ni-based catalysts including Co, Cu, and Ce.
- To further optimization of the catalyst composition regarding Ni loading and promoter/Ni molar ratio.

4.2 Abstract

In this phase of research, systematic screening of 29 catalysts synthesized using five supports: Al_2O_3, activated carbon (AC), TiO_2, ZrO_2, MgO, and three promoters: Co, Cu, Ce (with two different Ce precursors) was performed. Then, the optimization of the Ni-Ce/Al_2O_3 catalyst was carried out by varying Ni loading (four levels) and Ce/Ni molar ratio (two levels). All these catalysts were screened for supercritical water gasification (SCWG) of lignin under the operating conditions of 650 °C, 26 MPa and water to biomass mass ratio of 5 in a tubular batch reactor. Various characterization techniques were used to investigate the properties of these catalysts further. As a result, using different supports, the activity of Ni-based catalysts for SCWG of lignin was found in the order of Al_2O_3 > TiO_2 > AC > ZrO_2 > MgO. As the best promoter, Ce enhanced the hydrogen selectivity by promoting the Ni dispersion and weakening the Ni-Al_2O_3 interaction. Use of different precursors for the Ce promoter ($CeCl_3 \cdot 6H_2O$ or $Ce(NO_3)_3 \cdot 6H_2O$) showed no effect on the hydrogen yield. For a fixed Ni loading, hydrogen yield increased with an increase in Ce/Ni molar ratio. The 20Ni-0.36Ce/Al_2O_3 catalyst showed highest hydrogen yield of 2.15 mmol/g, which is 35% greater than that for the non-catalytic run. The better performance of Ni-Ce/Al_2O_3 catalyst can be attributed to enhanced coke resistance as well as increased reducibility for Ni by the addition of Ce promoter.

4.3 Introduction

Hydrogen is a clean source of various materials for the chemical industry. The traditional area for H_2 utilization including refinery, methanol, and ammonia manufacturing as well as emerging area of interest in Fisher-Tropsch industry, as well as fuel cell application, will increase the demand of hydrogen (Navarro et al. 2009, Chaubey et al. 2013).

Supercritical water gasification (SCWG) of biomass is considered a promising technology for sustainable hydrogen production, it combines the easy availability of biomass feedstock and the unique properties of water in its supercritical phase (Temperature ≥ 373 °C, Pressure ≥ 22.1 MPa). SCWG can give more gas yield at a relatively lower range of temperature. Accelerated hydrolysis of biomass in SCW can boost the decomposition of the polymeric structure of biomass.

It is well established that lignin, together with cellulose and hemicellulose, are three mother precursors of lignocellulosic biomass (Zakzeski et al. 2010). And its chemical structure indicates that it has high potential to be the source of various valuable chemicals using proper decomposition

and upgrading techniques. However, the cross-linked polymeric structure significantly increases the recalcitrance of lignin to different chemical reactions and make it the most difficult part of biomass conversion (Bulushev and Ross 2011). Thus, although the efforts of lignin conversion into various chemicals and fuels are scattered in the open literature, commercialization is hardly achieved (Raguskas et al. 2014). For biomass SCWG process, the effects of critical reaction parameters such as temperature, pressure as well as water to biomass ratio were studied in the absence of the catalyst, on the yield of the process (Kang et al. 2015, Resende et al. 2008).

Use of catalysts is crucial for lignin conversion (Zakzeski et al. 2010). First, in SCWG, high specific heat of water, as well as the high-pressure demand, will greatly increase the cost of construction, operation as well as maintenance of the SCW reactor, so it is crucial to reduce the temperature needed in this process that could be achieved by using catalysts (Azadi, Afif, et al. 2012). Second, the structural complexity of lignin will obviously render the gasification efficiency. Therefore, an effective catalyst with high activity as well as H_2 selectivity is of great importance to reach desirable H_2 yield under mild operating conditions in SCW (Lu, Li, and Guo 2014).

Various catalysts have been tested for SCWG of biomass, yet most of them came directly from or developed based on catalysts used in industry (Azadi and Farnood 2011). Recently, there is a trend of research focus shifting to the heterogeneous catalyst, due to their advantages in selectivity, recyclability and environmental friendliness (Guo et al. 2010). Regarding the heterogeneous category, it could be divided as activated carbon (AC) catalysts, transition metal catalysts, and metal oxides. To be more specific, transition metal catalysts can be further split into two categories namely: Ni catalysts and novel metal catalysts. Indeed, many researchers have reached promising results from novel metal catalysts that use metals such as Ru, Rh, Pt, and Pb for SCWG process (Byrd, Pant, and Gupta 2008, Lu et al. 2006), but these catalysts may not beat Ni catalysts in the long term perspective for first, the relatively low cost, second, the comparable activity. Above all, modification of Ni catalysts may provide a cost-effective solution for the SCWG of biomass.

Above all, there are still gaps in the current body of knowledge, which could be briefly summarized as: first, although different catalysts have been tested for SCWG of lignin, a systematic comparison, and screening of these catalysts, especially Ni based catalysts with different supports and promoters, are missing from the literature. Second, limited catalyst screening work found in this area are done by means of simpler biomass model compounds, e.g., glucose (Zhang, Champagne,

and Xu 2011). However, catalysts working for glucose may not work for lignin due to its structural complexity. Additionally, catalyst modification study based on screening work mentioned above will also be important since most of the previous studies focused on the identification of useful catalysts.

To fulfill the knowledge gaps as identified above, in this study: 1) screening of five supports for Ni-based catalysts such as Al_2O_3, activated carbon (AC), TiO_2, ZrO_2 and MgO, 2) screening of three promoters for Ni-based catalysts including Co, Cu and Ce, and 3) further optimization of the catalyst recipe in terms of Ni loading and promoter/Ni molar ratio were carried out. The uniqueness of this study lies in: first, this is a systematic study for SCWG experiments to test the catalyst activity and hydrogen production as well as various characterizations to relate their properties to their performances. Second, by covering a broad range of materials, this study is also significant in its comprehensiveness and should be valuable for future work in this area. Third, since the catalysts evaluated are for SCWG of lignin, which is the toughest ingredient from biomass, the data presented in this study should also be valuable for developing an effective catalyst for biomass SCWG.

4.4 Experimental section

4.4.1 Catalyst preparation

Impregnation method was applied for the development of the catalysts studied in this research. Precursors for active metal or promoters for the impregnation were water–soluble metal salts including $Ni(NO_3)_2 \cdot 6H_2O$, $Cu(NO_3)_2 \cdot 2.5H_2O$, $Co(NO_3)_2 \cdot 6H_2O$, $CeCl_3 \cdot 6H_2O$, $Ce(NO_3)_3 \cdot 6H_2O$ all supplied by Sigma-Aldrich (Oakville, ON, CANADA). Catalyst supports used in this study including Al_2O_3, TiO_2, ZrO_2, and MgO were supplied by Alpha Aesar (Ward Hill, USA). The activated carbon (AC) support used in this study was previously prepared by this research group (Azargohar and Dalai 2005).

Regarding the synthesis procedure, the amount of precursors used was pre-calculated based on the composition of the catalyst. First, the precursor was dissolved in water. Then, a 1-mL syringe was used to impregnate the metal solution onto the support. Before calcination, the catalyst was equilibrated for two hours and then, dried in an oven at 105 ^oC for eight hours. The dried catalyst (except Ni/AC) was then calcined in flowing air at 650 ^oC for four hours. The calcination of Ni/AC catalyst was performed in the nitrogen atmosphere at 650 ^oC for four hours.

4.4.2 Material, SCW reactor, and test procedure

Lignin sample was commercial chemical obtained from Sigma-Aldrich (Oakville, ON, CANADA). A batch type SCW reactor was used for performing all the SCWG tests, which has been described in detail in last chapter. In this phase of research, for each catalytic SCWG test, 0.65 g lignin and 0.65 g of catalyst were fed to the reactor together with 3.25 g of water (no catalyst for the blank experiment). All the experiments are performed under the SCW conditions of 26MPa, 650 °C. The water to biomass ratio was maintained at five for all tests. The procedure for experiments as well as production collection could be referred to the description in Chapter 3.

4.4.3 Catalyst characterization

For calcined fresh catalysts, the wide-angle powder X-ray diffraction (XRD) analysis was conducted by a Rigaku diffractometer using CuKα radiation in the scanning range of 10–90 degree. The BET surface area, pore volume, and pore size of the catalysts were measured using a Micromeritics ASAP 2000 physisorption system via low-temperature N_2 adsorption–desorption isotherms. The CO adsorption of the fresh catalyst (~ 0.1 g) was measured using the Micromeritics ASAP 2020 chemisorption equipment. H_2-temperature programmed reduction (H_2-TPR) of the fresh catalysts was performed using TPD/TPR-2720 Micromeritics (USA) instrument (Badoga et al. 2012).

For spent catalysts, the carbon formation on the spent catalysts was investigated by TG/DTG (thermogravimetry/derivative thermogravimetry) analysis using a TGA Q500 Thermogravimetric Analyzer supplied by TA Instruments (New Castle, USA). For each test, 10 - 20 mg sample was used. The runs were performed in the air atmosphere (60 mL/min). Sample heating was from room temperature to 800 °C at a ramp rate of 10 °C/min and kept at 800 °C for 10 min.

4.4.4 Characterization of supercritical water gasification products

Analysis of the gas phase products was performed using Agilent GC 7890A gas chromatograph. Helium was used as carrier gas, and column pressure was maintained at 22 kPa. Compounds were separated following a linear temperature program of 50-280 °C (10 °C /min) and then at 280 °C for 10 min. The run time in total was 40.5 min.

To calculate the weight of each component in the gas phase products, the molar amount of N_2 gas was used as a reference. Specifically, the molar amount of N_2 used to pressurize the reactor before each run could be calculated based on the initial pressure and volume of the reactor. Then,

according to the molar ratio of each gas component to N_2, the molar amount of the component was calculated. Finally, the weight of each gas component was calculated using the molar amount and molecular weight of each component.

Fourier transform infrared spectroscopy (FT-IR) analysis of the SCWG char was performed using a Spectrum GX FTIR spectrometer (PerkinElmer Inc., USA) using KBr technique, within the range of 400-4000 cm^{-1} under transmittance mode and 16 accumulations applied for a single acquisition. The elemental composition of char product was analyzed by an "Elementar Vario III" elemental analyzer. Through high-temperature decomposition, solid products are converted into gasses through combustion. 4 to 6 mg sample was used for each analysis.

4.4.5 Data interpretation

For the results from SCWG tests, the definitions of the hydrogen and gas yield, and hydrogen selectivity reported here were given in the last phase. For the composition of catalysts, the numbers of (2.5, 5, 10, and 20) before Ni indicates the weight percentage of Ni with respect to the weight of the catalyst support. The number before the promoter (Ce, Co, Cu) indicates the specific molar ratio of the promoter to Ni. As an example, 5Ni-0.36Ce/Al_2O_3 has 5 wt% Ni and a Ce to Ni molar ratio of 0.36, and Al_2O_3 is the support. Based on the number of repeats for each experiment, the average value of each parameter (such as H_2 selectivity) is calculated and the standard deviation given shows the largest difference of experimental values from this average value.

4.5 Results and discussion

4.5.1 Screening of different supports

4.5.1.1 Results of SCWG tests and catalyst characterization

Supporting material is crucial for the heterogeneous catalyst used in SCWG considering the high temperature and pressure employed in the process. The first step of this study was to identify useful supports for hydrogen generation from SCWG of lignin. In this study, in total five supports including Al_2O_3, AC, MgO, TiO_2, and ZrO_2 were used in the catalyst structure.

The results of SCWG tests and BET analysis of catalysts using different supports are given in Table 4.1. In the case of 10 wt% Ni loading group, 10Ni/TiO_2 showed higher hydrogen yield (1.83 mmol/g), followed by 10Ni/Al_2O_3 and 10Ni/AC, which produced 1.64 mmol/g and 1.47 mmol/g H_2, respectively. While regarding gas yield, Ni catalyst supported by Al_2O_3 showed the best

activity (16.8 wt%), followed by AC (14.4 wt%) and TiO_2 (13.7 wt%). Specifically, the effectiveness of the supports regarding gas yield are in the order of Al_2O_3 > AC > TiO_2 > ZrO_2 > MgO. As is shown in Table 1, the BET surface area decreased in the order of AC > Al_2O_3 > MgO > TiO_2 > ZrO_2. Additionally, with different Ni loading of 10 and 20 wt% on TiO_2, similar gas yield was observed.

Table 4.1 Surface property of Ni catalysts with different supports and their effects on gas yield, hydrogen yield, and hydrogen selectivity

	BET surface area (m^2/g)	Total pore volume (cm^3/g)	Pore size (nm)	Gas yield (wt%)	H_2 yield (mmol/g)	H_2 selectivity
No-catalyst	-	-	-	16.1 ± 0.3	1.59 ± 0.04	0.31± 0.01
10Ni/Al_2O_3	230	0.65	8	16.8 ± 0.3	1.64 ± 0.07	0.44 ± 0.00
10Ni/AC	474	0.34	5	14.4 ± 0.3	1.47 ± 0.08	0.75 ± 0.02
10Ni/MgO	41	0.21	20	2.7 ± 0.1	0.36 ± 0.11	0.56 ± 0.01
10Ni/TiO_2	11	0.03	19	13.7 ± 0.7	1.83 ± 0.06	0.58 ± 002
20Ni/TiO_2	-	-	-	13.7 ± 0.5	1.78 ± 0.09	0.75 ± 0.04
10Ni/ZrO_2	9	0.02	13	7.7 ± 0.5	0.72 ± 0.06	0.52 ± 0.02

The XRD patterns of 10Ni catalysts with different supports are given in Figure 4.1. The Figure indicates that in fresh catalysts NiO is evident from peaks with 2Θ values of 37°, 43°, 62.5°. The presence of the small variance of peak locations amongst different catalysts could be attributed to the difference in interactions between Ni and the support material (Lu et al. 2014).

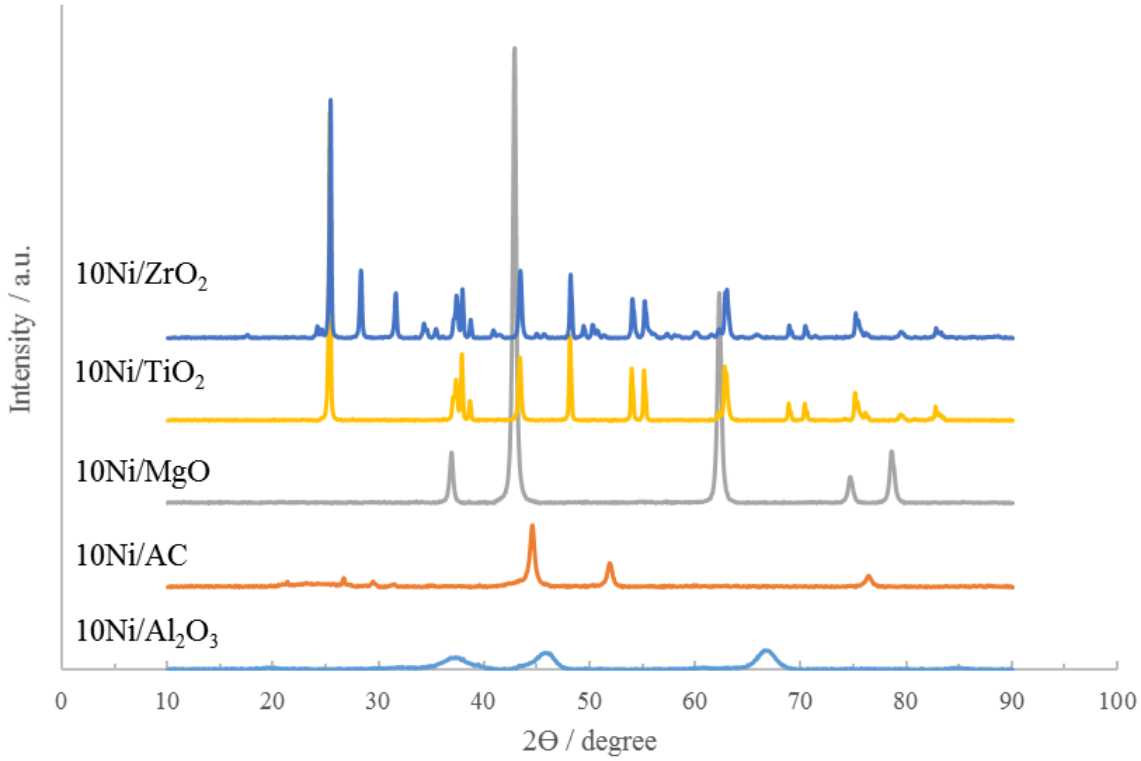

Figure 4.1 XRD patterns of 10Ni catalyst with different supports

4.5.1.2 Discussion on the effects of different supports

Al_2O_3 is the most commonly used catalyst support for steam reforming of methane (Yung, Jablonski, and Magrini-Bair 2009). Activated carbon (AC) was reported to catalyze water gas shift reaction and to promote the carbon gasification efficiency of glucose in the temperature range of 575 °C to 725 °C (Lee and Ihm 2008). MgO supported Ni catalyst with 10 wt% Ni loading is reported to show the best performance in SCWG of lignin at 400 °C, with a 30 mol% carbon yield (Furusawa et al. 2007). TiO_2 supported Ru catalyst showed stable activity in SCWG of lignin at 400 °C (Osada, Sato, Arai, et al. 2006). ZrO_2 was also reported to be stable in SCWG of p-cresol at 350 °C and 17-23 MPa (Elliott, Sealock Jr, and Baker 1993). Above all, they were all reported as potential candidates for catalyst supports in SCWG.

In this study, they performed quite differently with Ni loading of 10 wt%; catalytic activity was found to increase with an increase in the surface area, but the trend was not observed in this study. Specifically, although AC has the highest surface area of 474 m^2/g, 10Ni/AC showed lower activity than that of 10Ni/Al_2O_3 having a surface area of 230 m^2/g. A similar difference in activity

was also observed in a previous research (Zhang, Champagne, and Xu 2011), where the lower activity of Ni/AC catalyst than Ni/γ-Al_2O_3 in SCWG of glucose is attributed to lower dispersion of Ni on the AC support. Other factors which might reduce the activity of Ni/AC catalyst include the coke formation on the metallic surface, as well as sintering of Ni in SCW (Lee 2011).

The lowest activity in this study is given by 10Ni/MgO catalyst, with the gas yield of 2.7 wt%. The failure of this catalyst could be explained using the poor dispersion of Ni on MgO support. This is evident in the XRD patterns in Figure 4.1, as with the same Ni loading of 10 wt%, the intensity of NiO peaks at 2Θ of 43° and 62.5° in the case of 10Ni/MgO is significantly higher than in regard to other catalysts studied. Also, according to the literature, one disadvantage of using MgO support for SCWG process is the phase change of MgO into $Mg(OH)_2$ under SCWG operating conditions (Li et al. 2013).

Two parameters such as gas yield and hydrogen selectivity determine the hydrogen yield. The gas yield reflects catalyst activity, as, by definition, it is directly proportional to the mass of lignin conversion into the gas phase. As such, although 10Ni/TiO_2 showed higher hydrogen yield (1.83 mmol/g) than 10Ni/Al_2O_3 (1.64 mmol/g), Ni/Al_2O_3 was considered as the best performer as the gas yield of 10Ni/Al_2O_3 (16.8 wt%) was higher than that of 10Ni/TiO_2 (13.7 wt%). Both 10Ni/TiO_2 and 10Ni/ZrO_2 showed moderate activity in this study. As they are reported to be stable in SCW, further evaluation of these catalysts with promoters was performed and reported in the next section.

Above all, it is concluded that for SCWG of lignin, the high surface area is beneficial but the highest surface area may not lead to highest catalytic activity. Other properties of the catalyst such as metal dispersion, metal particle size as well as metal-support interaction might have more significant influence.

4.5.2 Screening of different promoters

4.5.2.1 Results of SCWG tests and catalyst characterization

Promoter, even with a small quantity, may bring in high activity, selectivity, or stability (Richardson 1989). In this study, in total three promoters such as Ce, Cu, and Co were investigated. Specifically, Ce was reported as a useful promoter for Ni-Ce/ZrO_2 catalyst for H_2 production from methane steam reforming (Roh et al. 2002), as well for Ni-Ce/Al_2O_3 catalyst used for CO_2 reforming of methane (Wang and Lu 1998a). Also, another study showed that in SCWG of glucose, use of Ce as a promoter in Ni/γ-Al_2O_3 enhanced both the activity and selectivity of the catalyst (Lu

et al. 2010). Cu as a promoter of Ni/γ-Al_2O_3 catalyst is reported to have two functions in SCWG of glucose: one is to promote the methane steam reforming reaction resulting in enhanced hydrogen yield, the other is that to some degree it may prevent Ni from sintering in SCW (Li et al. 2011). Co-rich Ni-Co/Al_2O_3 was proved to be effective for dry reforming of methane, as Co is highly active for the decomposition of methane (San-José-Alonso et al. 2009).

To compare the performances of different promoters, SCWG tests of corresponding Ni-based catalysts were performed, the results are given in Table 4.2. As the results indicate, the effectiveness of various promoters regarding hydrogen yield was in the sequence of Ce (1.65 mmol/g) > Co (0.97 mmol/g) > Cu (0.81 mmol/g) with Ni loading of 10 wt%, and promoter/metal molar ratio 0.1. Interestingly, compared to the no-promoter catalyst, use of promoter did not increase the gas yield. However, it promoted the production of hydrogen by increase the hydrogen selectivity, e.g., hydrogen selectivity of 10Ni-0.1Ce/Al_2O_3 and non-catalytic run was 0.63 and 0.44, respectively. Specifically, the order of hydrogen selectivity is: Ce (0.63) = Co (0.63) > Cu (0.53).

Table 4.2 Effects of Ni catalyst with different promoters on gas yield, hydrogen yield, and hydrogen selectivity

	Gas yield (wt%)	H_2 yield (mmol/g)	H_2 selectivity
10Ni/Al_2O_3	16.8 ± 0.3	1.64 ± 0.07	0.44 ± 0.00
10Ni-0.1Ce/Al_2O_3	13.5 ± 0.4	1.65 ± 0.07	0.63 ± 0.04
10Ni-0.1Cu/Al_2O_3	8.9 ± 0.3	0.81 ± 0.02	0.53 ± 0.04
10Ni-0.1Co/Al_2O_3	9.5 ± 0.2	0.97 ± 0.09	0.63 ± 0.01
10Ni-0.1Ce/TiO_2	12.2 ± 0.7	1.94 ± 0.10	0.82 ± 0.01
20Ni-0.1Ce/TiO_2	12.1 ± 0.5	1.49 ± 0.09	0.68 ± 0.01
10Ni-0.1Ce/ZrO_2	14.0 ± 0.3	1.16 ± 0.04	0.36 ± 0.02
20Ni-0.1Ce/ZrO_2	13.9 ± 0.7	1.58 ± 0.13	0.59 ± 0.01

What should be clarified here is that to maintain the consistency of operating conditions, fixed amount (3.25g) of water was used for both non-catalytic test and catalytic tests, however, considering the limited volume of the SCW reactor (~6ml), and the fact that to a certain amount, higher water density is beneficial for lignin decomposition in SCW (Osada, Sato, Watanabe, et al. 2006). The contact between SCW and the biomass might be better in the case of the non-catalytic test.

In this phase, 10Ni-Ce/TiO_2 and 10Ni-Ce/ZrO_2 were also tested to evaluate the effect of Ce promoter on these catalysts. The results are given in Table 4.2. As observed, the 10Ni-0.1Ce/TiO_2,

in comparison with 10Ni/TiO_2 (Table 4.1) showed higher hydrogen selectivity (0.82 vs. 0.58), but with similar gas yield (12.2 wt% vs. 13.7 wt%). The effect of Ce addition to ZrO_2 support also showed that the gas yield significantly increased, e.g., from 7.73 wt% for 10Ni/ZrO_2 to 13.95 wt% for 10Ni-0.1Ce/Al_2O_3. As another trend, for the same Ce/Ni ratio, following an increase in Ni loading to 20 wt%, gas yield showed no significant change for both TiO_2 and ZrO_2 supported catalysts.

4.5.2.2 Discussion on the effects of different promoters

It is reported that Ce has a high capacity for oxygen storage so that it can store or release a lot of active oxygen species during SCWG process (Roh et al. 2002). Moreover, the oxidative property may lead to inhibition of carbon deposition as the active oxygen-containing species react with carbon deposits on the catalyst (Wang and Lu 1998a, Lu et al. 2010). It was also reported that the addition of Ce weakens the interaction between Ni and the catalyst support, which in turn leads to higher reducibility as well as Ni dispersion (Wang and Lu 1998a). Another benefit of using Ce as a promoter, which is of particular importance for Ni/γ-Al_2O_3 catalyst, is that the presence of Ce may prevent the phase change of Al_2O_3 support from γ to α phase due to shifting towards higher temperature in SCWG (Morterra, Bolis, and Magnacca 1996).

The beneficial effect of Cu and Co as promoters is less pronounced in this study. Regarding Co, one possible reason is that the Ni loading of 10 wt% is too high. Specifically, as was pointed out in a recent research, for the Ni-Co/ZrO_2 catalyst used in dry reforming of methane, to maintain long-term activity and prevent carbon deposition, one essential condition is that Ni and Co particles must be finely dispersed, which cannot be achieved when Ni and Co loading in total exceeds 6 wt% (Djinović et al. 2012). Regarding Cu, the reason might be its inactivity in C—C bond cleavage (Zhang, Champagne, and Xu 2011). Above all, Ce is considered a better promoter for Ni/Al_2O_3 catalyst used for SCWG of lignin, more detailed discussion is covered in the following section.

4.5.3 Optimization of Ni-Ce/Al_2O_3 catalyst composition

The third step of this study was to optimize the recipe of the Ni-Ce/Al_2O_3 catalyst. In total five Ni metal loading including 2.5, 5, 10 and 20 wt% with two Ce/Ni molar ratio of 0.1 and 0.36 were tested. Also, the effect of 2 different precursors for Ce promoter including $CeCl_3 \cdot 6H_2O$ and $Ce(NO_3)_3 \cdot 6H_2O$ were examined. Using SCWG tests and catalyst characterization the roles of Ni

and Ce as well as their interaction with the Al_2O_3 promoters were investigated. The results of SCWG tests are summarized in Table 4.3.

4. 5.3.1 Effect of Ni metal loading

As given in Table 4.3, Al_2O_3 is not active for lignin SCWG as it gives similar hydrogen yield as the blank run (1.50 mmol/g vs. 1.59 mmol/g). Also, without the presence of Ce, the hydrogen yield was in the order of 10Ni > 5Ni > 20Ni > 2.5Ni. Specifically, the highest hydrogen yield was given by $10Ni/Al_2O_3$. It was 1.64 mmol/g that was about five times greater than that of the $2.5Ni/AL_2O_3$ (0.26 mmol/g). Although the hydrogen selectivity of these two catalysts is comparable (0.44 vs. 0.51), the gas yield of $10Ni/Al_2O_3$ (16.8 wt%) was significantly higher than that of the $2.5Ni/Al_2O_3$ (3.21 wt%). Also, as shown in Figure 4.3, within each Ni loading group, without Ce, the hydrogen yield was lower than Ce promoted catalysts. Another trend is that when Ce is added, the average hydrogen yield increased with Ni loading.

Table 4.3 Effects of Ni loading and Ce/Ni molar ratio on gas yield, hydrogen yield, and hydrogen selectivity

Catalyst	Ni loading (wt%)	Ce/Ni molar ratio	Gas yield (wt%)	H_2 yield (mmol/g)	H_2 selectivity
Control group					
No-catalyst	0	0	16.1 ± 0.3	1.59 ± 0.04	0.31 ± 0.01
Al_2O_3	0	0	8.4 ± 0.1	1.5 ± 0.06	1.00 ± 0.02
0.1Ce/Al_2O_3(10Ni)	0	0.1	10.8 ± 0.3	1.47 ± 0.05	0.69 ± 0.02
0.36Ce/Al_2O_3(10Ni)	0	0.36	9.7 ± 0.1	1.13 ± 0.06	0.60 ± 0.02
Experimental group					
2.5Ni/Al_2O_3	2.5	0	3.2 ± 0.1	0.26 ± 0.01	0.51 ± 0.01
2.5Ni-0.1Ce/Al_2O_3	2.5	0.1	14.9 ± 0.7	1.34 ± 0.07	0.37 ± 0.01
2.5Ni-0.36Ce/Al_2O_3	2.5	0.36	10.4 ± 0.2	1.57 ± 0.05	0.86 ± 0.02
5Ni/Al_2O_3	5	0	6.9 ± 0.3	0.91 ± 0.05	0.63 ± 0.02
5Ni-0.1Ce/Al_2O_3	5	0.1	11.0 ± 0.3	1.90 ± 0.07	1.09 ± 0.03
5Ni-0.36Ce/Al_2O_3	5	0.36	14.3 ± 0.4	2.11 ± 0.08	0.67 ± 0.02
10Ni/Al_2O_3	10	0	16.8 ± 0.3	1.64 ± 0.07	0.44 ± 0.00
10Ni-0.1Ce/Al_2O_3	10	0.1	13.5 ± 0.4	1.65 ± 0.07	0.63 ± 0.03
10Ni-0.36Ce/Al_2O_3	10	0.36	11.0 ± 0.2	1.86 ± 0.06	0.86 ± 0.03
20Ni/Al_2O_3	20	0	8.2 ± 0.2	0.78 ± 0.03	0.59 ± 0.01
20Ni-0.1Ce/Al_2O_3	20	0.1	14.6 ± 0.5	2.10 ± 0.07	0.77 ± 0.02
20Ni-0.36Ce/Al_2O_3	20	0.36	12.9 ± 0.1	2.15 ± 0.04	0.95 ± 0.03
Different precursors for Ce					
10Ni-0.1Ce/Al_2O_3-2	10	0.1	11.1 ± 0.1	1.71 ± 0.04	0.77 ± 0.02
10Ni-0.36Ce/Al_2O_3-2	10	0.36	10.7 ± 0.3	1.82 ± 0.06	0.75 ± 0.02

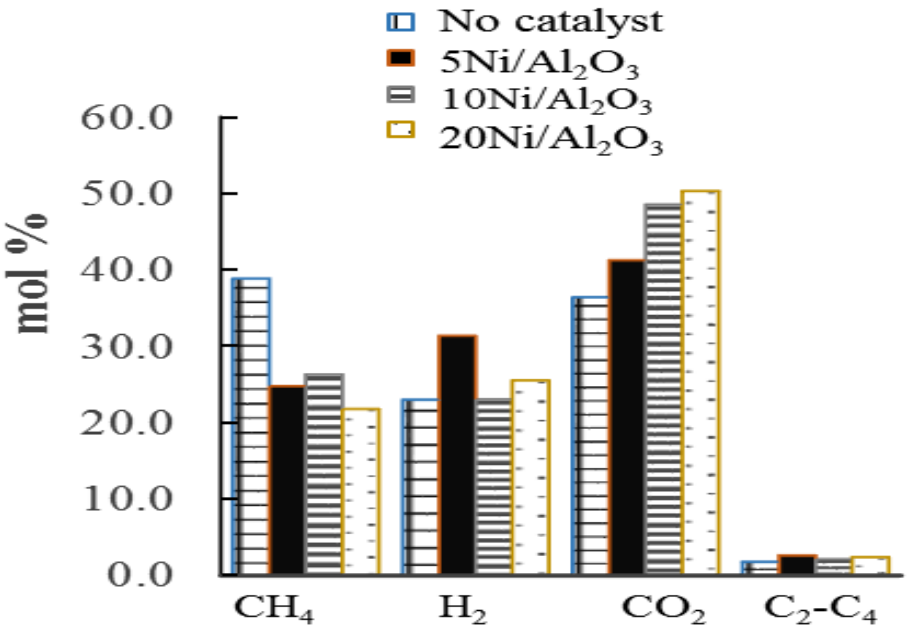

Figure 4.2 Effect of Ni loading on gas composition

The effect of Ni loading (without Ce) on gas composition is shown in Figure 4.2. First, $5Ni/Al_2O_3$ catalyst produced gas with a slightly higher percentage of hydrogen. Second, compared to non-catalytic runs, the use of Ni/Al_2O_3 reduced the proportion of CH_4 in the product gas. However, as a more obvious trend, when the loading of Ni increased, the percentage of CO_2 increased significantly and exceeded 50% with $20Ni/Al_2O_3$.

It is well established that Ni catalyst is active for various reactions in the SCWG process including tar cracking, water-gas shift reaction, as well as methanation reaction (Resende and Savage 2010). However, Ni catalysts are prone to carbon deposition (Fang 2014) and suffer from other problems such as sintering and support decomposition in SCW (Li et al. 2011). Lower Ni loading (e.g., 2.5 wt%) did not show promising gas yield which might only because of the lack of the active component. The failure of higher Ni loading (e.g., 20 wt%), however, could be attributed to two reasons. One is the relatively poorer Ni dispersion caused by the high loading. The other is the change in Ni morphology as was confirmed by the XRD patterns in Figure 4.3.

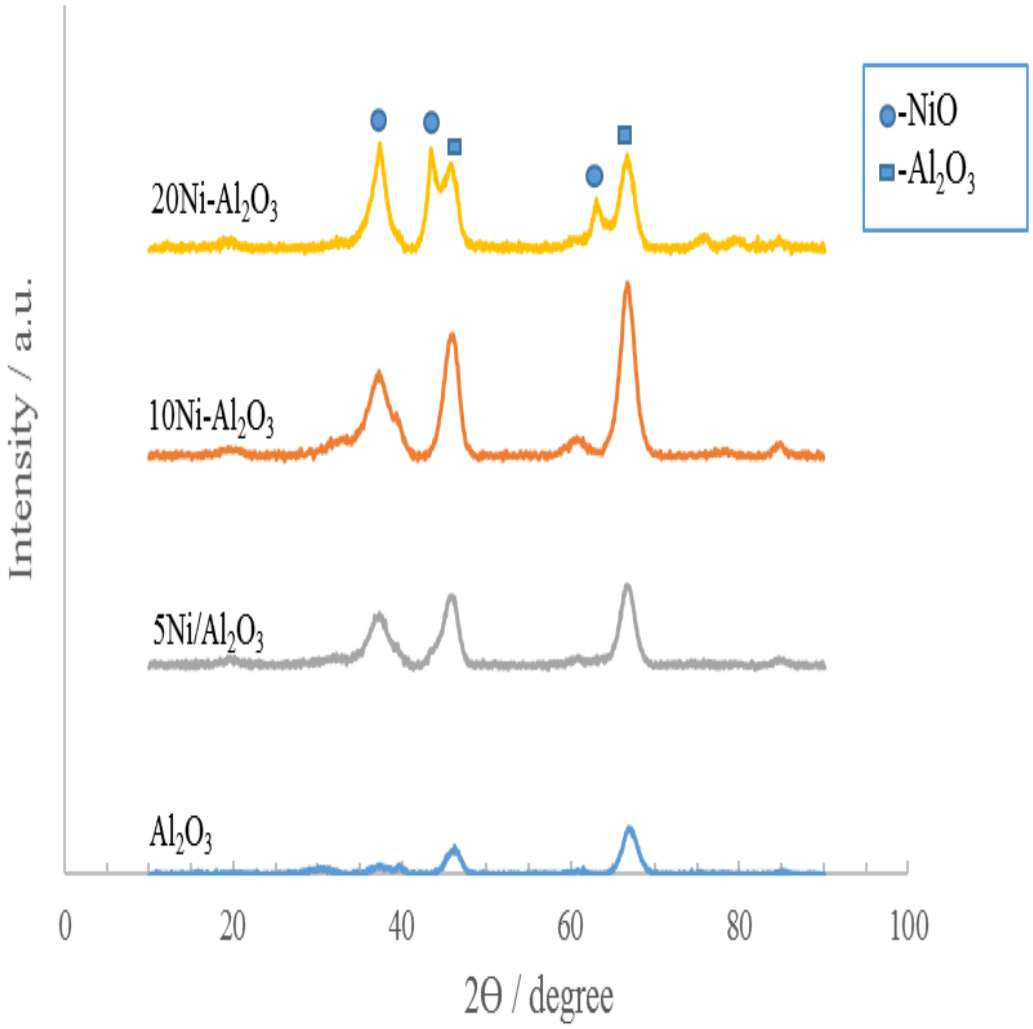

Figure 4.3 XRD patterns of Ni/Al_2O_3 catalyst with different Ni loadings

Specifically, although some of the peaks of γ-Al_2O_3 (46° and 66.7°) and NiO (37°, 43°, and 62.5°) are broad and overlapped. With an increase in Ni loading from 5 to 10 wt%, the peak intensity increased significantly, indicating that NiO became more detectable. Further, when Ni loading increases to 20 wt%, two new peaks appear at 2Θ degrees of 43.7° and 63.3°, which also belong to NiO (Chen and Ren 1994). However, since metallic Ni was reported to be the only active form in SCWG, increase in NiO, which is not active in SCWG (Azadi and Farnood 2011), may have a negative effect on the catalytic activity depending on the particular species. Additionally, the result also indicates that different species of nickel oxide may exist in the catalysts, which is reported by a previous study (Kumar, Sun, and Idem 2008), a more detailed discussion will be offered later.

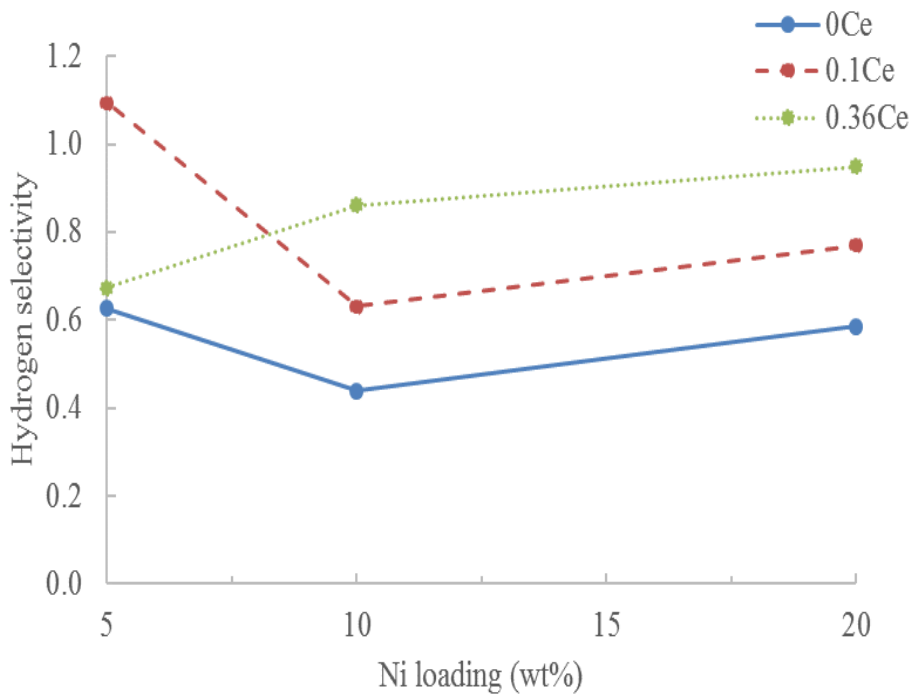

Figure 4.4 Effect of Ce/Ni molar ratio on hydrogen selectivity

Based on above, we conclude that Ni/Al_2O_3 is active for hydrogen production from lignin SCWG. A certain amount of Ni is needed to enhance the gas yield, however, increase in Ni loading have a tendency to decrease CH_4 but increase the CO_2 proportion in the product gas. Without the promoter, Ni loading 10 wt% performed best in this study.

4.5.3.2 Effect of Ce/Ni molar ratio

As given in Table 4.3, adding Ce to Al_2O_3 without Ni did not increase the hydrogen yield. Moreover, the addition of Ce showed different effects with different Ni loading. Specifically, it is clear from Figure 4.4 that when Ni loading was 10 or 20 wt%, the hydrogen selectivity increased significantly with the increase in Ce/Ni ratio, however, when Ni loading was 5 wt%, Ce/Ni molar ratio of 0.1 showed maximum hydrogen selectivity of 1.09. This observation probably indicates that there is an interaction effect between Ni loading and Ce/Ni ratio. As shown in Figure 4.5, it is evident that within each Ni loading group, when Ce/Ni molar ratio increased from 0.1 to 0.36, the hydrogen yield showed an only limited increase. It can be concluded: Ce addition mainly enhances the H_2 selectivity, but not the gas yield.

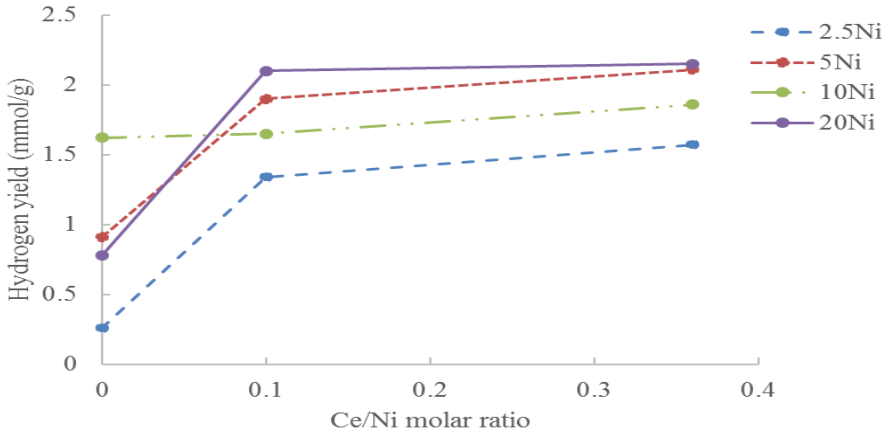

Figure 4.5 Effect of Ni loading and Ce/Ni molar ratio on hydrogen yield

A clear picture of the effect of Ce on the gas composition is given in Figure 4.6. For both 5Ni (Figure 4.6.a) and 20Ni (Figure 4.6.b) catalysts, with Ce, the hydrogen percentage was always higher. However, the trends showing in 5Ni and 20Ni are different. Specifically, for the 5Ni group, with an increase in Ce/Ni molar ratio, the hydrogen proportion increased then decreased, the optimum value was observed at Ce/Ni molar ratio of 0.1. Differently, in the 20Ni group, with an increase in Ce/Ni molar ratio to 0.36, the share of hydrogen increased consistently. It suggests that higher Ce/Ni molar ratio might be needed for optimum hydrogen yield when Ni loading is high (e.g., 20 wt%).

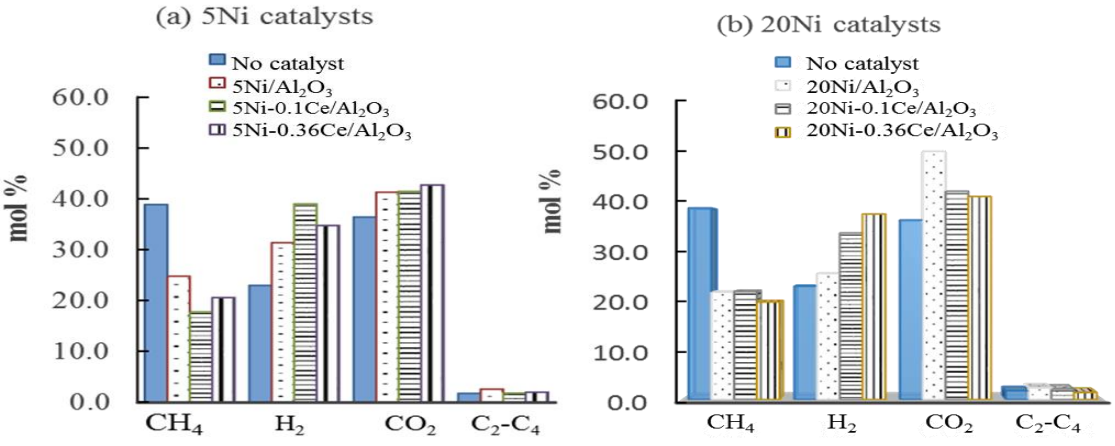

Figure 4.6 Effect of Ce/Ni molar ratio on gas composition

Based on the discussion above, another reasonable thought is that as a promoter, the primary role of Ce is to enhance the hydrogen selectivity, and there is one optimum Ce ratio corresponding to any specific Ni loading that can result in the highest H_2 yield.

4.5.3.3 Effect of different precursors for Ce promoter

In this study, the performance of 10Ni-Ce/Al_2O_3 catalysts with the various precursors for Ce ($CeCl_3 \cdot 6H_2O$) is also evaluated. The results are listed in Table 3, where they were denoted by 10Ni-0.1Ce/Al_2O_3-2 and 10Ni-0.36Ce/Al_2O_3-2. The reason is that a previous study in this research group used similar precursor ($CeCl_3$) for Ni-Ce/AL_2O_3 for SCWG of pinewood and cellulose (Ding et al. 2014). The most commonly used precursor in other studies is $Ce(NO_3)_3 \cdot 6H_2O$ (Zhang, Champagne, and Xu 2011). However, use of different precursors may change the performance of the catalyst. One reason is that introduction of Cl ions to Ni/Al_2O_3 may alter the acidity of the catalyst (Richardson 1989). Another reason is that Cl ions may poison the Ni metal as the similar effect was reported on Ru catalyst (Yamaguchi et al. 2008). As is shown in Table 4.3, no significant difference in hydrogen yield was observed by using different precursors of Ce, e.g., 10Ni-0.36Ce/Al_2O_3 (1.86 mmol/g) and 10Ni-0.36Ce/Al_2O_3-2 (1.82 mmol/g). The reason might be that the calcination process removed the Cl ions contained in the precursor at 650 °C.

4.5.4 Characterization of fresh and spent catalysts

To develop an effective catalyst for future application, a better understanding of the Ni-Ce/Al_2O_3 catalyst will be necessary. So, after discussion focusing mainly on SCWG tests, deeper insight into why Ni-Ce/Al_2O_3 showed better performance is provided via the characterization of catalysts and other products. Moreover, a detailed discussion is given for different characterization studies as follow:

4.5.4.1 CO Chemisorption

In this study, CO chemisorption was performed for selected fresh Ni catalyst with different Ce/Ni molar ratios. The results in Table 4.4 indicate that: first, the addition of Ce (Ce/Ni molar ratio 0.36) enhanced the Ni dispersion for both 5Ni/10Ni catalysts, and this effect is more significant with higher Ni loading. Specifically, e.g., with Ce promoter, the Ni dispersion increased from 1.1 % to 6.6 %. Second, with an increase in Ni loading from 5 to 10 wt%, Ni dispersion decreased from 2.6 % to 1.1 %. Also, data in Table 4.4 show that higher dispersion also leads to smaller crystallite size and larger metallic surface area.

Table 4.4 Effect of Ce/Ni molar ratio of metal dispersion

Catalyst	Metal dispersion （%）	Metallic surface area (m^2/g sample)	Metallic surface area (m^2/g metal)	Crystallite size (nm)
5Ni-Al_2O_3	2.6	1.2	19.2	35.9
5Ni-0.36Ce/Al_2O_3	4.3	1.4	28.9	23.3
10Ni-Al_2O_3	1.1	0.8	7.7	88.2
10Ni-0.36Ce/Al_2O_3	6.6	4.4	43.8	15.4

Higher Ni metal dispersion is generally desirable in a sense that finely dispersed Ni particles may have better resistance to sintering (Zhang, Champagne, and Xu 2011). As another advantage, smaller metal particle size, which is normally the result of better dispersion, may enhance the coke resistance of the catalyst (Zhang, Wang, and Dalai 2008). As shown in Table 4.3, although in both cases of 5Ni and 10Ni catalysts, the addition of Ce increased hydrogen yield, the reason is quite different. For example, 5Ni/Al_2O_3 and 5Ni-0.36Ce/Al_2O_3 showed similar hydrogen selectivity (0.63 and 0.67, respectively), but the gas yield doubled when Ce was used (6.9 at % vs. 14.3 wt %). For 10Ni/Al_2O_3 and 10Ni-0.36Ce/Al_2O_3, gas yield reduced but hydrogen selectivity increased significantly from 0.44 to 0.86 mmol/g. Also, it is interesting to observe that with the increase in metal dispersion. The hydrogen selectivity always increased, specifically, as metal dispersion increased in the order of: 10Ni/AL_2O_3 (1.1 %) < 5Ni/Al_2O_3 (2.6 %) < 5Ni-0.36Ce/Al_2O_3 (4.3 %) < 10Ni-0.36Ce/Al_2O_3 (6.6), and their corresponding hydrogen selectivity were: 10Ni/AL_2O_3 (0.44) < 5Ni/Al_2O_3 (0.63) < 5Ni-0.36Ce/Al_2O_3 (0.67) < 10Ni-0.36Ce/Al_2O_3 (0.86).

Thus, in SCWG of lignin, it is hard to correlate Ni metal dispersion to the gas yield, and a similar phenomenon was also observed previously in SCWG of glucose, in which the researchers found that catalyst particle size affected neither gasification efficiency nor gas composition (Azadi, Afif, et al. 2012). However, the difference observed in this study is that higher Ni dispersion leads to higher hydrogen selectivity.

4.5.4.2 H_2 TPR

H_2-TPR study was performed to test the reducibility, as well as Ni species in fresh 5Ni catalysts. As confirmed by a past study, the metallic form Ni is the active phase of the catalyst in SCWG of glucose (Zhang, Champagne, and Xu 2011). Since the considerate amount of hydrogen is produced in the process, the reduction of Ni might happen in-situ automatically. However, since different forms of Ni co-exist in the catalyst, so the reduction temperature of different Ni species, as well as the proportion of these Ni species, plays a major role in the catalytic activity. In this study, as the

reaction temperature was 650 °C, the reduction of Ni species which reduced at low temperature are considered important.

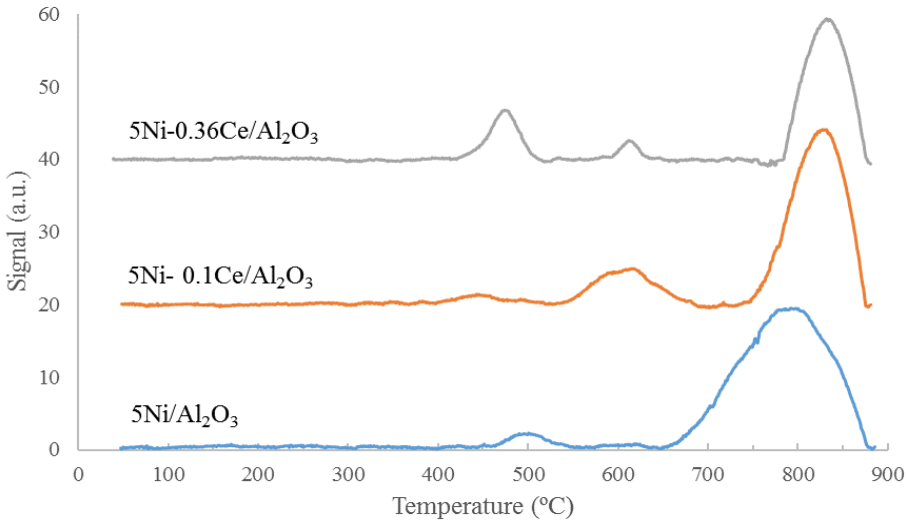

Figure 4.7 TPR profiles of 5Ni-Ce/Al_2O_3 catalysts

The TPR profiles of 5Ni catalysts are given in Figure 4.7. Several reduction peaks appeared in the temperature range of 450 - 840 °C. Specifically, peak positions were: for 5Ni/Al_2O_3, a small peak at 500 °C, followed by a hump at around 600 °C and a huge peak at 780 °C; and for Ce added 5Ni catalysts, a hump at 450 °C (0.1Ce/Ni molar ratio)-a peak at 479 °C (0.36Ce/Ni molar ratio), another peak at 616 °C, and a huge peak at 835 °C. In this study, low-temperature peaks (450 °C, 479 °C) could be assigned to the reduction of surface NiO which has a weak interaction with the support, while the peak appearing at around 500 °C to 700 °C is caused by the reduction of fixed NiO species. The interaction between the fixed NiO and the support is stronger than that of the surface NiO (Dong et al. 2002, Li, Hu, and Hill 2006).

For more details, the surface NiO is described as highly dispersed and amorphous, while the fixed NiO was described as spherical nickel crystallites covered by a shell formed by material like nickel aluminate(Li, Hu, and Hill 2006). The peaks appeared at higher than 700 °C, which is not relevant in this study, could be assigned to the reduction peak of $CeAlO_3$ (Kumar, Sun, and Idem 2008). in Ce promoted catalysts (835 °C), while the peak at 780 °C for 5Ni/Al_2O_3, could be assigned to a spinel phase of Ni^{2+} ions in a diluted form, which could not be identified by XRD characterization (Rynkowski, Paryjczak, and Lenik 1993).

Based on the above, first, the low-temperature peaks below 500 °C in Ce added catalysts indicate that Ce increased the reducibility of 5Ni catalysts. Thus, the Ce promoter eased the reduction by enabling it at a lower temperature. Second, when Ce was added, although two low-temperature peaks are observed at similar positions (first peak: 450 °C ~ 479 °C, second peak: 600 °C), increase in reducibility became more pronounced with increase in Ce/Ni ratio from 0.1 to 0.36 as the area of the first peaks increased. The reasons are as follows: 1) more Ce provides a better dispersion of Ni on the catalyst surface, as was already confirmed by chemisorption results, and 2) Ce weakened the interaction between Ni species.

4.5.4.3 TG/DTG

Several reasons may lead to catalyst deactivation in SCWG of lignin, which could be summarized as crystallite sintering, the phase change of support and coke deposition (Lu, Li, and Guo 2014). To investigate the coke resistance of the catalyst, TG/DTG analysis was performed on spent Ni-Ce/Al_2O_3 catalysts. The TG (Thermogravimetry), as well as DTG (Derivative Thermogravimetry) profiles up to 800 °C, are given in Figure 4.8.

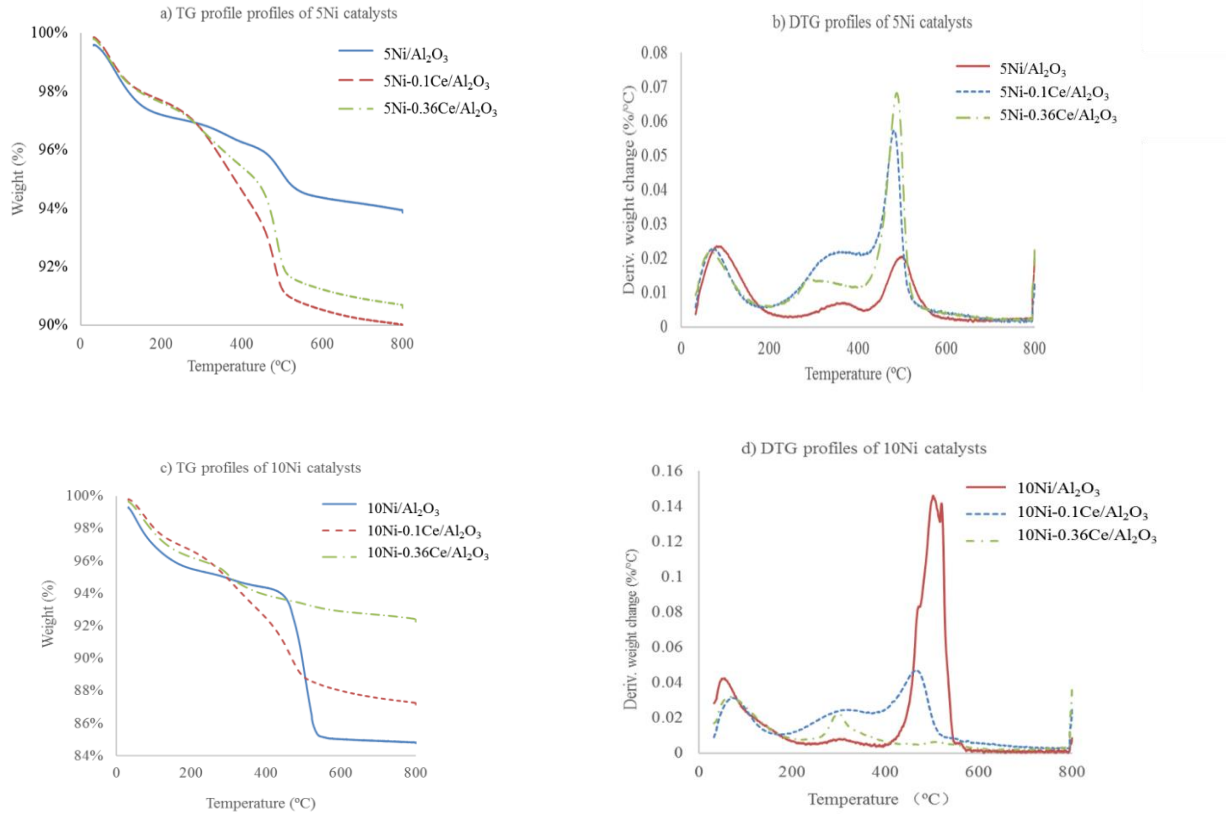

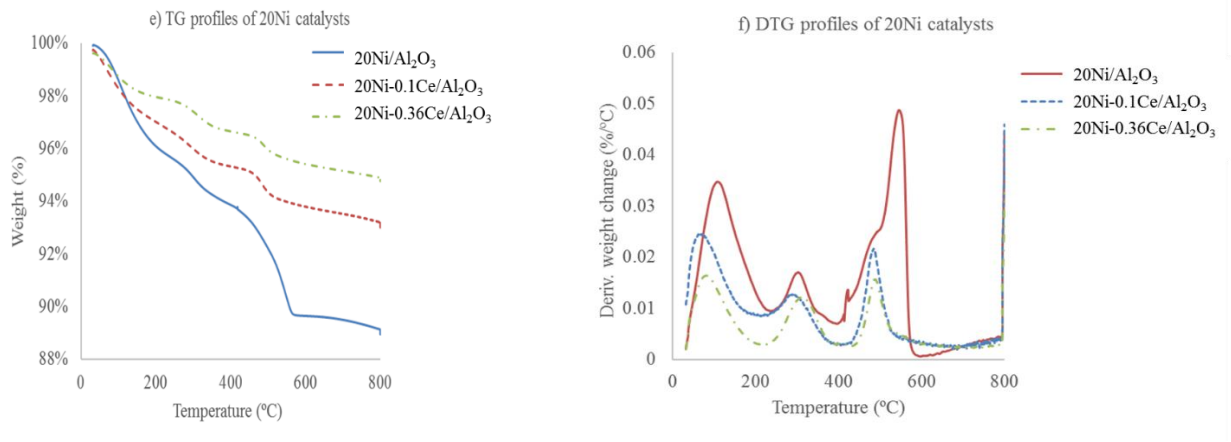

Figure 4.8 TG/DTG profiles of the spent Ni-Ce/Al_2O_3 catalysts

A quantified overview of coke formation could be obtained from TG curves. As shown in Figure 4.8, without Ce, the weight loss was in the order of 10Ni (15%) > 20Ni (11%) > 5Ni (6%), which indicates that Ni loading of 5 wt% showed the lowest coke accumulation. This could be attributed to the better Ni dispersion at lower Ni loading, which is partly confirmed by chemisorption results (Table 4.4). To add more details, from TG profiles of a fixed Ni loading, effect of different Ce/Ni molar ratio is different. For example, for 5Ni catalysts, the coke formation was 0.1Ce > 0.36Ce > 0Ce, more coke was accumulated on Ce promoted catalyst. At 10Ni or 20 Ni, however, coke formation was in the order: 0.36Ce < 0.1Ce < 0Ce, which means that increase in Ce enhanced the coke resistance. This indicates that there is an interaction between Ni and Ce, and for higher Ni loading (> 5 in this study), an increase in Ce decreases the coke.

Qualitative evaluation of the coke is based on the DTG curves. As summarized in previous research, two categories of carbon deposits could be found: oxidation peaks appearing at low temperature belong to amorphous carbon accumulated on Ni surface (Wang and Lu 1998b), while oxidation peaks appearing at high temperature belongs to crystallized carbon deposits with various extents of graphitization (Natesakhawat et al. 2005). The surface carbon is highly active and relatively easier to oxidize as compared to the crystallized carbon (Natesakhawat et al. 2005). In 5Ni group (Figure 4.8b), with a shift of the peak towards low temperature in the DTG profile, the results indicate that coke formed on Ce promoted catalysts is easier to oxidize. In 10Ni group (Figure 4.8d), the peak at 500 °C shows strong coke formation without Ce. However, the peak shifted towards low temperature with Ce addition. For 10Ni-0.36Ce/Al_2O_3, only one small peak appears at 300 °C. In 20Ni group (Figure 4.8f), a form of crystallized carbon was observed on 20Ni/Al_2O_3

with a sharp peak near 550 °C, but with the increase of Ce, the peak shifted towards lower temperature and intensity also decreased.

Above all, suitable coke resistance can be achieved in two ways: 1) coke formation in less quantity and 2) less graphite coke deposits. In this study, without Ce, when Ni loading is higher than 10 wt%, an increase in Ce loading will increase coke resistance in both ways. However, with low Ni loading (e.g., 5 wt%), the quantity of coke may increase with the presence of Ce, however, the tendency of coke to be amorphous was also observed.

4.5.4.4 XRD

Figure 4.9 shows XRD patterns of 5, 10 as well as 20Ni-Ce/Al_2O_3 catalysts with different Ce/Ni molar ratio. In Figure 4.9, the peaks with 2Θ of 28.6°, 33.4°, 47.7° and 56.6° were assigned to CeO_2 (Lu et al. 2010), while peaks appear at 2Θ of 46° and 66.8° were assigned to Al_2O_3 support.

Figure 4.9a indicates that in the 5Ni group, Ce promoted the dispersion of Ni. Specifically, the peak intensity of NiO with the 2Θ value of 37.5°, 61° decreased. Moreover, this trend is identical to the chemisorption results where the Ni dispersion of 5Ni-0.36Ce/Al_2O_3 (4.3%) increased significantly as compared to 5Ni/Al_2O_3 (2.6%) (Table 4).

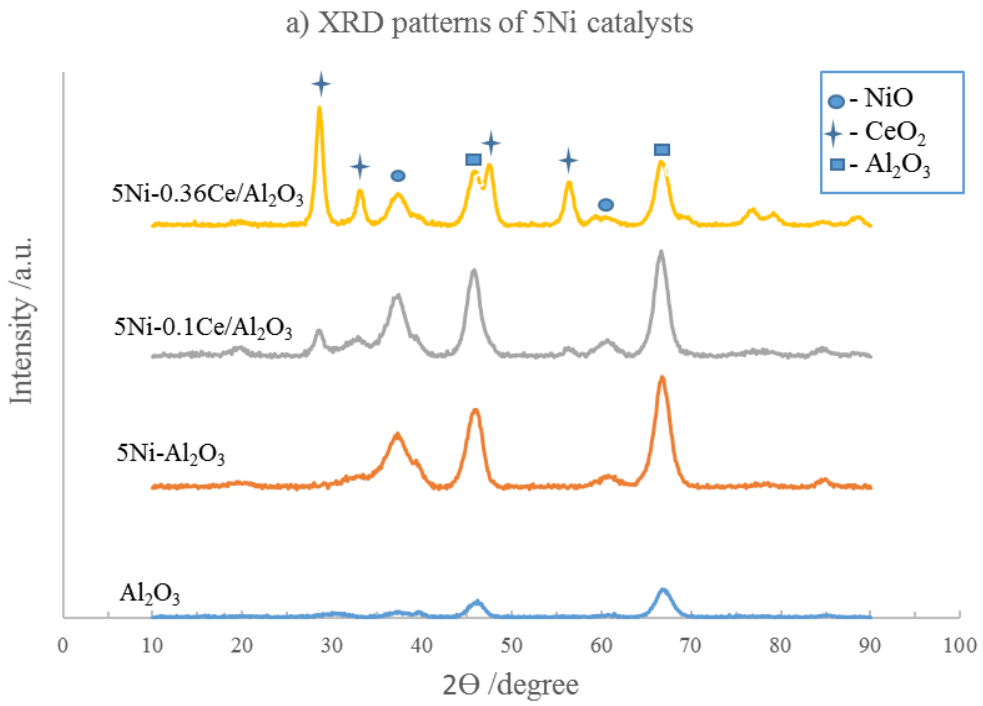

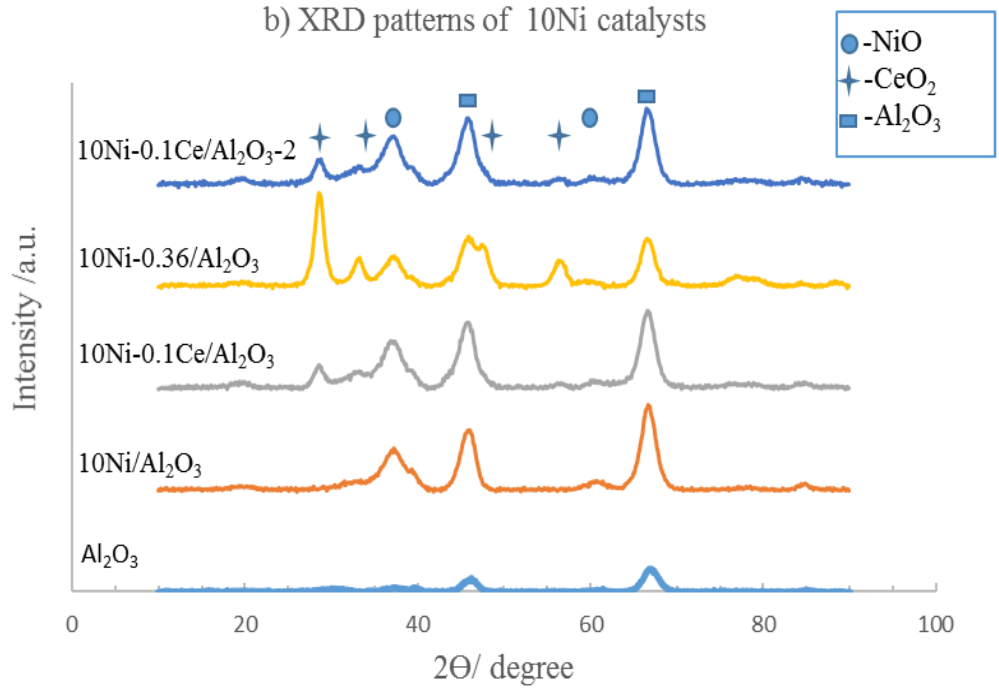

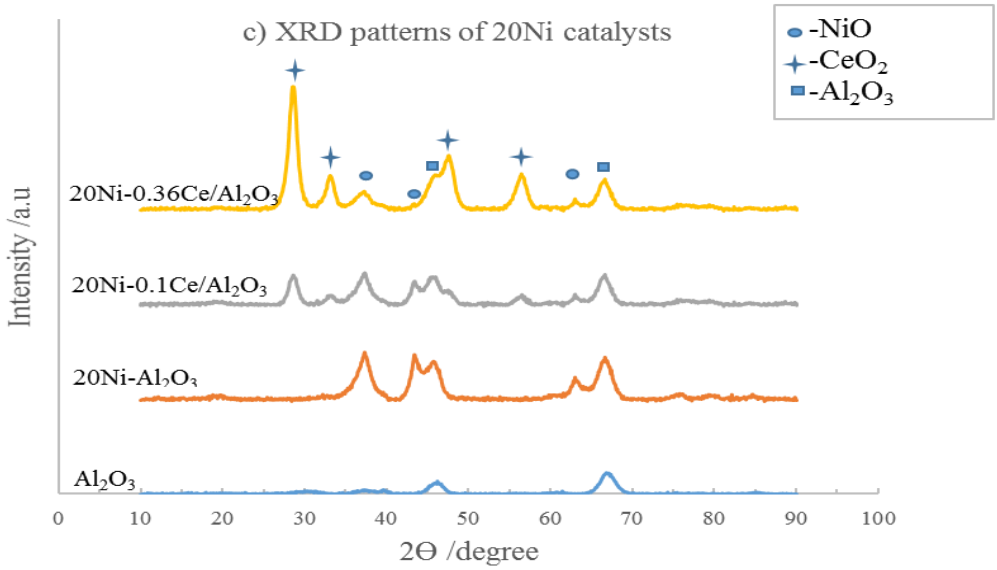

Figure 4.9 XRD patterns of 5/10/20Ni-Ce/Al_2O_3 catalysts with different Ce/Ni molar ratios

Figure 4.9b indicates that in the 10Ni group, an increase in Ce ratio from 0.1 to 0.36 also increased the dispersion of Ni, as the peak intensity of NiO decreased. This figure also shows that the use of

different precursors for Ce (10Ni-0.1Ce/Al_2O_3-2) did not change the diffraction pattern of the catalyst. Figure 4.9c shows the XRD patterns of the 20Ni group, as similar as above, Ni dispersion also increased with the increase in Ce ratio, however, a difference in the 20Ni group was that an additional NiO peak at 43.7° was observed. This peak became less visible with an increase in Ce/Ni molar ratio, and could be attributed to one of the NiO species that was discussed with TPR results. Additionally, $NiAl_2O_4$ peaks, which are located at 2Ɵ of 19°, 31.4°, 45°, 55.7°, 59.7° or 65.5° (Ragupathi, Vijaya, and Kennedy), were not detected. Above all, as confirmed by XRD results, the addition of Ce helps the dispersion of Ni. Use of different precursors for Ce promoter did not affect Ni morphology of the 10Ni catalysts.

4.5.5 Characterization of SCWG char

4.5.5.1 FT-IR

FT-IR analysis was performed to specify the functional groups of the solid-phase product (SCW char); the spectra are given in Figure 4.10. Compared to catalytic SCWG chars, the peaks in the range of 600-900 cm^{-1} in non-catalytic char spectrum are significant. These peaks confirm the presence of aromatics including phenols and substituted phenols as common compounds in the biomass gasification products (Williams and Onwudili 2006). The result indicates that under the test condition, lignin SCWG is not efficient without Ni catalyst. The reason might be incomplete lignin-decomposition under given condition. Specifically, to produce gaseous products, phenolic compounds must endure aromatic C—C bond cleavage (Kang et al. 2013), which is reported to be facilitated by Ni catalyst (Huber, Shabaker, and Dumesic 2003). Within the catalytic SCWG chars, the difference between 5Ni and 10Ni group was not significant, which might indicate the similar functional composition of the SCWG chars. However, one difference was found as a sharp peak at around 1076 cm^{-1} appeared only in the 5Ni SCWG chars. This peak was assigned to the skeletal vibration of C—O—C in pyranose rings (Sun et al. 2004). Also, with a fixed Ni loading, the increase in Ce/Ni molar ratio does not change the functional composition of the SCW significantly both for 5Ni and 10Ni catalysts.

Above all, the Ni-Ce/Al_2O_3 catalysts in this study showed high lignin-decomposition efficiency, which could be attributed to its high activity in C—C bond cleavage of aromatic rings.

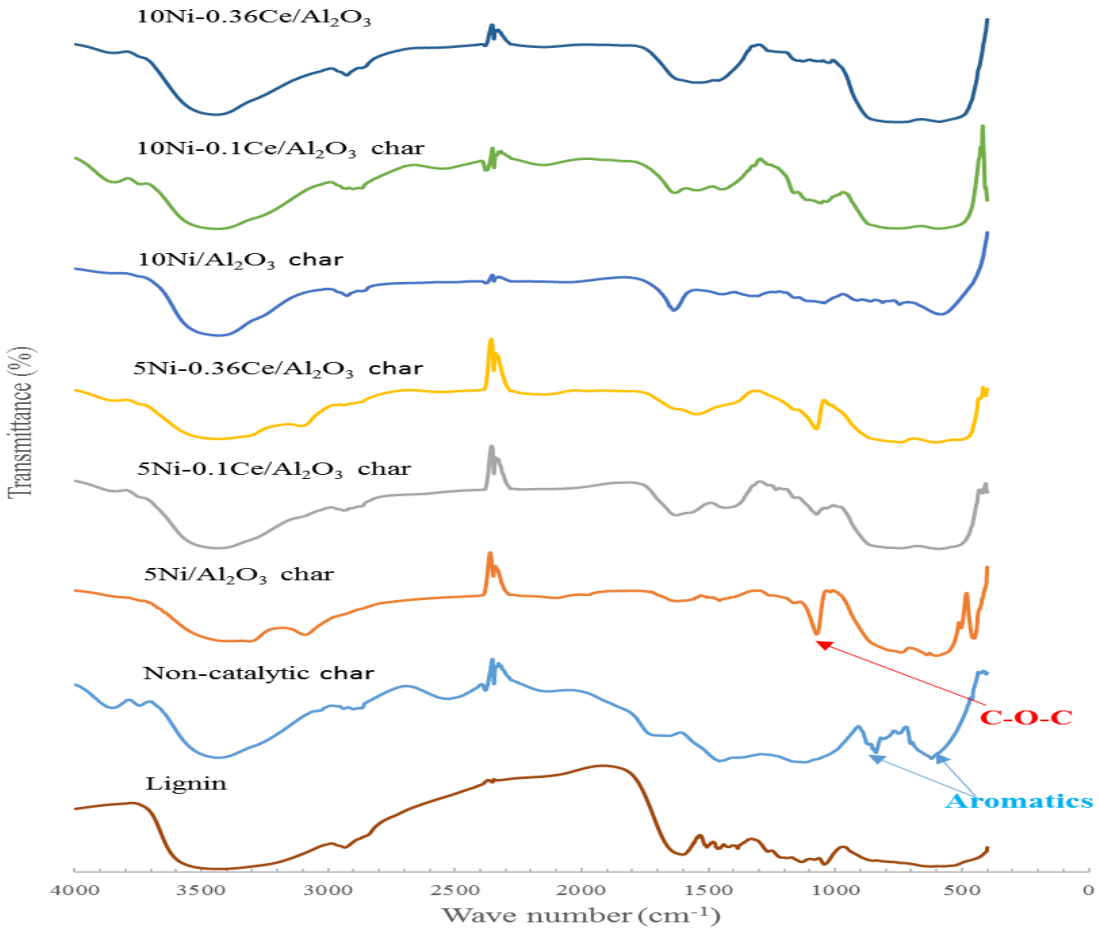

Figure 4.10 FT-IR spectra for fresh lignin sample and SCWG chars

4.5.5.2 Elemental analysis (CHNS)

The elemental analysis was performed to test the elemental composition of lignin sample as well as SCWG chars, the results are given in Table 4.5, and the data were reported in total dry basis. First, it is evident that as compared with lignin sample (Lignin, alkali), the chars produced by Ni-Ce/Al_2O_3 catalysts contain significantly less amount of carbon (C = 25.8-32.5 wt% vs. C = 48.2 wt%) as well as hydrogen (H = 0.7-1.0 wt% vs. H = 4.7 wt%), which indicates that the carbon conversion efficiency was enhanced by these catalysts. Second, with Ce/Ni molar ratio fixed at 0.36, with an increase in Ni loading from 2.5 to 10 wt%, the carbon content showed a decreasing trend. However, the similar carbon content was observed with 10Ni and 20Ni SCWG chars (25.5, 25.8 wt%, respectively). Additionally, compared to the lignin sample, catalytic SCWG char contains more ash, this observation is due to that ash is not reactive in SGWG reactions.

Table 4.5 Results of elemental analysis of lignin sample and SCWG chars

	Elemental composition （wt%）					
Sample source	N	C	S	H	O*	Ash
Lignin, alkali	0.12 ± 0.02	48.23 ± 0.19	4.59 ± 0.31	4.72 ± 0.10	25.84	16.5 ± 0.36
2.5Ni-Ce0.36/Al_2O_3	0.03 ± 0.00	32.46 ± 0.97	0.40 ± 0.02	1.03 ± 0.06	25.75	40.32 ± 0.86
5Ni-Ce0.36/Al_2O_3	0.06 ± 0.01	29.96 ± 6.94	1.01 ± 0.16	0.76 ± 0.07	14.71	53.49 ± 0.57
10Ni-Ce0.36/Al_2O_3	0.07 ± 0.00	25.53 ± 0.24	1.07 ± 0.04	0.67 ± 0.01	21.95	50.71 ± 0.51
20Ni-Ce0.36/Al_2O_3	0.07 ± 0.00	25.83 ± 0.66	1.19 ± 0.21	0.73 ± 0.07	17.17	55.01±1.20

*O is calculated by difference.

4.6 Conclusions

An intensive screening of catalysts synthesized from five supports: Al_2O_3, AC, TiO_2, ZrO_2 and MgO, and three promoters: Co, Cu, and Ce were performed, and further optimization of the Ni-Ce/Al_2O_3 catalyst was carried out for H_2 production from SCWG of lignin. Principal conclusions of this study are listed below:

1) Using different supports, the activity of Ni-based catalysts for SCWG of lignin was in the order of Al_2O_3 > TiO_2 > AC > ZrO_2 > MgO. High surface area is desirable but may not lead to high catalytic activity. Other properties of the catalyst such as Ni dispersion, Ni crystalline phase as well as metal-support interaction have more significant influence.

2) Using different promoters, the activity of Ni-based catalysts for SCWG of lignin were in the order of Ce > Co > Cu. Ce is considered as an efficient promoter of Ni-Ce/Al_2O_3 catalysts, and use of different precursors for the Ce promoter ($CeCl_3 \cdot 6H_2O$ or $Ce(NO_3)_3 \cdot 6H_2O$) showed no influence on hydrogen yield.

3) Ni/Al_2O_3 is active for hydrogen production using lignin SCWG. The Increase in Ni loading has a tendency to decrease CH_4 but increases the CO_2 proportion in the product gas. Without the promoter, Ni loading of 10 wt% performed the best.

4) As a promoter, Ce can enhance the hydrogen selectivity by promoting the Ni dispersion and weakening the Ni-Al_2O_3 interaction. The better performance of Ni-Ce/Al_2O_3 can be attributed to enhanced coke resistance as well as increased reducibility by the Ce promoter.

5) Hydrogen yield is dependent on both Ni loading and Ce/Ni molar ratio, the interaction between these two factors was observed. With a fixed Ni loading, when Ce/Ni molar ratio increased, the hydrogen yields always increased in this study.

6) In this study, 20Ni-0.36Ce/Al_2O_3 catalyst showed highest hydrogen yield of 2.15 mmol/g. As compare to non-catalytic run (1.59 mmol/g), the hydrogen yield increased by ~35%.

Chapter 5 Effect of Mg-Al and TiO_2 Supported Catalysts on Hydrogen Generation from Gasification of Lignin in Supercritical Water

This Chapter is based on a manuscript which is communicated for publication and currently under review.

Contributions of authors: KANG: (1) preparing the samples and the catalysts, (2) performing SCWG tests (3) performing characterizations for gasification products and catalysts, (4) analysing the experimental results, and (5) writing the manuscript and provide responses to reviewers' comments. Dr. Ramin Azargohar examined the experimental design, and reviewed the manuscript. Dr. Ajay K. Dalai and Dr. Hui Wang, performed overall supervision of this research, examined the research results, oversaw the preparation of the manuscript, and submitted the papers.

5.1 Knowledge gaps, hypothesis, and objectives

5.1.1 Knowledge gaps

- The effects of Ni-Co/Mg-Al catalysts on hydrogen yield from lignin SCWG have not been studied before.
- The effects of Ni/Ru catalysts supported by TiO_2 with different Ni loading and promoters on hydrogen yield from lignin SCWG have not been studied.

5.1.2 Hypothesis

- Novel catalysts may provide higher hydrogen yield.
- The activity/selectivity of the novel catalysts might be improved by appropriate modifications.

5.1.3 Objectives

To study the effects of Ni-Co/Mg-Al catalysts on hydrogen yield for lignin SCWG with different Mg-Al ratios and different preparation methods.

To study the effects of Ni/TiO_2 catalysts with different Ni loadings and promoters on hydrogen yield from SCWG of lignin.

5.2 Abstract

Two groups of catalysts including Ni-Co/Mg-Al and Ni/TiO_2 catalysts were developed for hydrogen production from supercritical water gasification of lignin. Catalyst evaluation was

performed at 650 ºC, 26 MPa in SCW. The water to biomass mass ratio was maintained at five for all experiments. For Ni-Co/Mg-Al catalyst group, the strong acidic sites within the temperature range of 400-600 °C is crucial for hydrogen production. The Cop.2.6Ni-5.2Co/2.6Mg-Al catalyst is the best performer of this group regarding gas yield and hydrogen yield. The better performance could be attributed to its high surface area, high coke resistance, and high strong acidic strength in the range of (400-600 ºC). For Ni/TiO_2 catalyst group, 5 wt% Ni loading is the optimum for hydrogen production. However, the addition of promoters such as Co, Ru, Ce, Mg did not improve the hydrogen yield. A detailed mechanism for catalytic SCWG of lignin is proposed. The mechanism addresses the roles of different catalyst components including active metal, supporting material, and promoter in the process individually and reveals the properties required for improving the hydrogen yield.

5.3 Introduction

A clean, sustainable hydrogen orientated energy system has every potential to be a solution for the world energy crisis, global warming as well as the atmospheric contamination (Teichmann et al. 2011, Dunn 2002). Yet, a major concern before the adoption of hydrogen energy is the large scale generation of hydrogen, where biomass could act as a sustainable precursor(Cortright, Davda, and Dumesic 2002). Supercritical water gasification (SCWG) could generate hydrogen from biomass cost-effectively, in a sense that it could handle biomass with high moisture content at relatively low temperatures.

As on of the most abundant polymeric material available in nature, lignin is of particular interest for biomass SCWG (Ragauskas, Beckham, Biddy, Chandra, et al. 2014). Lignin conversion is yet a severe challenge because of its highly cross-linked aromatic structure. To achieve lignin valorization, catalysis is considered as the key technology (Zakzeski et al. 2010). For the effective production of hydrogen via lignin SCWG, it is of vital importance to develop reliable catalysts which have both high stabilities under SCW process conditions and high hydrogen selectivity.

As the current scenario, two main categories of catalysts are used for SCWG of biomass, namely homogeneous (alkali metal) catalysts, and heterogeneous (transitional metal) catalysts. Without denying the importance of both, a review of research progress in supported heterogeneous catalysts will be provided below, combined with statements for motivation, objectives, and novelty of the present work. For supported heterogeneous catalysts, appropriate support is crucial, considering

the relatively harsh conditions of SCW environment. The appropriate support could provide not only better activity but more importantly, better stability. Catalyst supports including different types of Al_2O_3, metal oxides as well as activated carbon have been tested for this process. The results from these supports are scattered in the literature, and in-depth insight could be obtained from recent work (Guo et al. 2010, Azadi and Farnood 2011, Azadi, Afif, et al. 2012, Reddy et al. 2014).

Mg-Al support combines the high thermal stability of MgO (melting point 3073 ºC) and high specific surface area of Al_2O_3, it showed excellent stability in dry reforming process at 750 °C (Zhang, Wang, and Dalai 2007), therefore, it has every potential to be a good candidate support for SCWG process. Magnesium-aluminum hydrotalcite is a type of anionic clay which contains multi-layered hydroxides with exchangeable anions (Takehira et al. 2005). When heated with high tempreture maintains its stability by forming a mixture of Mg-Al oxides which is homogeneous (Takehira et al. 2004). It is a novel catalyst support for SCWG reactions which showed promising activity and hydrogen selectivity for the SCWG of carbohydrates at 380 °C(Azadi, Khan, et al. 2012). As another novel catalyst support for lignin SCWG, TiO_2 was found to give reasonable hydrogen yield for lignin SCWG when loaded with Ru (Yamaguchi et al. 2008). Also, in our previous work, it was found that Ni/TiO_2 is also active for lignin SCWG (Kang et al. 2016). Therefore, modification of Mg-Al and TiO_2 supported catalysts for SCWG of lignin for hydrogen production is considered.

It has been reported that for SCWG of lignin at 400 °C using 5 wt% Ni loading on activated carbon support (AC), the hydrogen yield of various catalysts was observed in the order of Pd > Ru > Pt > Rh > Ni (Yamaguchi et al. 2008). Ru/Al_2O_3 was found to be active for reforming of glycerol in SCW at 700 – 800 °C (Byrd, Pant, and Gupta 2008). Stability of Ru catalysts for lignin SCWG was studied using 5 wt% Ru/C, 5 wt% $Ru//\gamma\text{-}Al_2O_3$, 2 wt% Ru/TiO_2 catalysts and Ru/TiO_2 showed stable gasification activity for three subsequent runs at 400 °C (Osada, Sato, Arai, et al. 2006), however, according to a previous study, the Ru catalyst is prone to sulfur poisoning (Osada et al. 2007). Recently, because of the low cost of Ni compared to novel metals, modification of the Ni based catalyst attracted more research interest. Lots of work have been done to introduce a secondary metal to Ni catalysts for better performance, and this method is proved to be effective in enhancing the catalyst stability in SCW environment as well as improving the hydrogen selectivity (Li et al. 2011). As an example, Ni-Co combination was proved to be an excellent

combination for high temperature dry reforming reaction performed at 750 °C (Zhang, Wang, and Dalai 2007). Therefore, for active phase, Ni, Ru, Ni-Co combination, and the effects of different promoters are evaluated in the present paper.

In terms of preparation method, impregnation method is commonly applied for lab studies for its simplicity. However, co-precipitation method might provide better performance for the catalyst. For example, it was reported that co-precipitated Ni/Mg-Al catalysts with the metal loading of Ni: 26.3, Mg: Al: 7.2 and 24.1 wt% performed best for hydrogen production from glucose SCWG at 400 °C, and the hydrogen yield was eight times higher than that of the non-catalytic test (Li et al. 2013). Therefore, the effects of these two methods are more selectively compared in the present paper.

The main objective of this research is to evaluate and modify two groups of catalysts for hydrogen production via SCWG of lignin including 1) a group of Mg-Al supported Ni-Co catalysts. For this group, the effects of Mg to Al molar ratio, the effects of different preparation methods, and the effect of commercial Mg-Al hydrotalcite as catalyst support for hydrogen generation from SCWG of lignin are studied. 2) a group of TiO_2 supported catalysts with Ni as active phase. For this group, the effects of Ni loading and the promoters are studied. Also, to better understand the role of different catalyst components in the SCWG process, the mechanism of hydrogen production from lignin SCWG using various types of catalysts is proposed. The data in this paper should provide a valuable reference for understanding the properties and performance of these catalysts. In addition, the mechanism proposed here contains insight into the functions of different catalyst components in the SCWG process.

5.4 Experimental section

5.4.1 Materials

Lignin sample and metal precursors for catalysts including $Ni(NO_3)_2{\cdot}6H_2O$, $Co(NO_3)_2{\cdot}6H_2O$, $Ce(NO_3)_3{\cdot}6H_2O$, and $Mg(NO_3)_2{\cdot}6H_2O$ were purchased from Sigma-Aldrich (Oakville, Canada). Ruthenium(III) nitrosyl nitrate was supplied by Alfa Aesar (Ward Hill, USA).

TiO_2 used as catalyst support was provided by Alfa Aesar (Ward Hill, USA). The commercial Mg-Al hydrotalcite in powder form was purchased from Sigma-Aldrich (Oakville, Canada). Other Mg-Al catalyst supports used for impregnation were prepared by first, mixing $Al(OH)_3$ and

$Mg(OH)_2$ (purchased from Alfa Aesar) together with a specific mass ratio based on calculation. Then the mixture was dried and calcined at 800 °C for 6 hours before their use for impregnation.

5.4.2 Catalyst preparation

Most of the catalysts were prepared using impregnation method (Imp.). The Cop.2.6Ni-5.2Co/2.6Mg-Al catalyst evaluated in this research was prepared by coprecipitation (Cop.). The detailed procedure of the preparation procedure was described elsewhere (Wang et al. 2013). Basically, it was made by precipitating Ni, Co, Mg and Al from their nitrate salt solution by titration using aqueous ammonia solution. For the impregnation, calculated amount of metal precursor was converted into solution before impregnation onto the support. An oven drying procedure at 105 ^oC for eight hours was applied before the calcination. All Mg-Al supported catalyst were calcined at 800 °C and all TiO_2 supported catalysts are calcined at 650 °C in air. The time for calcination is six hours.

5.4.3 Reactor and SCWG test procedure

A batch-type SCW reactor was used to perform all experiments in this study. All the SCWG tests were performed in SCW reactor at 650 °C, 26 MPa. The water to biomass mass ratio was five for all tests. For each test, the reactor was loaded with 0.65g lignin, 0.65g catalyst, and 3.25g water. The calcined catalyst was loaded into the reactor without reduction. Details about the SCW reactor, as well as SCWG test procedure, are described in our previous work (Kang et al. 2016). For product separation and collection, the similar procedure described in Chapter 3 was followed. For the characterization, spent catalysts were spearated manually from the solid phase.

5.4.4 Characterization of gasification products and catalysts

Some of the characterizations performed in this study were described in Chapter 3 and Chapter 4. The TPD/TPR-2720 Micromeritics (USA) instrument was used to perform Ammonia temperature programmed reduction (NH_3-TPD) of the calcined catalysts.

5.4.5 Data interpretation

The performance of the catalysts was evaluated using hydrogen and gas yields. The definitions were given in chapter 3. Regarding the name of the catalysts, the numbers before active metal indicates the metal loading in terms of weight percentage. The number before the promoter represents the promoter to active metal molar ratio. The composition of the Mg-Al supported Ni-Co bimetallic catalysts are given in Table 5.1.

For the ease of discussion, three sub-groups of the Mg-Al supported catalysts were categorized in this paper. The first sub-group is three 5Ni-3Co catalyst supported by Mg-Al with the different Mg-Al ratio. The second sub-group is two 2.6Ni-5.2Co HT catalyst made with different preparation methods. The third one is the 5Ni-3Co catalyst support by a commercial Mg-Al hydrotalcite. For Mg-Al supported catalysts, Imp or Cop indicates the preparation method of the catalyst. As an example, the Cop.2.6Ni-5.2Co/2.6Mg-Al catalyst is prepared by coprecipitation method, it has 2.6 wt% Ni, 5.2 wt% Co as the active phase, Mg-Al as the support with 2.6 as the molar ratio of Mg to Al.

Table 5.1 Composition of Mg-Al supported catalysts and their effect on gas yield and hydrogen yield

Catalyst	Ni (wt%)	Co (wt%)	Mg/Al molar ratio	Gas yield (wt%)	Hydrogen yield (mmol/g)
1. Different Mg-Al molar ratio					
5Ni-3Co/2.7Mg-Al	5	3	2.7/1	4.9 ± 0.4	0.57 ± 0.03
5Ni-3Co/1.3Mg-Al	5	3	1.3/1	8.0 ± 0.4	1.45 ± 0.03
5Ni-3Co/0.7Mg-Al	5	3	0.7/1	7.8 ± 0.3	0.63 ± 0.03
2. Different preparation method					
Cop.2.6Ni-5.2Co/2.6Mg-Al	2.6	5.2	2.6/1	12.9 ± 0.5	2.36 ± 0.13
Imp.2.6Ni-5.2Co/2.6Mg-Al	2.6	5.2	2.6/1	4.7 ± 0.4	0.42 ± 0.01
3. Commercial support					
5Ni-3Co/Com.Hydrotalcite	5	3	3.0/1	8.9 ± 0.4	0.88 ± 0.01

5.5 Results and discussion

5.5.1 Effect of Ni-Co/Mg-Al catalysts

5.5.1.1 Results of SCWG tests

The results of SCWG tests of the Mg-Al supported Ni-Co bimetallic catalysts are given in Table 5.1. For the effects of the Mg-Al molar ratio, the intermediate value of 1.3 seems to be optimum, as the highest gas yield of 1.45 mmol/g was obtained using the 5Ni-3Co/1.3Mg-Al catalyst. By different preparation methods, the Cop.2.6Ni-5.2Co/2.6Mg-Al catalyst showed superior gas yield and hydrogen yield.

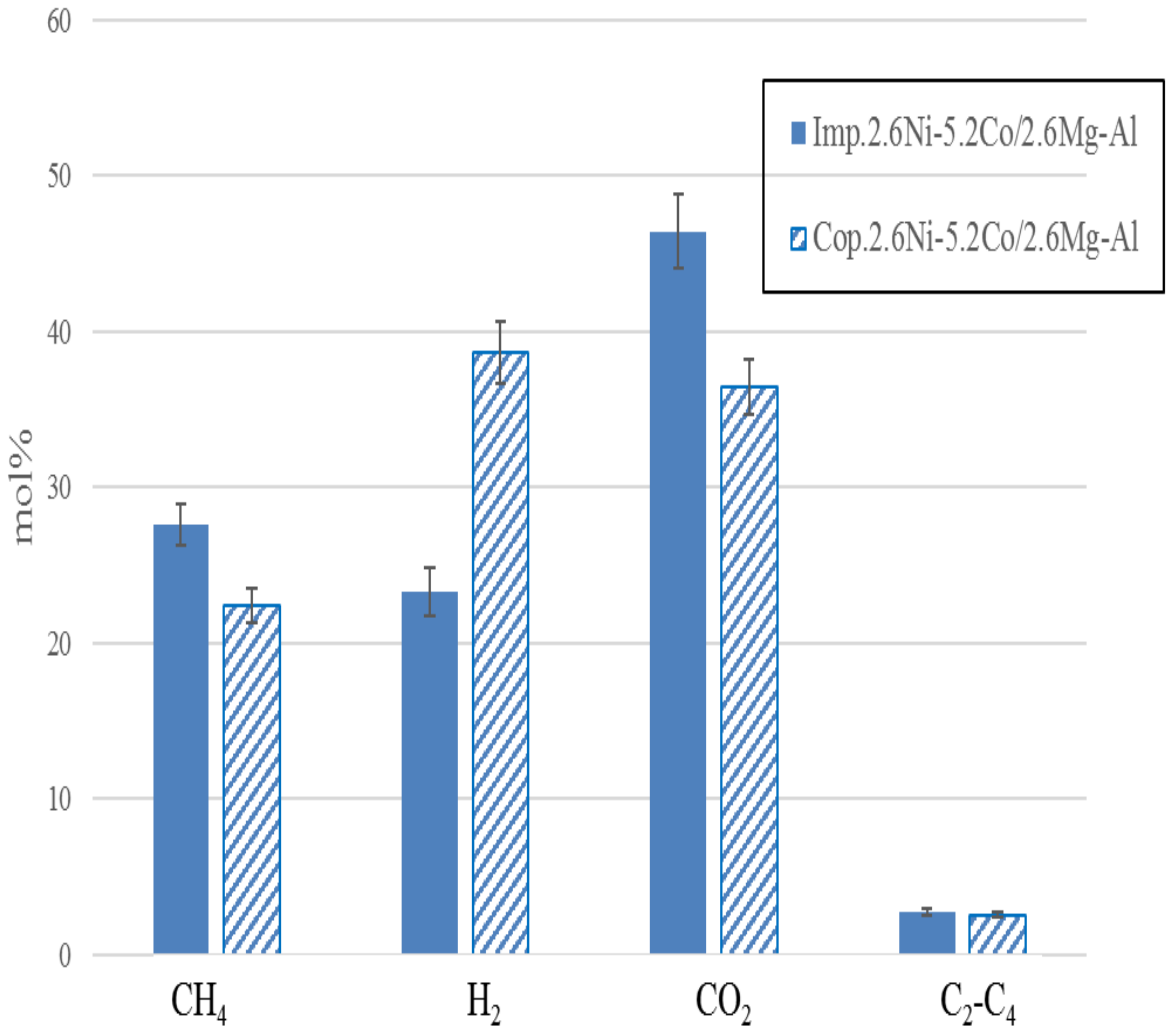

Figure 5.1 Effect of Ni-Co/Mg-Al catalysts on gas composition

Specifically, the gas and hydrogen yield were 12.9 wt% and 2.36 mmol/g, respectively, which are near three times as much in the gas yield and more than five times higher in hydrogen yield than that of the Imp. catalyst with the same composition. In addition, higher hydrogen selectivity was observed with the Cop catalyst. As indicated in Figure 5.1, the product gas from the Cop.2.6Ni-5.2Co/Mg-Al catalyst showed the significantly greater proportion of H_2 and a lower proportion of CO_2 and CH_4 than that of the Imp. catalyst. The C_2-C_4 in this figure represents C_2-C_4 hydrocarbons. The commercial hydrotalcite supported catalyst showed an intermediate hydrogen yield of 0.88 mmol/g. Therefore, the overall best performer in this group is the Cop.2.6Ni-5.2Co/2.6Mg-Al catalyst.

Table 5.2 Physico-chemical characteristics of the Mg-Al supported catalysts

Catalyst	S_{BET}* (m^2/g)	V_{pore}* (cm^3/g)	Metal dispersion (%)	Metallic surface area (m^2/g sample)	Metallic surface area (m^2/g metal)	Crystallite size (nm)
1. Different Mg-Al molar ratio						
5Ni-3Co/2.7Mg-Al	144	0.40	4.7	2.5	31.3	21.5
5Ni-3Co/1.3Mg-Al	164	0.32	2.0	1.1	13.4	50.4
5Ni-3Co/0.7Mg-Al	197	0.26	0.9	0.5	5.9	114.4
2. Different preparation method						
Cop.2.6Ni-5.2Co/2.6Mg-Al	183	0.30	1.0	0.5	6.7	101.3
Imp.2.6Ni-5.2Co/2.6Mg-Al	104	0.17	0.9	0.5	6.1	111.2
3. Commercial support						
5Ni-3Co/Com.Hydrotalcite	217	0.24	0.4	0.2	2.3	286.9

*S_{BET}: BET surface area; V_{pore}: pore volume

5.5.1.2 N_2 adsorption/desorption

Results from N_2 adsorption/desorption are given in Table 5.2. Regarding different Mg-Al molar ratios, when the Mg-Al molar ratio in the support decreased from 2.7:1 to 0.7:1, the BET surface area increased from 144 m^2/g to 197 m^2/g. This observation could be attributed to the fact that higher content of aluminum in the support eases the formation of ink bottle-like pores which lead to an increase in surface area, whilst higher magnesium content eases the formation of slit-shaped pores which led to the decrease of the surface area (Li et al. 2013).

For different preparation methods, the BET surface area is significantly higher on Cop.2.6Ni-5.2Co/2.6Mg-Al (183 m^2/g) than that of the Imp.2.6Ni-5.2Co/2.6Mg-Al (104 m^2/g), which suggests that the coprecipitation method is beneficial for maintaining surface area of the Mg-Al supported catalysts as compared to impregnation. Larger pores were observed on the Cop. catalyst. According to the literature, this is possibly caused by the application of the coprecipitation method. Specifically, coprecipitation enables complete metal-support interaction which allows the active metal to have a direct influence on the support structure (Zieliński 1993). Highest BET surface area of 217 m^2/g was found on 5Ni-3Co/Com.Hydrotalcite catalyst, this indicates that difference in the supporting material also matters for these characteristics.

5.5.1.3 CO-chemisorption

Results from CO-chemisorption are given in Table 5.2. Comparing different Mg-Al ratios, the metal dispersion increased with increase in Mg-Al molar ratio, followed by an increase in metallic surface area and a decrease in crystalline size. This could be explained by the fact that presence of Mg inhibited the incorporation of nickel into the Al_2O_3 lattice and adjusted the interaction between nickel and alumina, therefore, improved the Ni dispersion, led to the formation of smaller metal particles and provided a larger metallic surface area (Sánchez-Sánchez, Navarro, and Fierro 2007). The preparation method was found to have minimum impact on the metal dispersion. Specifically, the metal dispersions of the 2.6Ni-5.2Co/2.6Mg-Al catalysts were nearly identical (0.9% for Imp. vs. 1.0% for Cop.). The commercial hydrotalcite supported catalyst gives lowest metal dispersion (0.4 %), possibly due to the formation of metal clusters formed as highest crystallite size was observed (286.9 nm).

5.5.1.4 XRD

The XRD patterns of the Mg-Al supported catalysts are provided in Figure 5.2 and 5.3, with the pattern of the uncalcined commercial hydrotalcite for reference. The fresh commercial hydrotalcite support showed the highly crystallized double-layered structure of hydrotalcite. The hydrotalcite structure was evident from the diffraction peaks in the 2Θ range of 20-30° and other asymmetric peaks in the 2Θ range of 30–50° (Dixit et al. 2013).

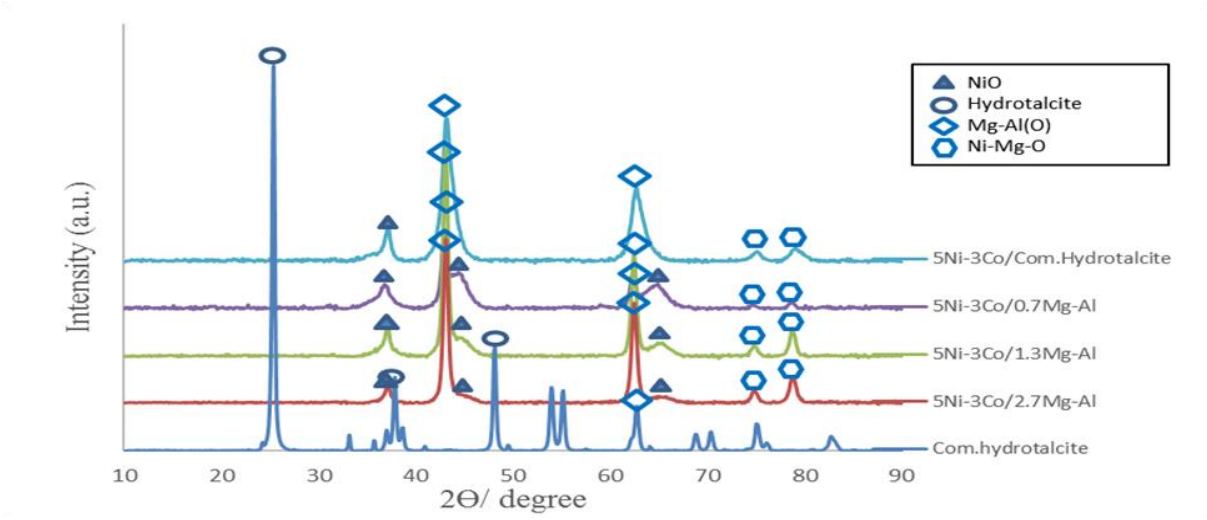

Figure 5.2 XRD patterns of commercial hydrotalcite and 5Ni-3Co/Mg-Al catalysts

On calcined catalysts, the presence of Mg(Al)O mixed oxides are proved by their characteristic diffractions at 2Θ positions of 43 and 63° (Reyero et al. 2013). Also, the NiO was confirmed by

its characteristic peaks at 2Θ values of 37.3°, 43.4°, 63° (Sajjadi et al. 2013). And the peaks at the 2Θ position of 75.1° and 79° could be assigned to the of Mg-Ni-O solid solution (Takehira et al. 2004).

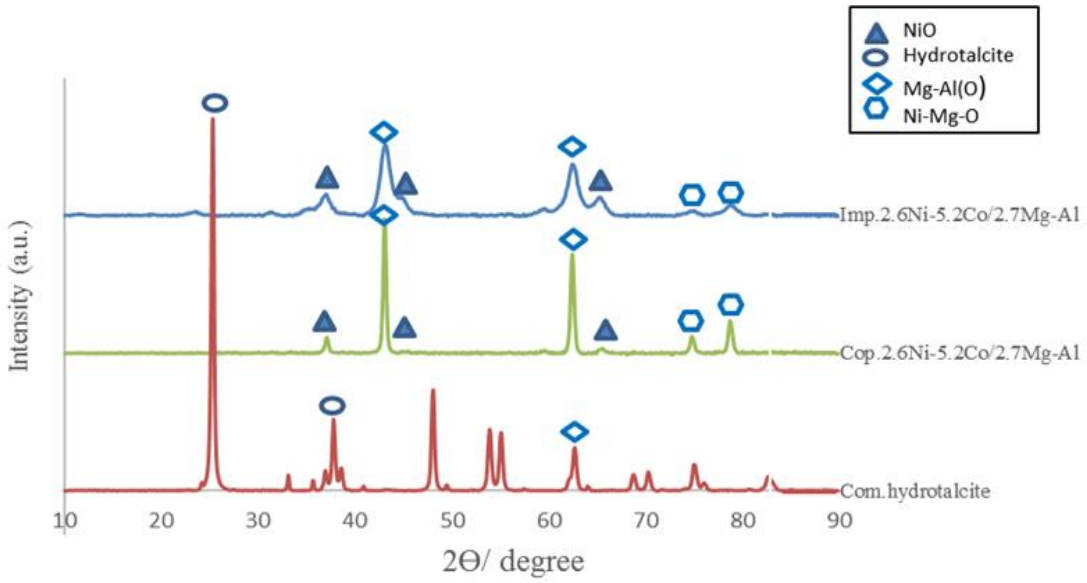

Figure 5.3 XRD patterns of commercial hydrotalcite and Ni-Co/Mg-Al catalysts prepared by different methods

According to the literature, alloying of the Ni-Co might occur in calcination. However, the spinel-type solid solution and spinel phases are not distinguishable by XRD due to their similarity (Zhang, Wang, and Dalai 2007). Therefore, the discussion here is based on Ni, and Co will be considered indistinguishable from different Ni phases. The effect of Mg-Al ratio and effect of commercial hydrotalcite could be compared from Figure 5.2.a. The intensity of NiO characteristic peak at 43.4°C decreased with increase in Mg-Al ratio, which could be explained by better dispersion with higher Mg content. This is in coherence with the CO-chemisorption result (Table 5.2).

Also, with more Mg present, the Ni-Mg-O peaks becomes more and more intensive. What's more, the pattern of the commercial hydrotalcite supported catalyst shows that calcination changed the hydrotalcite structure as the characteristic peaks of hydrotalcite was not observed. To compare the effects of different preparation methods, it is clear in Figure 5.2.b that the intensity of the Ni-Mg-O increased on the pattern of the Cop.2.6Ni-5.2Co/2.6Mg-Al, indicating that coprecipitation method eased the formation of the solid solution.

Table 5.3 NH_3–TPD results for the Mg-Al supported catalysts

Catalyst	acid amount (µmol/g)			total acid mount (µmol/g)
	weak (100 - 200 °C)	medium (200 - 400 °C)	strong (400 - 600 °C)	
1. Different Mg-Al molar ratio				
5Ni-3Co/2.7Mg-Al	25	230	36	291
5Ni-3Co/1.3Mg-Al	82	200	288	570
5Ni-3Co/0.7Mg-Al	0	2,304	35	2,339
2. Different preparation method				
Cop.2.6Ni-5.2Co/2.6Mg-Al	0	1,646	587	2,233
Imp.2.6Ni-5.2Co/2.6Mg-Al	42	73	0	115
3. Commercial support				
5Ni-3Co/Com.Hydrotalcite	120	148	106	374

5.5.1.5 NH_3-TPD

The acidic properties of the Mg-Al supported catalysts were characterized using NH_3-TPD technique and the results are reported in Table 5.3. Comparing different Mg-Al ratios, the total acid amount decreased from 2339 µmol/g to 291 µmol/g when the Mg-AL molar ratio from increased from 0.7:1 to 2.7:1. This is because the increase of Mg content decreased the surface acidity by neutralization effect (Sánchez-Sánchez, Navarro, and Fierro 2007). The Cop. catalyst showed the significantly higher total acid amount of 2233 µmol/g than that of the Imp. catalyst (115 µmol/g). This observation could be illustrated by the fact that by coprecipitation method, incorporation of MgO into Al_2O_3 matrix creates moderate acidity (Kumar et al. 2004). The commercial hydrotalcite supported catalyst showed the total acid amount of 374 µmol/g, although the Mg-Al ratio is 3.0, indicating that the preparation method of the catalyst support influences the acidity.

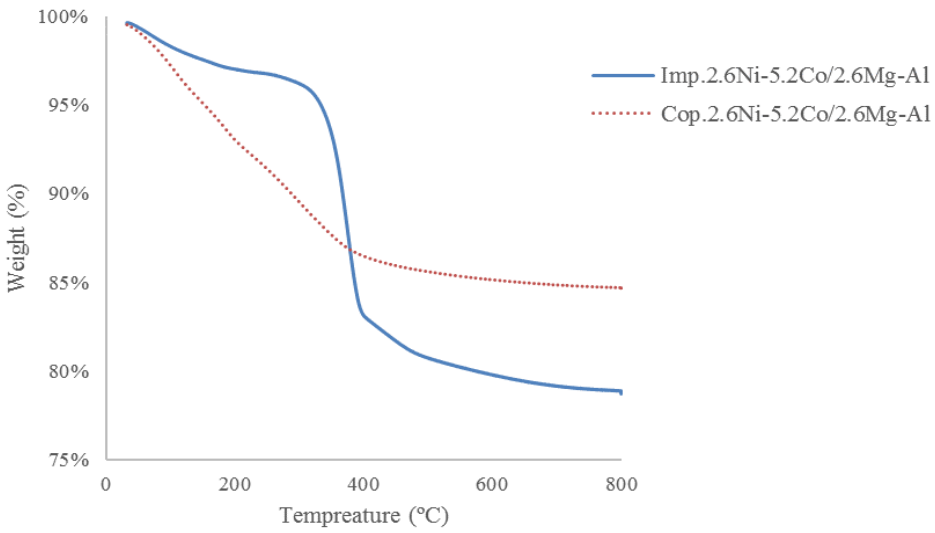

Figure 5.4 TG profiles of 2.6Ni-5.2Co/Mg-Al catalysts prepared by different methods

5.5.1.6 Thermogravimetric analysis

Spent catalysts were characterized by TG/DTG analysis to compare the effects of preparation method on coke resistance of the Ni-Co/HT catalyst. The results are given in Figure 5.4. It was indicated by the TG profiles (Figure 5.3.a) that the weight loss of the Cop. catalyst (15.3 wt%) was less than that of the Imp. catalyst (21.3 wt%), which indicates that less coke was accumulated on the surface of Cop. catalyst.

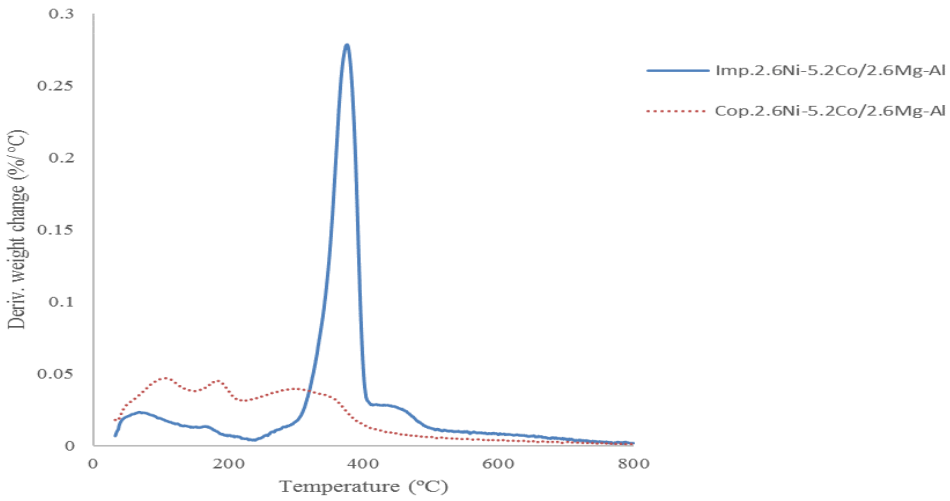

Figure 5.5 DTG profiles of 2.6Ni-5.2Co/Mg-Al catalyst prepared by different methods

What's more, from the DTG profiles (Figure 5.5), the sharp peak of the Imp. catalyst around 378 °C indicates that the coke formed on the nickel surface is mainly amorphous carbon (Wang

and Lu 1998b). According to the literature, the improved coke resistance of the Cop. the catalyst may be introduced by the synergy between Ni and Co (Zhang, Wang, and Dalai 2007).

5.5.2 Further discussion about Ni-Co/Mg-Al catalysts

5.5.2.1 Surface and porous properties

Generally, properties such as high surface area as well as high metal dispersion are desirable for catalyst applications. However, for the group of Mg-Al supported catalysts, relationship between catalyst activity/selectivity with surface properties such as BET surface area and metal dispersion is not clear, e.g., the commercial hydrotalcite supported 5Ni-3Co catalyst with the BET surface area of 217 m^2/g, which is highest in the group, showed hydrogen yield of 0.88 mmol/g. This is less than that for 5Ni-3Co/1.3Mg-Al (1.45 mmol/g) with a lower BET surface area of 164 m^2/g. The highest metal dispersion was observed on the 5Ni-3Co/2.7Mg-Al catalyst. However, the hydrogen yield was 0.57 mmol/g, which was second lowest in this group.

5.5.2.2 Acidity

The importance of catalyst acidity is observed for lignin SCWG. According to the literature, one key step during lignin SCWG to generate gaseous products is the decomposition of low-molecular-weight depolymerized intermediates in the liquid phase, including the C—C bond cleavage of phenolic compounds (Kang et al. 2013). Also, it was found that in fast pyrolysis of lignin, the acid sites on catalyst were effective in converting the intermediates into smaller molecules and preventing the re-polymerization and coke formation (Ma, Troussard, and van Bokhoven 2012). The researchers have also found that the strong acidic sites (400-700 °C) were effective for different reactions including decarboxylation, cracking, and dealkylation. All these reactions are beneficial for enhancing the hydrogen production by breaking down the lignin structure and making the hydrogen atoms more accessible for the reactions.

Specifically, based on the results listed in Table 5.1, and Table 5.3, generally, hydrogen yield increased with the increase in the total acid amount of the catalyst. However, one exception is the 5Ni-3Co/0.7Mg-Al catalyst, which has a high total acid amount of 2339 μmol/g, but the hydrogen yield is significantly lower than that of the Cop. 2.6Ni-5.2Co/2.6Mg-Al catalyst, which has a similar total acid amount of 2233 μmol/g. Comparing the acidity profile of these two catalysts, it is clear that the Cop. 2.6Ni-5.2Co/2.6Mg-Al catalyst has the significantly higher amount of strong acidic sites in the range of 400-600 °C (587 μmol/g) than the other (35 μmol/g). Also, by different

preparation methods, it is observed that coprecipitation is more effective than impregnation in increasing the acidity (2233 vs. 115 μmol/g), especially the strong acidic sites above 400 °C (587 vs. 0 μmol/g).

Based on these results, a reasonable assumption is: for the Ni-Co/Mg-Al catalysts, strong acidity is needed for high hydrogen yield. For the verification of this assumption, a mathematical linear regression was performed using the strong acidic amount as independent variable (X) and hydrogen yield as dependent variable (Y), and the results are shown in Figure 5.6. According to the results, the R^2 value of the linear regression is as high as 0.996; this means that 99.6% of the variation in the observed hydrogen yield could be explained by the linear equation shown in the figure (Kang et al. 2015). This result indicates that higher strong acidic strength (400-600 °C) leads to higher hydrogen yield. Therefore, a higher amount of strong acidic sites might be the key reason for the better performance of the Cop. catalyst.

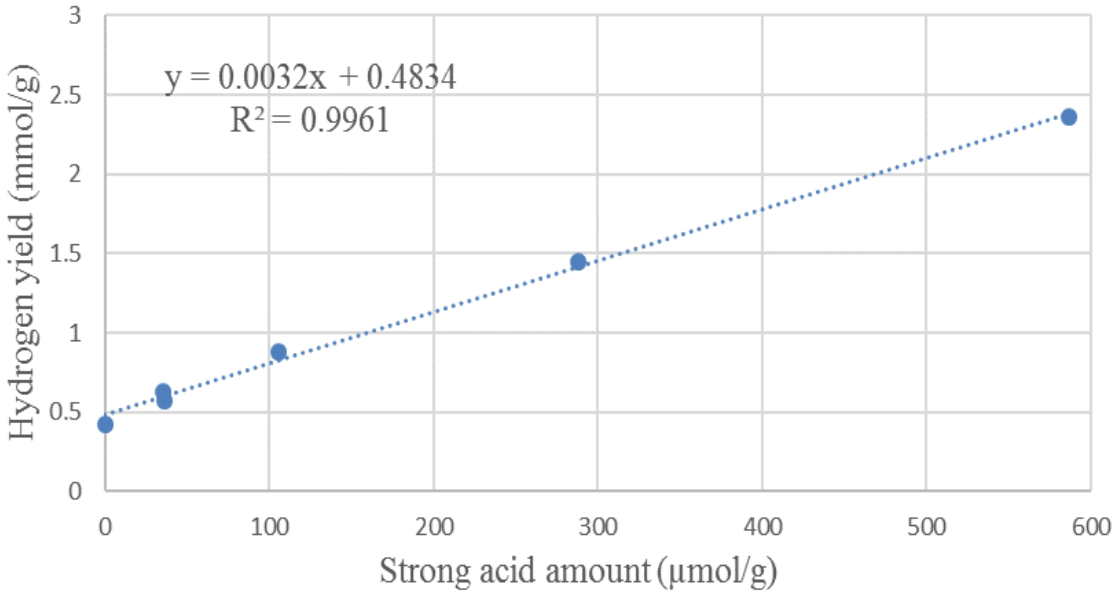

Figure 5.6 Correlation curve of hydrogen yield versus strong acid amount for Mg-Al supported catalysts

As a brief summary for this group of catalyst, first, for Ni-Co/Mg-Al catalysts, the hydrogen yield could be well correlated with the strong acidic strength within the range of 400-600 °C. Secondly, in terms of preparation method, coprecipitation is better than impregnation as it is effective in maintaining the surface area, coke resistance and the strong acidic strength of the catalyst.

5.5.3 Effect of TiO_2 supported Ni or Ru catalysts

5.5.3.1 Effect of Ni metal loading on TiO_2 support

With appropriate loading, Ni was proved to be active in SCWG related reactions, including tar cracking and water gas shift reaction (Resende and Savage 2010). Lack of Ni leads to low activity, whereas Ni overloading might also lead to low activity caused by problems such as poor dispersion as well as clustering of the metal particles. The results of both N_2-adsoption/desorption and the SCWG test on Ni/TiO_2 with different loadings are given in Table 5.4.

Table 5.4 Characteristics of Ni/TiO_2 catalysts and the effect of Ni metal loading on gas and hydrogen yield

Catalyst	Ni (wt %)	S_{BET} (m^2/g)	V_{pore} (cm^3/g)	Gas yield (wt%)	Hydrogen yield (mmol/g)
TiO_2	0	37	0.29	8.1 ± 0.4	0.53 ± 0.02
$2.5Ni/TiO_2$	2.5	36	0.16	9.2 ± 0.4	0.67 ± 0.07
$5Ni/TiO_2$	5	27	0.12	11.6 ± 0.5	1.82 ± 0.02
$10Ni/TiO_2$*	10	11	0.03	13.7 ± 0.7	1.83 ± 0.06
$20Ni/TiO_2$*	20	12	0.03	13.7 ± 0.5	1.78 ± 0.09

*Part of the data has been reported in chapter 4, they are listed for reference.

As the result shows, with the increase in Ni metal loading from 2.5 to 20 wt%, the BET surface area of the catalyst decreased from 36 m^2/g to 12 m^2/g, respectively. Also, the pore volume decreased from 0.16 cm^3/g to 0.03 cm^3/g. This is not surprising given the fact that the TiO_2 catalyst support itself only has a low BET surface of 37 m^2/g. By impregnation, loaded metal covers pore walls and eventually occupies all the pore space (AKSOYLU et al. 1996).

The XRD patterns of TiO_2 support and Ni/TiO_2 catalysts with different Ni loadings are given in Figure 5.7. The patterns clearly show that the TiO_2 support used in this study is in anatase phase (JCPDS card No. 21-1272) (Chen et al. 2009). With different Ni loadings, the main peak of NiO at 2Ɵ position of 43.4° was not observed until Ni loading reached 10 wt% (Sajjadi et al. 2013). This observation indicates that at lower Ni loadings, the nickel particles are finely dispersed on the TiO_2 support, whereas the poor dispersion of nickel is caused by high Ni loadings. Another reason might be that NiO formed a solid solution with TiO_2 caused by the strong metal-support interaction (Zein and Mohamed 2004).

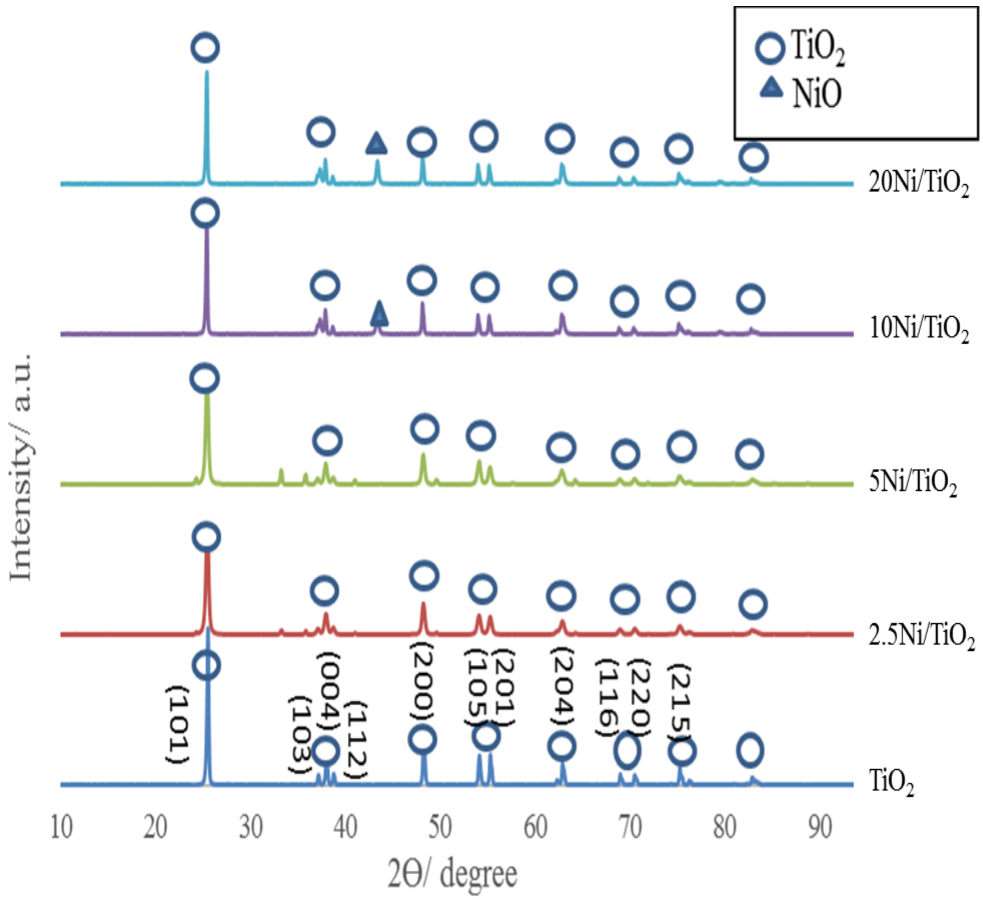

Figure 5.7 XRD patterns of TiO_2 support and Ni/TiO_2 catalysts with different Ni loadings

In terms of hydrogen yield, the results show that first, TiO_2 support itself is not active, proved by the poor hydrogen yield of 0.53 mmol/g (Table 5.4). Also, the $2.5Ni/TiO_2$ catalyst did not show enough activity with a low hydrogen yield of 0.67 mmol/g. The poor performance of this catalyst could be explained by the lack of active metal in the catalyst. With the increase in Ni loading from 2.5 to 5 wt%, the hydrogen yield increased dramatically from 0.67 to 1.82 mmol/g, almost tripled. But, further, increase in Ni loading to 10 and 20 wt% did not improve the hydrogen yield (Kang et al. 2016). This might be due to the fact that overloading of nickel caused poor metal dispersion on the catalyst, which is proved by the XRD results. Based on the result of this study, it was considered that 5 wt% Ni loading is the optimum for Ni/TiO_2 catalysts.

5.5.3.2 Effect of promoters on 5Ni/TiO₂ catalysts

Modification of the $5Ni/TiO_2$ catalyst was made by adding promoters including Ru, Co, Ce, and Mg. The XRD patterns of unpromoted/promoted $5Ni/TiO_2$ catalysts were plotted in Figure 5.8, with the pattern of TiO_2 for reference.

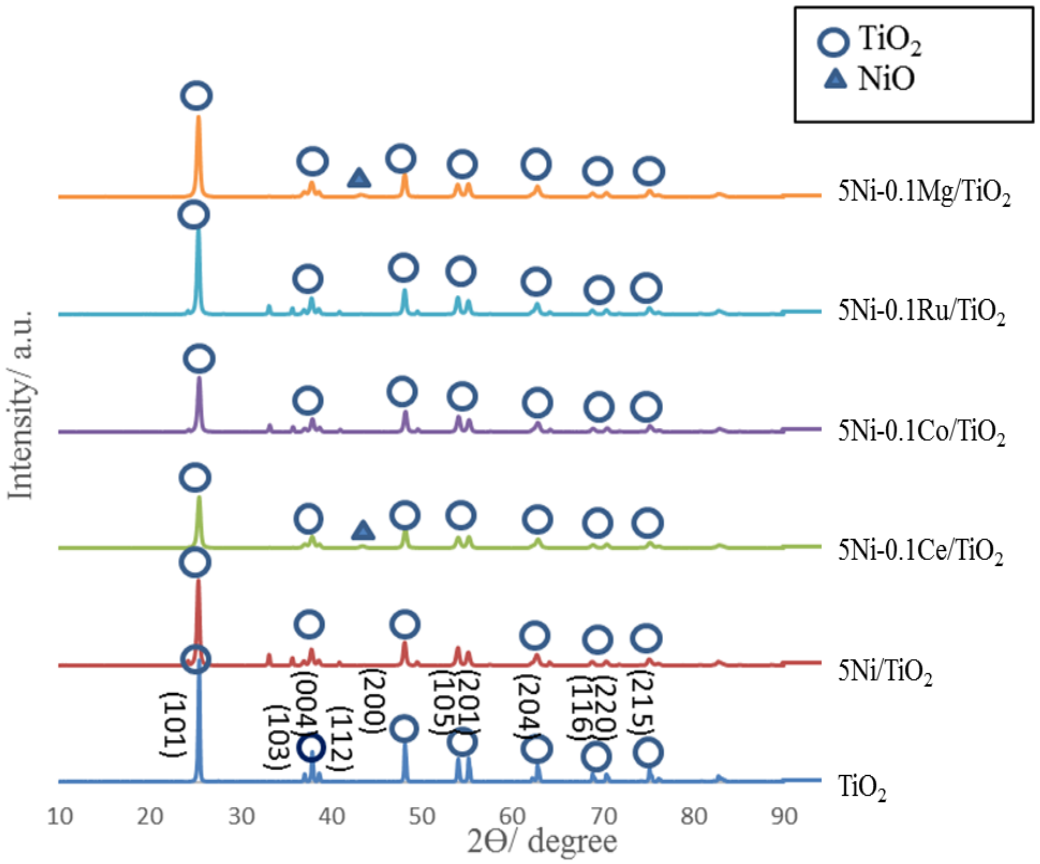

Figure 5.8 XRD patterns of TiO_2 support and 5Ni/TiO_2 catalysts with different promoters

Since a very low amount of the promoters are applied, their corresponding peaks were not detected. By adding promoters, the TiO_2 maintained its anatase phase as characteristic peaks of TiO_2 did not change. However, the intensity (101) peak varied, indicating that the interaction between Ni and TiO_2 changed by adding promoters. Although not detectable on the 5Ni/TiO_2 catalyst, the main peak of NiO (43.4°) was detected on Ce and Mg promoted catalysts. This indicates that poor dispersion of Ni was caused by the addition of Mg or Ce as promoters.

In addition, investigation of the carbon formation on the Ni-promoter/TiO_2 catalyst group was performed by TG/DTG analysis using spent catalyst, and the profiles are given in Figure 5.9 and 5.10. It is clear from the TG profiles (Figure 5.9) that in terms of coke resistance, the unpromoted 5Ni/TiO_2 catalyst out-performed those with promoters. Specifically, the weight loss of the spent catalyst was 3.3 % for 5Ni/TiO_2, followed by 4.1 % for 5Ni-0.1Co/TiO_2. Ce and Ru promoted 5Ni/TiO_2 catalyst showed a similar weight loss of 5.4 % and 5.9 %, respectively.

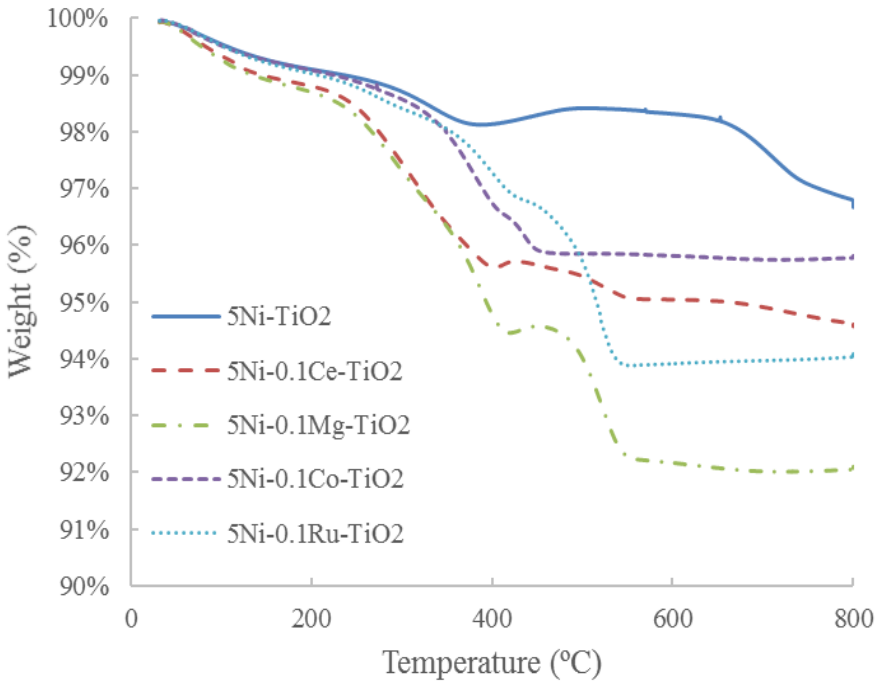

Figure 5.9 TG profiles for spent 5Ni - promoter/TiO_2 catalysts

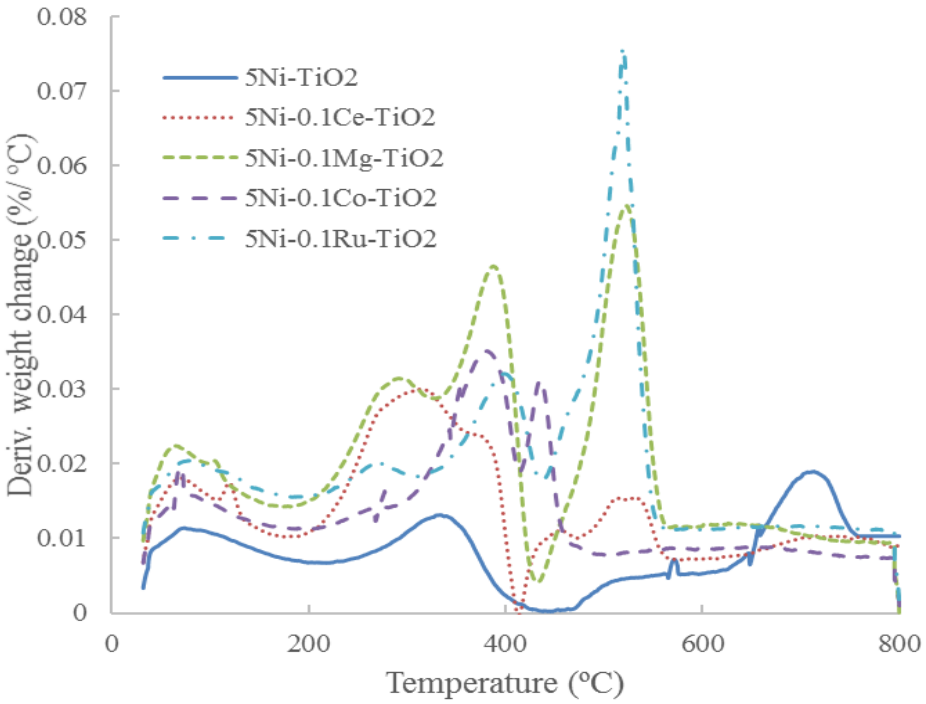

Figure 5.10 DTG profiles for 5Ni - promoter/TiO_2 catalysts

Maximum weight loss was observed with 5Ni-0.1Mg/TiO_2 catalyst. In terms of DTG (Figure 5.10), the observed peaks can be simply assigned to two kinds of carbon species, e.g., low-temperature peaks represent mainly amorphous carbon deposits, which could be easily oxidized (Wang and Lu 1998b). The high-temperature peaks appearing after 500 °C represent hard to oxidize graphite-like crystalline carbon deposits (Natesakhawat et al. 2005). In the SCWG reactions, the formation of crystalline carbon might cover the active site of the catalyst thus leading deactivation (Zhang, Champagne, and Xu 2011). Based on this, different degrees of amorphous carbon deposition were found on all the TiO_2 supported catalysts, however, with huge peaks occurring at around 530 °C, the Mg, Ru promoted catalyst experienced more extensive crystalline carbon deposition.

The results of SCWG test were given in Table 5.5. The hydrogen yield with different promoters was found in the order of Co > Ru > Ce > Mg. However, the un-promoted 5Ni/TiO_2 catalyst gave highest hydrogen yield of 1.82 mmol/g. Therefore, no improvement of hydrogen yield was found using promoters. Interestingly, although 5Ni-0.1Co/TiO_2 gave less hydrogen yield than 5Ni/TiO_2, the addition of Co as promoters improved the gas yield. As a dramatic increase in gas yield from 11.6 wt% to 15.8 wt% was observed. This could be explained by its relatively high activity for lignin decomposition but poor hydrogen selectivity in the gas phase. Also, the poor performance of the Ce and Mg catalyst could be explained by poor nickel dispersion which is proved by the XRD results. As a brief summary, first, the best performer is 5Ni/TiO_2, which gave highest hydrogen yield of 1.82 mmol/g. Second, use Co, Ru, Ce, Mg as promoters did not improve the hydrogen yield of these catalysts.

Table 5.5 Composition of promoted Ni/TiO_2 catalysts and their effects on gas and hydrogen yield

Catalyst	Ni (wt%)	Promoter	Gas yield (wt%)	Hydrogen yield (mmol/g)
5Ni/TiO_2	5	No	11.6 ± 0.5	1.82 ± 0.02
5Ni-0.1Ru/TiO_2	5	Ru	9.58 ± 0.6	0.93 ± 0.06
5Ni-0.1Co/TiO_2	5	Co	15.8 ± 0.7	1.67 ± 0.06
5Ni-0.1Ce/TiO_2	5	Ce	9.4 ± 0.5	0.66 ± 0.02
5Ni-0.1Mg/TiO_2	5	Mg	8.8 ± 0.2	0.56 ± 0.02

5.5.4 Proposed reaction mechanism for hydrogen production from catalytic SCWG of lignin

Based on all results as well as literature knowledge, a reaction scheme (Figure 5.11) is proposed for SCWG of lignin to better address functions of different catalysts/catalyst components in lignin SCWG.

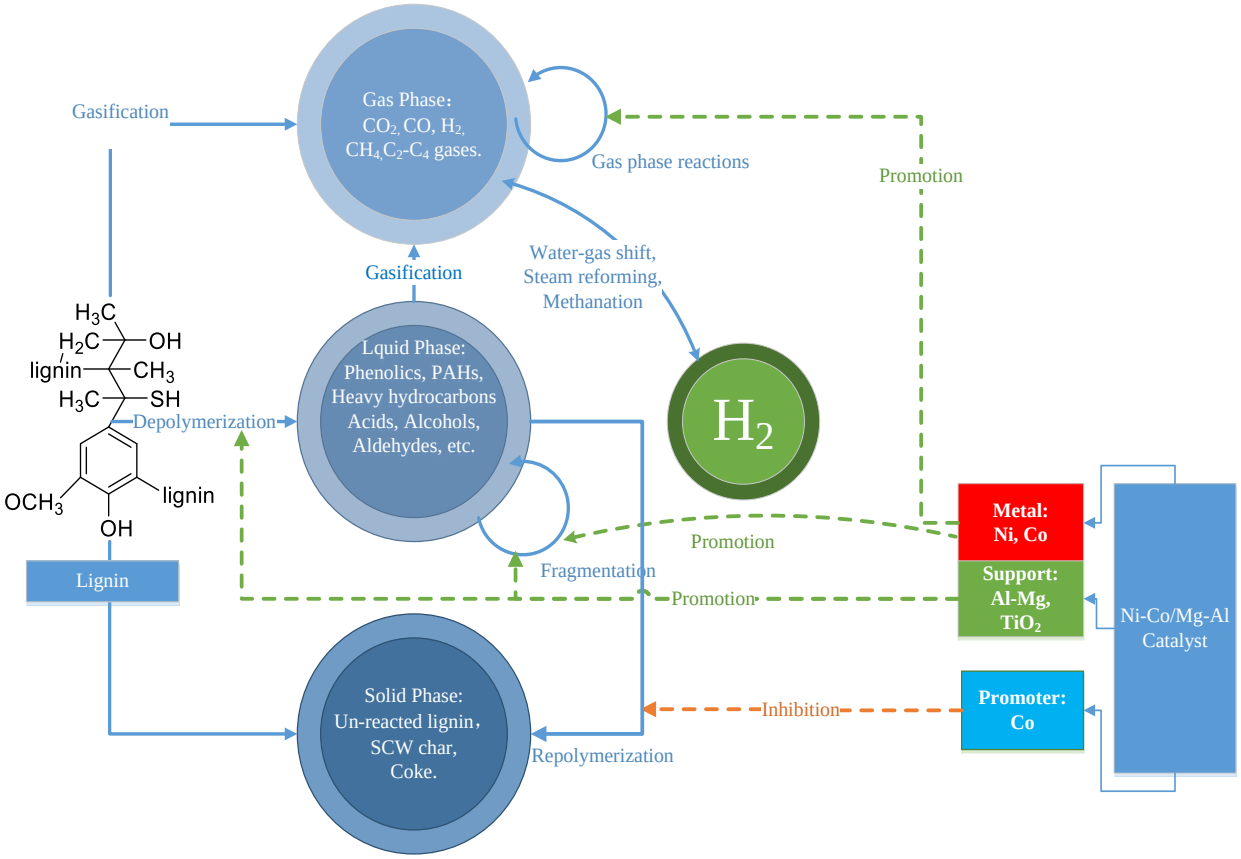

Figure 5.11 Proposed scheme of hydrogen production from lignin SCWG, and effects of different catalysts

As the main focus of current research, it was found that all three basic components of the heterogeneous catalyst including active metal, support, and promoter, as well as their interactions affect the hydrogen yield of lignin SCWG. To be more specific, without catalyst, under SCW conditions, lignin decomposition happens and four different phases co-exist in the reactor namely: 1) oil phase including main phenolics, PAHs and heavy hydrocarbons; 2) aqueous phase which includes mainly acids, aldehydes, alcohols, and phenols; 3) gas phase including CO_2, H_2, CO, and C_1–C_4 hydrocarbons; and 4) solid phase including products such as undissolved lignin, oligomers, monomers (Fang et al. 2008). Here in Scheme 1, for the ease of discussion 1) oil phase, and 2)

aqueous phase were combined as the liquid phase. Saisu et al. proposed the mechanism of lignin decomposition in SCW (2003). For the two stage mechanism, the first stage is the lignin depolymerization via hydrolysis and dealkylation. The product of this stage is mainly lower-molecular-weight compounds in the liquid phase. These compounds including main phenolics, hydrocarbons, PAHs, alcohols, and aldehydes which all contain reactive functional groups. The second stage is the lignin repolymerization. In this stage, the reactions happen among these intermediates and un-reacted lignin. These reactions cause the formation of undesirable products such as SCW char and coke. Later, a more comprehensive network for lignin SCWG was developed (Kang et al. 2013), and two more stages were introduced to the mechanism namely Stage 3. fragmentation: the secondary decomposition of the lower-molecular-weight liquid products via the cleavage of aromatic C–C bond in phenolic products; Stage 4. gas-phase reactions: during this stage, the products in the gas phase react with each other and led to the change of gas composition of the product. For the fourth stage, the reactions might happen as listed below:

Water-gas shift reaction: $CO + H_2O \rightleftharpoons CO_2 + H_2$……...……(5.1)

Steam reforming reaction: $CH_4 + H_2O \rightleftharpoons CO + 3H_2$……..(5.2)

Methanation reaction: $CO_2 + 4H_2 \rightleftharpoons CH_4 + 2H_2O$…….(5.3)

For catalytic SCWG of lignin, since the repolymerization step leads to coke formation, this stage could be considered as a good evaluator for the coke resistance of the catalyst. In addition, the fragmentation step leads to liquid-gas conversion whereas the gas-phase reaction step affects the hydrogen content in the gas phase, so these two steps correspond well to catalyst activity and selectivity, respectively.

Based on the heterogeneous catalyst studied in this paper, the active metal Ni mainly plays its role in the gas-phase reaction as well as the fragmentation stage. Specifically, the active metal Ni is active for water-gas shift reaction and steam reforming reaction (reactions 1-2), therefore, can improve not only the gas yield by helping the lignin decomposition but also can improve the hydrogen selectivity in the gas phase (Resende and Savage 2010, Bengaard et al. 2002). This effect was observed in this study, specifically, as is shown in Table 5.4, the gas yield from $5Ni/TiO_2$ is higher than that of the TiO_2 support (11.6 wt% vs. 8.1 wt%). What's more, as is shown in Figure

5.9, the percentage of hydrogen in the product gas from 5Ni/TiO_2 is considerably greater than that of the TiO_2 support (35.2 mol% vs. 19.0 mol%).

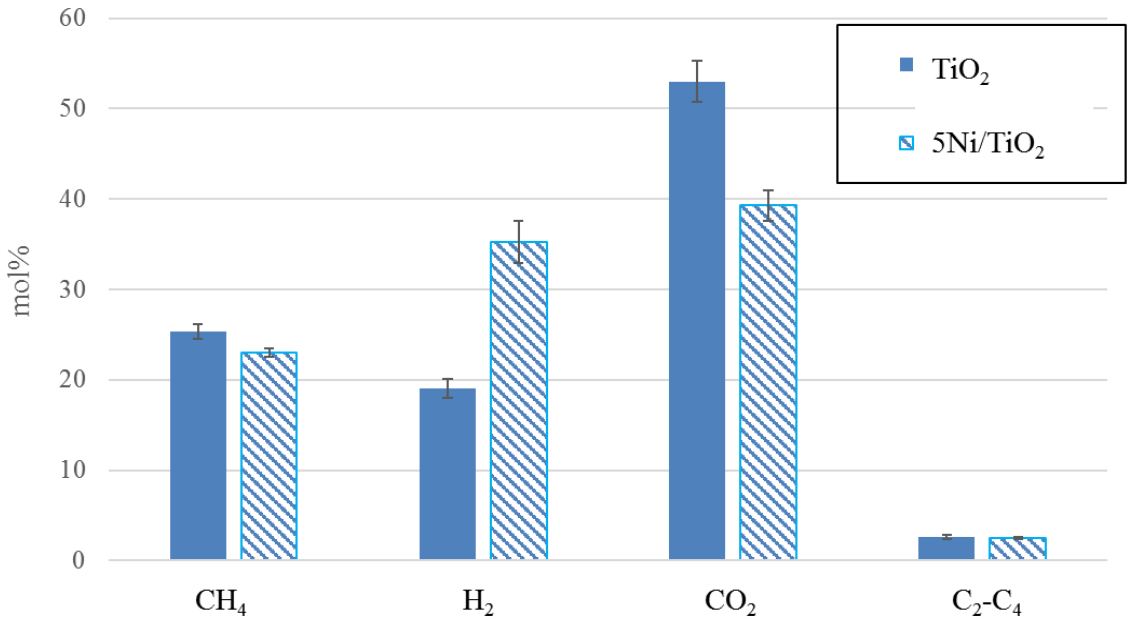

Figure 5.12 Effect of TiO_2 support and 5Ni/TiO_2 catalyst on gas composition

The main role of the secondary metal or the promoter was found to be in hindering the repolymerization reactions and to improve the catalyst coke resistance or activity. For example, the better coke resistance was observed with the Cop.2.6Ni-5.2Co/2.6Mg-Al catalyst with Co as a secondary metal in the catalyst. And the main reason for the better coke resistance is the Ni–Co interaction (Zhang, Wang, and Dalai 2007). For TiO_2 supported Ni catalyst, Co helped to enhance the gas yield. In this case, for 5Ni/TiO_2 catalyst, Co functioned as a promoter and improved the catalyst activity.

In terms of support, the main effects are in the depolymerization as well as fragmentation stage. It was found that for the Mg-Al hydrotalcite supported a catalyst; strong acidity always leads to higher hydrogen yield. As discussed before, acidic sites are active for C—O and C—C bond cleavage, thus stabilizing the liquid phase intermediates and leading to improved gas yield (Ma, Troussard, and van Bokhoven 2012). Therefore, strong acidic sites enhanced the depolymerization as well as fragmentation. The acidity could be fine-tuned by changing the Mg to Al ratio as well as the preparation method. The interaction between the active metal and support is also important in the lignin SCWG process. For example, the better coke resistance showed by the Cop.2.6Ni-

5.2Co/2.6Mg-Al catalyst might be caused by the strong metal–support interaction (Zhang, Wang, and Dalai 2007).

It was summarized that use of the homogeneous alkaline catalyst, including K_2CO_3, KOH, NaOH could significantly improve the H_2 yield for biomass SCWG, and the efficiency of gasification will increase with an increase in the catalyst loading (Fang 2014). However, the reaction mechanism is quite different from the heterogeneous catalyst. Taking K_2CO_3 as one example, for one thing, it helps the decomposition of alcohols and acids which are part of the fragmentation stage thus helping to enhance the gas yield in this process, for another thing, it may form a formate salt (KOOCH). Then format salt reacts with water to produce hydrogen. The reactions mechanism are reported as the reactions 4-7 (Onsager, Brownrigg, and Lødeng 1996).

$$H_2O + K_2CO_3 \rightarrow KHCO_3 + KOH \quad (5.4)$$

$$KOH + CO \rightarrow KCOOH \quad (5.5)$$

$$KCOOH + H_2O \rightarrow H_2 + KHCO_3 \quad (5.6)$$

$$2KHCO_3 \rightarrow H_2O + K_2CO_3 + CO_2 \quad (5.7)$$

Based on the mechanism been proposed, the heterogeneous catalyst is a highly flexible tool for SCWG process as: first, each of its components has its unique role in SCWG. Thus, it provides more routes to improve the process. What's more, fine-tuning of the properties of heterogeneous catalysts could be achieved by thoughtful catalyst design and preparation.

5.6 Conclusions

Two groups of catalysts including Ni-Co/Mg-Al and Ni/TiO_2 catalysts were prepared, characterized and evaluated for producing hydrogen from SCWG of lignin. For the Ni-Co/Mg-Al catalysts, the hydrogen yield could be well correlated with the strong acidic sites within the temperature range of 400-600 °C. For catalyst preparation, coprecipitation is more efficient than impregnation. The better performance of the Cop.2.6Ni-5.2Co/2.6Mg-Al catalyst could be attributed to its high surface area, high coke resistance, and the higher strong acidic strength. For the Ni/TiO_2 catalysts, 5 wt% Ni loading is the optimum for hydrogen production. However, adding Co, Ru, Ce, Mg as promoters did not improve the hydrogen yield. A detailed mechanism for hydrogen production from catalytic SCWG of lignin is proposed. The mechanism provides insight into the roles of different catalyst components including active metal, supporting material, and

promoter in the process, as well as properties required to improve the hydrogen yield. The mechanism also reveals the high flexibility of heterogeneous catalysts for hydrogen production from the SCWG process.

Chapter 6 Hydrogen Production from Lignin, Cellulose, and Waste Biomass via Supercritical Water Gasification: Catalyst Activity and Process Optimization Study

This Chapter is based on: Kang, K., Azargohar, R., Dalai, A.K., Wang, H. Hydrogen production from lignin, cellulose and waste biomass via supercritical water gasification: Catalyst activity and process optimization study. *Energy Conversion and Management*. 117 (2016) 528-37.

Contributions of authors: KANG: (1) preparation of samples and catalysts, (2) performing SCWG tests (3) performing characterizations for gasification products and catalysts, (4) analysing the experimental results, and (5) writing the manuscript and provide responses to reviewers' comments. Dr. Ramin Azargohar examined the experimental design, and reviewed the manuscript. Dr. Ajay K. Dalai and Dr. Hui Wang performed overall supervision of this research, examined the research results, oversaw the preparation of the manuscript, and submitted the papers.

6.1 Knowledge gaps, hypothesis, and objectives

6.1.1 Knowledge gaps

- The performances of promising catalysts identified in this research and in the literature need to be compared under identical reaction conditions.
- The optimization of the process parameters is critical to determine the favorable process conditions to achieve maximum hydrogen production.
- Characterizations of biomass samples for evaluation of the feedstock for SCWG is missing from the literature.

6.1.2 Hypothesis

- Evaluation of catalysts using various feedstocks can provide a better idea of performances of the catalysts.
- Use of Taguchi experimental design and statistical analysis helps to identify the optimum reaction conditions for hydrogen production from catalytic SCWG process.
- Biomass characterization could provide profound insight into the role of feedstock in the process.

6.1.3 Objectives

- To find the best performers as promising homogeneous/heterogeneous catalysts by using both lignin and cellulose as a feedstock.
- To perform Taguchi optimization for four reaction parameters including temperature, biomass type, catalyst type, and catalyst loading to produce hydrogen with maximum yield via catalytic SCWG of lignin.
- To characterize the biomass used in this study to achieve a better understanding of the role of different biomass in the process.

6.2 Abstract

Optimization of process parameters for catalytic biomass supercritical water gasification process (SCWG) was performed. By catalysts screening using cellulose and lignin as biomass model compounds, K_2CO_3, and 20Ni-0.36Ce/Al_2O_3 were identified as the best catalysts. Then, an optimization study based on Taguchi experimental design was conducted, and waste biomass including wheat straw, canola meal, and timothy grass was used as feedstock. The effects of different parameters are studied. The relative importance of different process parameters for hydrogen production follows the order of temperature > catalyst loading > catalyst type > biomass type. High temperature (~650 °C) and high catalyst loading (~100%) based on biomass loading are desirable for hydrogen production. Using different waste biomass, the average hydrogen yield was in the order of canola meal > wheat straw > timothy grass.

6.3 Introduction

Supercritical water gasification (SCWG) refers to gasification with the presence of supercritical water (SCW), which is obtained at pressures above 22.1 MPa and temperatures above 374 °C. It is a promising technology for hydrogen production from biomass.

Catalysis is necessary for hydrogen production from SCWG, as the use of catalyst helps to bring down the high reaction temperature needed for the gasification reactions, which may potentially bring down the cost of the SCWG process. Both hetero/homogeneous catalysts have been tested in SCWG in previous studies. For the homogenous category, catalytic effects of alkaline salts such as K_2CO_3, Na_2CO_3, $KHCO_3$, and NaOH have been evaluated for subcritical and supercritical water gasification (Guo et al. 2010). The mechanism of hydrogen production using alkali salts as

catalysts involving the production of simpler intermediates which could be easily converted to hydrogen. Also, via absorption of produced carbon dioxide, alkali catalysts could also enhance the water-gas shift reaction to generate hydrogen (Fang 2014). In terms of heterogeneous catalysts, both Ni and Ru based catalysts were proved to be effective for SCWG (Guo et al. 2010, Onwudili and Williams 2016). The main route for hydrogen production from these catalysts is through the steam reforming reactions of different hydrocarbons (Fang 2014). The promising activity of Ni-Ru bimetallic catalysts for SCWG of indole was reported in a recently published work(Guo et al. 2015). The main advantage of Ru based catalyst is its high activity whereas Ni based catalyst is favorable because of the low cost and considerable activity.

In literature, different biomass model compounds were used as feedstocks for SCWG to understand the process. Also, technology for hydrogen production from real waste biomass via SCWG process is under development (Hosseini, Wahid, and Ganjehkaviri 2015). In our previous studies, lignin was used as a model biomass to optimize the reaction parameters for a batch type SCW reactor, and the screening/modification of various Ni based catalysts was conducted. As the first step, parameters for non-catalytic SCWG of lignin, three parameters including temperature, pressure, and water to biomass ratio was optimized using Central Composite Design (CCD) with parameters varied in the range of 400 −650 °C, 23 −29 MPa, and 3 −8, respectively. It was found that up to 650 °C, higher temperature is desirable for hydrogen production; however, change of pressure did not show a significant effect (Kang et al. 2015). A similar effect of temperature was observed on the SCWG of marine biomass, where the increase in temperature from 300 to 600 °C improved the hydrogen yield (Deniz et al. 2015). Then, for catalytic SCWG of lignin, under the operation conditions of 650 °C, 26 MPa and water to biomass mass ratio of five, it was observed that: using different supports, the activity of Ni-based catalysts was in the order of Al_2O_3 > TiO_2 >AC > ZrO_2 > MgO. Regarding promoters, the activity of the catalysts were in the order of Ce > Co > Cu (Kang et al. 2016).

Generally, studies based on model biomass provide more fundamental information about the process whereas studies on real biomass provide more information on the performance of the SCWG reactors at various operating conditions (Azadi, Khan, et al. 2012). This study is performed to further understand the effects of reaction parameters in the catalytic SCWG process, and optimize the process operating conditions.

Based on the literature, several gaps need to be filled: first, the performances of promising catalysts identified in the literature need to be compared under identical reaction conditions; also, the performances of catalysts should be evaluated for real biomass rather than model biomass; what's more, the optimization of the process parameters is critical to determine the favorable process conditions to achieve maximum hydrogen production. To fill the knowledge gaps, we present the results from SCWG test of different catalysts, catalyst characterization, biomass characterization, and parameter optimization study of hydrogen yield using Taguchi approach.

One contribution of this work is its comprehensiveness by the broad coverage of biomass materials. Specifically, for the catalyst comparison, lignin and cellulose are used as feedstock. Lignin and cellulose are two main components of biomass, yet, in the plant body, they have different functions. Specifically, cellulose functions as the dominant reinforcing phase in plant structures (Siró and Plackett 2010), whereas lignin functions as glue to hold the lignocellulose matrix together (Zakzeski et al. 2010). Therefore, the effects of the structural difference between them on the catalyst performance provide more insight knowledge for application of each catalyst for real biomass. In addition, for the optimization study, three types of waste biomass such as canola meal (CM), wheat straw (WS), and timothy grass (TG) were used. Wheat straw and Timothy grass are all abundant biomass in the province of Saskatchewan. Canola meal is the by-product of the biodiesel industry and is generally used for animal feed. However, the issue of oversupply drives the need to utilize canola meal as a renewable energy source (Azargohar et al. 2013). To the best of our knowledge, the effects of timothy grass and canola meal for hydrogen production via SCWG were studied the first time. The characterization data presented in this paper provides better insight into the role of different biomass in the process, and the information would also be valuable for a researcher with various research interests.

As another novelty, Taguchi experimental design is applied for the first time for optimization of the SCWG process. Taguchi experimental design is a classic experimental design method dedicated to the optimization of process performance, quality and minimizes its cost (Taguchi 1986). In recent years, application of Taguchi method has been introduced into many research fields, such as chemical engineering, thermal engineering, etc. (Bao et al. 2013). The method involves the use of Taguchi orthogonal array (OA), which is developed based on factorial design (Taguchi 1987). The use of orthogonal array enables the researcher to optimize process parameters with a minimum number of experiments (Lu, Li, and Guo 2014). Also, Taguchi method effectively

maintains the statistical accuracy of the experiments (Chen, Chen, and Hung 2013). Specifically, statistical analysis of the data including analysis of variance (ANOVA) as well as effects of parameters/interactions provide information about the statistical significance of different parameters/interactions and helps to determine the optimum combination of reaction parameters (Venkata Mohan and Venkateswar Reddy 2013). In addition, the application of the Taguchi method enables the evaluation of the relative importance of different reaction parameters.

The work presented in this paper is also significant due to the wide range of catalysts used. First, the effect of different methods including impregnation and coprecipitaion, on the performance of Ni-Ce/Al_2O_3 are reported for the first time. In addition, this paper reports results from SCWG tests of various homo/heterogeneous catalysts combined with data from systematic characterizations of both catalysts and biomass samples. Information in this chapter should be helpful to explore the mechanism of each catalyst function for gasification of biomass model compounds as well as real biomass under supercritical water condition.

6.4 Material and method

6.4.1 Catalyst preparation

Catalysts tested in this study were prepared by impregnation (Imp.) or coprecipitation (Cop.) method. Chemicals used for the catalyst preparation including $Ni(NO_3)_2{\cdot}6H_2O$, $CeCl_3{\cdot}6H_2O$, $Al(NO_3)_3{\cdot}9H_2O$ were supplied by Sigma-Aldrich (Oakville, Canada). Ruthenium(III) nitrosylnitrate was supplied by Alpha Aser (Ward Hill, USA). Catalyst supports such as Al_2O_3 and TiO_2 both were supplied by Alpha Aesar (Ward Hill, USA).

Before preparation, the amount of precursors used were calculated based on the composition of the catalyst. For the impregnation, the precursor was dissolved in water. Then, a 1-mL syringe was used to impregnate the solution into the support. Before calcination, the catalyst was dried in an oven at 105 ^oC for 8 hours. The catalyst was then calcined in flowing air at 650 °C for 6 hours. The coprecipitation (marked as Cop. with their name) method was employed for precipitating Ni, Ce, and Al in their nitrate solution with aqueous ammonia. After filtration, the precipitate was washed and dried and calcined under the same condition with the impregnated catalysts.

6.4.2 Material, SCW reactor, and procedure for SCWG tests

Model biomass sample including lignin and cellulose were purchased from Sigma-Aldrich (Oakville, ON, Canada). Waste biomass samples used were canola meal, wheat straw, and timothy

grass. Canola meal was provided by Milligan Biofuels Inc. (Foam Lake, SK, CANADA). Wheat straw and timothy grass were all collected from a local farm (Saskatoon, SK, Canada). The compressed nitrogen gas (N_2) with high purity (> 99.9%) was purchased from Praxair Canada Inc. (Saskatoon, SK, Canada).

Detailed specifications and schematics of the batch SCW reactor and the experimental procedure could be found in Chapter 3. For the screening tests, operating conditions were all kept at 650 °C, and at 26 MPa with water to biomass mass ratio of five.

6.4.3 Characterization of biomass samples/SCWG char

Moisture and ash content were determined by using ASTM 3173-87(Designation 1996), and ASTM 3174-04 methods (Standard), respectively, using a laboratory muffle furnace (Holpack, USA). Fourier transform infrared spectroscopy (FT-IR) analysis of the biomass samples/SCWG chars were performed using a Spectrum GX FTIR spectrometer (PerkinElmer Inc., USA) using KBr technique, within the range of 400–4000 cm^{-1} under transmittance mode. The elemental composition of biomass samples/SCWG chars were analyzed by an ‘‘Elementar Vario III” elemental analyzer. Through high-temperature decomposition, solid samples were converted into gasses through combustion. 4–6 mg sample was used for each analysis. The higher heating values (HHV) of the biomass samples were measured using an oxygen bomb calorimeter (Parr® 6400 Calorimeter, IL, USA) following ASTM D 5865 method (Standard 2007).

6.4.4 Characterization of catalysts and gas phase product

Characterizations for the fresh catalysts including the N_2 adsorption–desorption, the CO-chemisorption of the fresh catalyst, the wide-angle powder X-ray diffraction (XRD) analysis, and the ammonia temperature programmed desorption (NH_3-TPD). Carbon formation on the spent catalysts was investigated by TG/DTG (thermogravimetry/derivative thermogravimetry) analysis. Analysis of the gas phase products was performed using Agilent GC 7890A gas chromatograph. Helium was used as carrier gas. The molar percentage composition of the gas phase was calculated by using peak normalization method, and the molar amount of N_2 gas was used as a reference. The details of these characterizations could be found in previous chapters.

6.4.5 Data interpretation

The definitions of hydrogen and gas yield reported in this paper can be found in previous chapters. For the composition of catalysts, the numbers (e.g., 5, 20) before active metal such as Ni/Ru

indicates the weight percentage of Ni/Ru with respect to the weight of the catalyst. The number before the promoter (e.g., Ce) indicates the specific molar ratio of the promoter to the active metal. For several Al_2O_3 supported catalysts, Cop. in their name indicates that the catalyst was prepared by coprecipitation method. For example, the Cop.20Ni-0.36Ce/Al_2O_3 catalyst is prepared by coprecipitation method and supported by Al_2O_3, it has 20 wt% Ni as the active phase, with Ce as the promoter, Ce/Ni molar ratio is 0.36.

6.4.6 Taguchi experimental design for optimization study

For the optimization of reaction parameters, the effects of four parameters including catalyst type, temperature, biomass type and catalyst loading were investigated and optimized. Taguchi approach was followed to design the experiments (DOE), and the DOE was performed using Minitab software. Taguchi approach establishes a series of experimental runs with parameters at different levels referred to as orthogonal array to reduce errors and to enhance the efficiency and reproducibility of the laboratory experiments (Venkata Mohan and Venkateswar Reddy 2013). The performance of the Taguchi approach is measured by the deviation between a characteristic from the target value and the loss function derived from statistics (Liao and Kao 2010). The loss function (L(y)) can be formulated in a quadratic form as:

$$L(y) = k \times (y-m)^2 \quad \text{.....(6.1)}$$

where k is the average loss coefficient which is dependent on the the magnitude of the characteristic, y is the observed response by experiments, and m is the targeted response. In this study, the loss function works under the objective of maximization of the hydrogen yield. Design parameters investigated as well as their types/levels are listed in Table 6.1. The other conditions were controlled at: pressure = 26 MPa, water to biomass ratio = 5, and biomass loading = 0.65 g. According to the experimental design ($L_{18} = 2^1 \times 3^3$ orthogonal array), eighteen runs was required, and the interaction between factors A: catalyst type, and C: biomass type was taken into account.

Table 6.1 Operating parameters and levels used for conducting Taguchi experimental design

Factors	Control parameters	Type/Level Settings		
		1	2	3
A	Catalyst type	Best homogeneous catalyst	Best heterogeneous catalyst	
B	Temperature (°C)	450	550	650
C	Biomass type	Canola Meal (CM)	Wheat straw (WS)	Timothy grass (TG)
D	Catalyst loading (%)	25	50	100

6.5 Result and discussion

6.5.1 Effect of catalysts on hydrogen yield

As the first step of this study, comparison of homo/heterogeneous catalysts for hydrogen production was performed using lignin/cellulose as model biomass. The performance of two homogenous and five heterogeneous catalysts was evaluated for hydrogen production from both lignin and cellulose, and the results are listed in Table 6.2. Considering the small volume of the SCW reactor, the volume of catalyst/support may affect the contact between SCW and biomass (Kang et al. 2016). Therefore, to avoid the impact of this issue, SCWG test with Al_2O_3 was performed as a blank test and data were provided for reference.

As homogeneous catalysts, K_2CO_3 showed better performance than Na_2CO_3 in terms of hydrogen yield from SCWG of both lignin and cellulose. The highest hydrogen yield was observed from K_2CO_3 on SCWG of lignin at 2.86 mmol/g, which nearly doubled than that of Na_2CO_3. Similar trend was reported by Muangrat et al. (Muangrat, Onwudili, and Williams 2010), where SCWG of glucose at 330 °C temperature and 13.5 MPa was studied using various alkali catalysts, and catalyst performance for the hydrogen yield was in the ordered of NaOH > KOH > $Ca(OH)_2$ > K_2CO_3 > Na_2CO_3 > $NaHCO_3$.

Table 6.2 Effect of different homogeneous/heterogeneous catalysts on hydrogen/gas yield from lignin/cellulose

Catalyst group	Catalyst	Gas yield from lignin (wt%)	Hydrogen yields from lignin (mmol/g)	Gas yield from cellulose (wt%)	Hydrogen yields from cellulose (mmol/g)
Blank test					
	Al_2O_3	8.4 ± 0.1	1.50 ± 0.06	6.2 ± 0.05	0.40 ± 0.02
Homogeneous catalysts					
	Na_2CO_3	12.4 ± 0.2	1.48 ± 0.08	18.7 ± 0.8	1.52 ± 0.03
	K_2CO_3	18.0 ± 0.6	2.86 ± 0.08	23.3 ± 0.6	2.12 ± 0.10
Heterogeneous catalysts					
	20Ni-0.36Ce/Al_2O_3 *	12.9 ± 0.1	2.15 ± 0.08	17.8 ± 0.7	1.90 ± 0.08
	20Ni/Al_2O_3 *	8.2 ± 0.2	0.78 ± 0.03	12.8 ± 0.4	1.18 ± 0.06
	Cop.20Ni/Al_2O_3	6.5 ± 0.2	0.43 ± 0.03	11.8 ± 0.3	0.84 ± 0.03
	Cop.20Ni-0.36Ce/Al_2O_3	6.1 ± 0.2	0.37 ± 0.02	8.9 ± 0.5	0.61 ± 0.05
	5Ru-Al_2O_3	9.2 ± 0.3	1.13 ± 0.02	6.8 ± 0.3	0.94 ± 0.05

*The results on lignin have been reported in Chapter 4, they are listed here for reference.

In their study, two functions of these alkali salts were summarized as: first, promote biomass decomposition in SCW, second, enhance the hydrogen yield via water-gas shift reaction, and inhibit coke formation. The better performance of K_2CO_3 observed could be due to its higher basicity than that of the Na_2CO_3. The main function of the alkaline catalysts in SCWG is to strengthen the basicity of the medium, which in turn leads to the decomposition of biomass into gasifiable intermediates (Muangrat, Onwudili, and Williams 2010).

In terms of the heterogeneous catalyst group, the best performance was found to be for 20Ni-0.36Ce/Al_2O_3 catalyst prepared by impregnation, which showed the highest hydrogen yield of 2.15 mmol/g from lignin. The 5Ru/Al_2O_3 catalyst showed higher hydrogen yield (1.13 mmol/g) than that of 5Ni/Al_2O_3 catalyst that was tested in a previous study with lignin (0.91 mmol/g) (Kang et al. 2016). This observation confirms that, when supported by Al_2O_3 with the same metal loading of 5 wt%, Ru is more active than Ni for hydrogen production via SCWG of lignin.

The surface and porous properties of heterogeneous catalyst/catalyst supports are reported in Table 6.3. The results indicate that for both Al_2O_3 and TiO_2 support, the impregnation of active metals leads to a considerable decrease in BET surface area. The highest surface area of the group was shown by Cop.20Ni/Al_2O_3 catalyst (287 m^2/g), followed by 5Ru/Al_2O_3 (226 m^2/g). Based on the results listed in Table 2, however, high BET surface area will not lead to high hydrogen yield. In

terms of metal dispersion, the highest value was observed on 5Ru/Al_2O_3, which is 8.7 %. But similar to BET surface area, based on SCWG results, no dependency of hydrogen yield on metal dispersion was observed.

Table 6.3 Surface and porous properties of different heterogeneous catalysts/catalyst support

Catalyst	BET surface area (m^2/g)	Total pore volume (cm^3/g)	Pore size (nm)	Metal dispersion (%)	Metallic surface area (m^2/g sample)	Metallic surface area (m^2/g metal)	Crystallite size (nm)
Al_2O_3	262	0.74	11	NA	NA	NA	NA
20Ni-0.36Ce/Al_2O_3	202	0.53	10	2.1	3.5	14.9	47.0
20Ni/Al_2O_3	195	0.5	10	1.7	2.3	11.4	59.3
Cop.20Ni/Al_2O_3	287	0.39	5	4.0	5.3	26.5	25.4
Cop.20Ni-0.36Ce/Al_2O_3	280	0.38	5	1.3	2.4	9.7	87.2
5Ru-Al_2O_3	226	0.65	12	8.7	1.6	31.9	15.1

6.5.2 Further discussion on effect of 20Ni-Ce/Al_2O_3 Catalyst group

6.5.2.1 Effect of preparation method

Results in Table 6.2 show that for 20Ni/AL_2O_3 catalyst group, impregnation method is better than coprecipitation. Specifically, the highest hydrogen yield was obtained by using 20Ni-0.36Ce/Al_2O_3, which is 2.15 mmol/g from lignin and 1.90 mmol/g from cellulose. In comparison, the lowest yield was found by using Cop. 20Ni-0.36Ce/Al_2O_3, which was 0.37 mmol/g with lignin, and 0.61 mmol/g with cellulose.

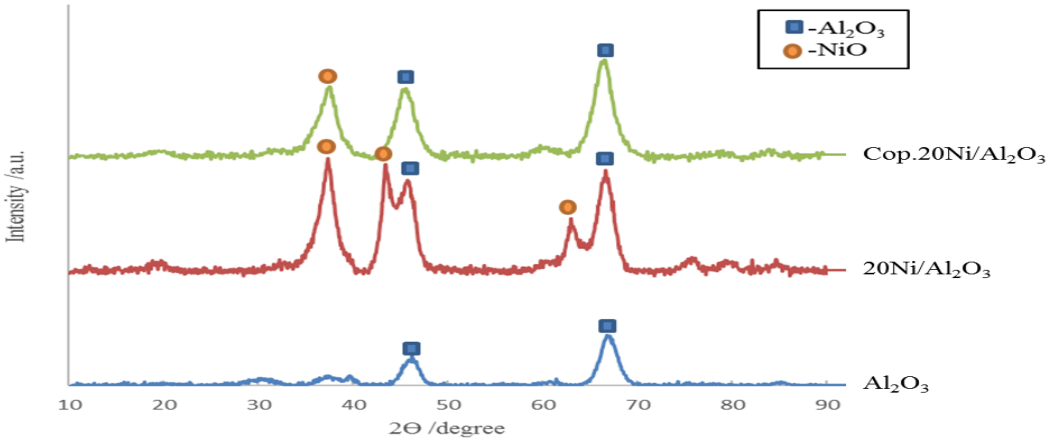

Figure 6.1 XRD patterns of 20Ni catalysts and Al_2O_3 catalyst support

Characterization results in Table 6.3 indicate that coprecipitation method leads to higher BET surface area of the catalyst. However, the effect of preparation method on metal dispersion was

not clear. Specifically, without Ce promoter, the Cop.20Ni/Al_2O_3 catalyst showed higher metal dispersion than the impregnated 20Ni/Al_2O_3 catalyst: 4.0 % and 1.7 %, respectively. However, with Ce promoter, the reverse trend was observed where Cop.20Ni-0.36Ce/Al_2O_3 showed lower metal dispersion (1.3 %) than the Imp. catalyst (2.1 %). The XRD patterns of 20Ni/AL_2O_3 catalysts prepared by both methods were plotted in Figure 6.1 with the pattern of Al_2O_3 support for reference. As the XRD patterns show, the intensity of NiO diffraction peaks at 2Θ positions of 34.7°, 43.0° and 63.2° decreased or even became undetectable with the change of preparation method from impregnation to coprecipitation.

Table 6.4 NH_3-TPD results for the 20Ni-Ce/Al_2O_3 catalyst group

Catalyst Name	Acid content (umol/g)			
	Weak (100-200 °C)	Medium (200-400 °C)	Strong (400-600 °C)	Total
20Ni-Al_2O_3	122	0	37	160
20Ni-0.36Ce/Al_2O_3	0	28	117	145
Cop.20Ni-Al_2O_3	50	480	11	541
Cop.20Ni-0.36Ce/Al_2O_3	10	66	0	76

Surface acidity of this catalyst group was investigated by NH_3-TPD technique, and the results are given in Table 6.4. Based on these results, no clear effect of preparation method was found on the total acid amount of the catalyst. However, a number of strong acid sites, which was assigned to the acidic site in the temperature range of 400-600 °C, were increased by using impregnation method. It was found in this study that different surface acidity is needed for effective conversion of different biomass components, and detailed description is discussed later.

6.5.2.2 Effect of Ce promoter

Results in Table 6.2 show that for impregnated 20Ni/Al_2O_3 catalyst, the addition of Ce promoter significantly improved the hydrogen yield for both lignin and cellulose. However, for the coprecipitated catalyst, less hydrogen yield was observed with Ce promoter. A detailed discussion of Ce promoter on impregnated Ni/Al_2O_3 could be found in our previous paper (Kang et al. 2016).

As our previous conclusion, with impregnation, Ce promoter could effectively enhance the coke resistance as well as reducibility of the catalyst by promoting the Ni dispersion and weakening the interaction between Ni and Al_2O_3 (Kang et al. 2016). The finding is confirmed here: first, as is shown in Table 3, for impregnated catalysts, the higher metal dispersion was given by Ce promoted 20Ni/Al_2O_3 catalyst. Second, the TG/DTA profiles of spent 20Ni/Al_2O_3 catalysts with/without Ce

promoter (Figure 6.2) from SCWG of cellulose proves that Ce promoted 20Ni/Al_2O_3 catalyst have better coke resistance.

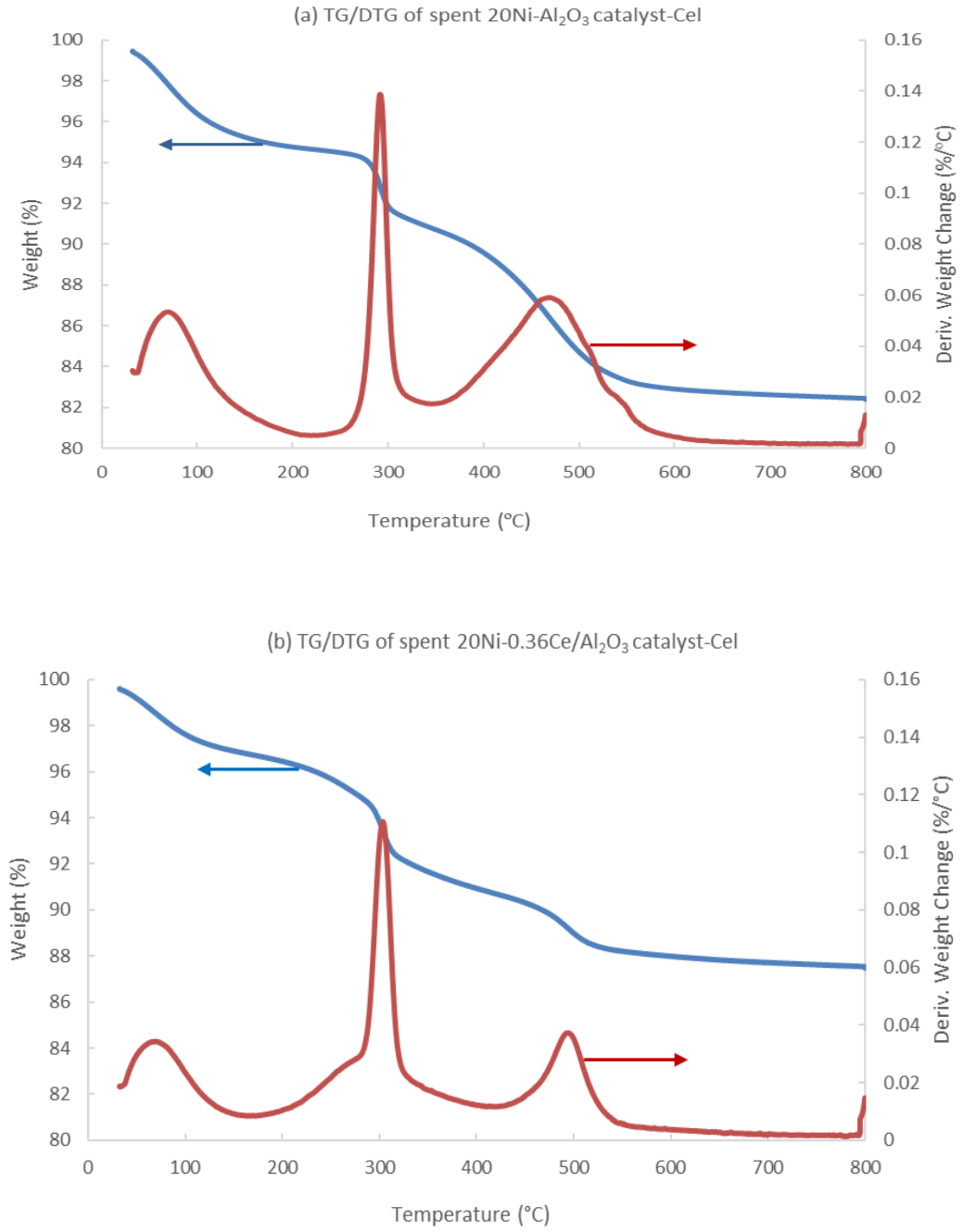

Figure 6.2 TG/DTG profiles of spent 20Ni-0.36Ce/Al_2O_3 catalyst from cellulose

Specifically, as illustrated in the TG profiles, the spent 20Ni-0.36Ce/Al_2O_3 catalyst showed less weight loss than that of the spent 20Ni/Al_2O_3 catalyst (12.5 wt% vs. 17.6 wt%). This observation

confirms that in terms of quantity, less coke was accumulated on the Ce promoted catalyst during the reaction. What's more, on the DTG profiles, smaller oxidation peaks in the range of 400-500 °C were observed when Ce was used as the promoter. Generally, oxidation peaks appearing in high-temperature range could be assigned to carbon deposits with various extents of crystallization and hard to oxidize (Natesakhawat et al. 2005). Therefore, in terms of quality, less crystallized carbon deposit was observed on the Ce promoted catalyst.

6.5.3 Statistical analysis for the optimization study

The results of optimization experiments, including controlling parameters as well as hydrogen yield are given in Table 6.5. The best catalysts in homo/heterogeneous group including K_2CO_3 and 20Ni-0.36Ce/AL_2O_3, respectively, were identified by the catalyst screening procedure mentioned above.

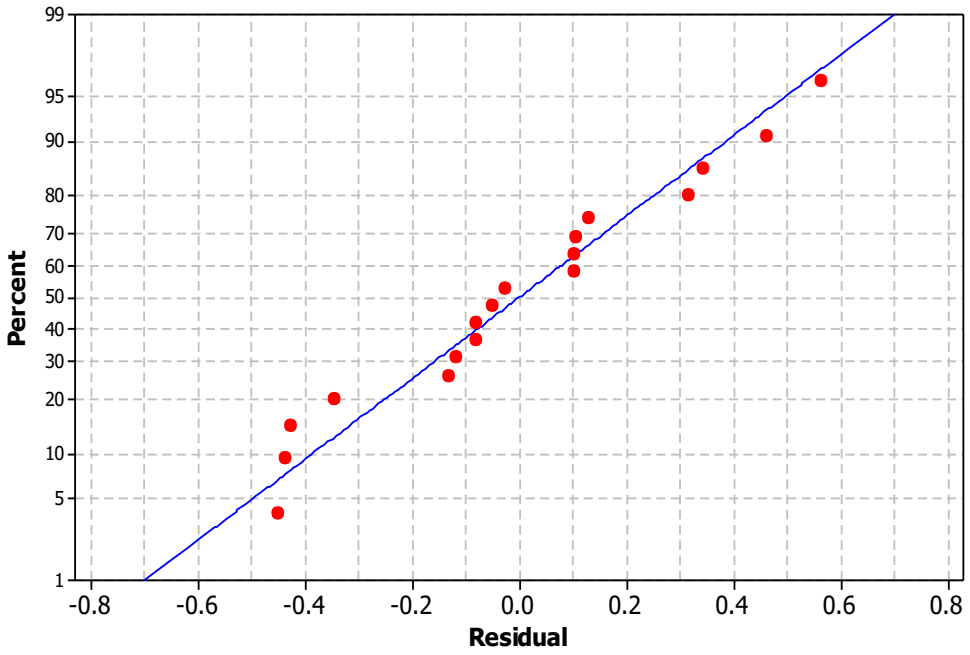

Figure 6.3 Normal probability plot of means for hydrogen yield

The normality of the experimental response (hydrogen yield) was checked by the normal probability plot shown in Figure 6.3. In this plot, the residuals were plotted versus their expected values when the distribution is normal. In this case, the normal distribution of the results is confirmed by the fact that most of the data points follow a straight line (Minitab 2006).

Table 6.5 Level combination from Taguchi experimental design (L18 orthogonal array) and results from corresponding experiments

Run No.	Catalyst type	Temperature (°C)	Biomass type	Catalyst loading (%)	Hydrogen Yield (mmol/g)
1	K_2CO_3	450	CM	25	0.42
2	K_2CO_3	550	CM	50	1.60
3	K_2CO_3	650	CM	100	3.36
4	K_2CO_3	450	WS	25	0.72
5	K_2CO_3	550	WS	50	1.43
6	K_2CO_3	650	WS	100	2.08
7	K_2CO_3	450	TG	50	0.14
8	K_2CO_3	550	TG	100	1.83
9	K_2CO_3	650	TG	25	1.36
10	20Ni-0.36Ce/AL_2O_3	450	CM	100	0.11
11	20Ni-0.36Ce/AL_2O_3	550	CM	25	0.86
12	20Ni-0.36Ce/AL_2O_3	650	CM	50	1.92
13	20Ni-0.36Ce/AL_2O_3	450	WS	50	0.25
14	20Ni-0.36Ce/AL_2O_3	550	WS	100	2.01
15	20Ni-0.36Ce/AL_2O_3	650	WS	25	0.87
16	20Ni-0.36Ce/AL_2O_3	450	TG	100	0.29
17	20Ni-0.36Ce/AL_2O_3	550	TG	25	0.48
18	20Ni-0.36Ce/AL_2O_3	650	TG	50	1.54
Predicted optimum condition and result	K_2CO_3	650	CM	100	2.89
Repeat of optimum condition and result	K_2CO_3	650	CM	100	3.31

Results from ANOVA of means of hydrogen yield are given in Table 6.6. In this table, p-values of individual parameters are all less than 0.05 (95% confidence level). However, the p-value of interaction between catalyst type and biomass loading is 0.577. The result indicates that all four parameters are significantly related to hydrogen yield but the interaction effect is not. What's more, sequential and adjusted sums of squares (Seq. SS & Adj. SS) in this table reflect the relative importance of individual parameters. Specifically, the factor with the largest sum of squares has the greatest impact on hydrogen yield, which is the temperature in this case.

Table 6.6 Analysis of variance for means for hydrogen yield

Source	DF	Seq. SS	Adj. SS	Adj. MS	F	P
Catalyst type	1	1.18	1.18	1.18	6.18	0.038
Temperature (°C)	2	7.36	7.36	3.68	19.24	0.001
Biomass type	2	0.59	0.59	0.30	1.55	0.001
Catalyst loading (%)	2	2.07	2.07	1.07	5.42	0.033
Catalyst type*Biomass type	2	0.23	0.25	0.11	0.59	0.577
Residual Error	8	1.53	1.53	0.19		
Total	17	12.97				

In addition, as the response of different levels of reaction parameters, the means of hydrogen yield were reported in Table 6.7. Data in this table provides a ranking of parameters based on the Delta statistics, which compares the relative importance of effects, and is calculated by the highest minus the lowest average for each factor (Minitab 2006).

Table 6.7 Response table for means of hydrogen yield

Level	Catalyst type	Temperature (°C)	Biomass type	Catalyst loading (%)
1	1.438	0.3216	1.378	0.7837
2	0.9253	1.3691	1.2266	1.1481
3		1.8542	0.9403	1.6131
Delta	0.5127	1.5326	0.4376	0.8294
Rank	3	1	4	2

The rank indicates that temperature is the most important parameter for hydrogen production. And relative importance of parameters was in the order of temperature > catalyst loading > catalyst type > biomass type. With the goal to increase hydrogen yield, significant parameters should be set at levels to produce the highest mean. The level average hydrogen yields in the response table show that the mean of hydrogen yield was maximized when T = 650 °C, catalyst loading = 100 %, catalyst type = K_2CO_3, and biomass type = CM. This combination has been tested the same in run 3. Also, the predicted hydrogen yield by the Taguchi design and repeat of experiments at optimum condition was listed in Table 5. Based on the result, the repeated run showed good repeatability with run 3 (hydrogen yield = 3.31 vs. 3.36 mmol/g), which is within the variance range of ± 5%. However, actual runs produced a higher amount of hydrogen than the predicted value (2.89 mmol/g). This could be explained by the relatively low value of adjusted coefficient of determination (R-squared), which is 74.9% from the linear model built by the Taguchi design. This

also means that the relationship between hydrogen yield and parameters investigated in this study cannot be fully explained by a linear model.

6.5.4 Effect of reaction parameters

6.5.4.1 Effect of catalyst type

The effect of the individual parameter on hydrogen yield can be seen from the main effect plot (Figure 6.4), where means of hydrogen yield versus each parameter at different levels are plotted. As the figure shows, catalyst 1 (K_2CO_3) produced higher hydrogen yield than catalyst 2 (20Ni-Ce/Al_2O_3) from real biomass.

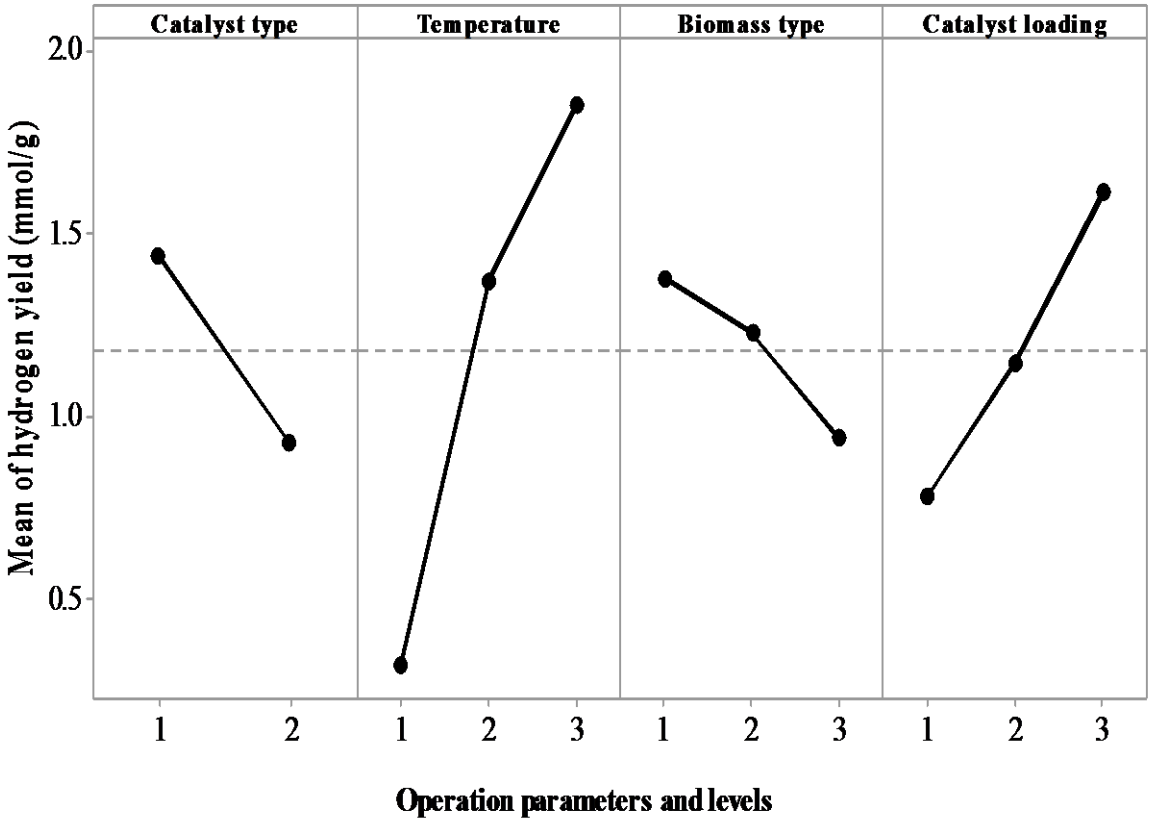

Figure 6.4 Main effects plot of hydrogen yield versus operating parameters

Also, data in Table 6.2 confirms that K_2CO_3 performed better than 20Ni-Ce/Al_2O_3 in SCWG of both lignin and cellulose. Specifically, the data shows that with model compounds, K_2CO_3 produces a higher amount of gas phase products than 20Ni-0.36Ce/Al_2O_3 on both of the model

biomass. However, the gas composition from both lignin and cellulose SCWG which is shown in Figure 6.5 indicates that change of catalyst type from K_2CO_3 (homogenous) to 20Ni-0.36Ce/Al_2O_3 (heterogeneous) has no significant effect on the gas composition of the final product.

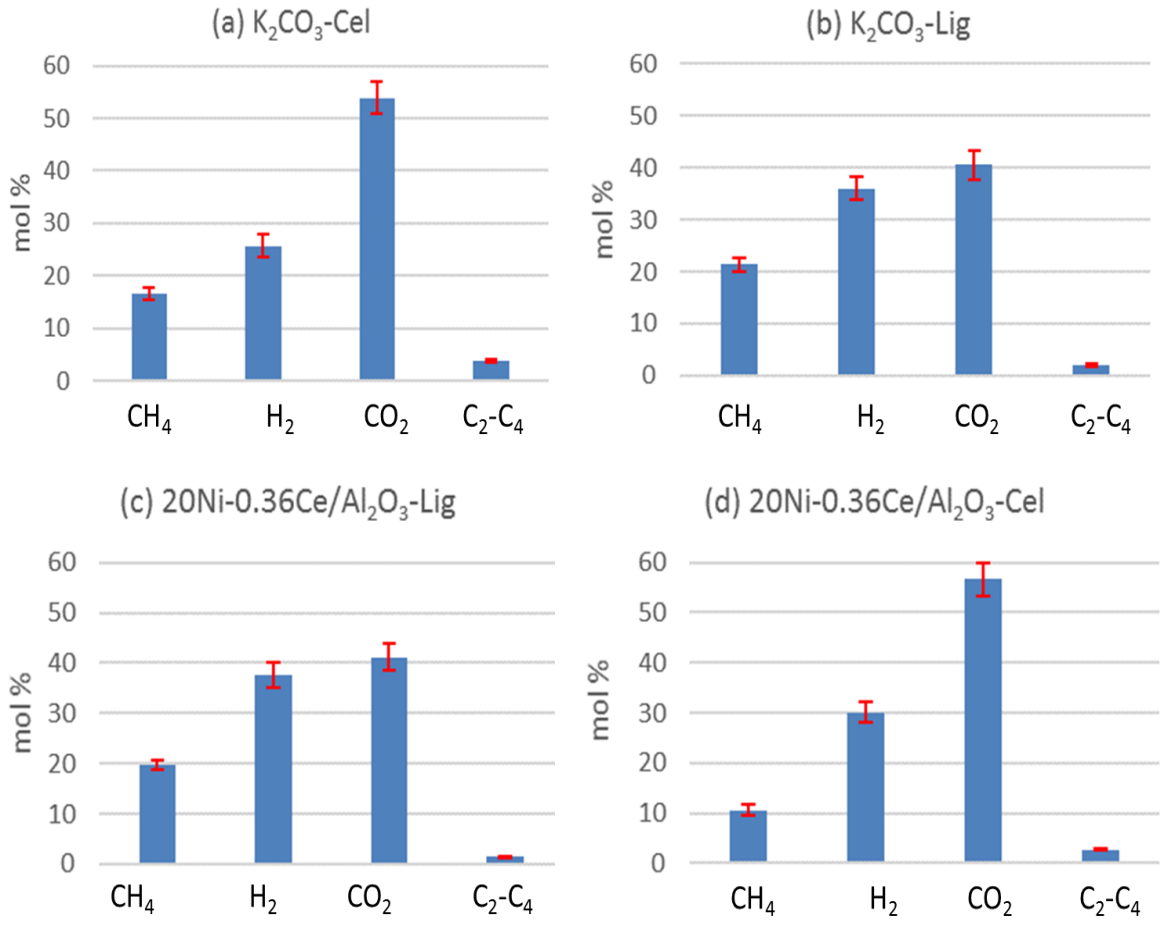

Figure 6.5 Gas phase composition from SCWG of lignin/cellulose using K_2CO_3 and 20Ni-0.36Ce/Al_2O_3 as catalysts

The effect of best homo/heterogeneous catalyst on the SCWG char was characterized by FT-IR and the spectra are given in Figure 6.6. First, compared to fresh CM sample, IR peaks at around 3278 cm^{-1} which are assigned to —OH stretching vibration as well as the peaks at 2854 and 2921 cm^{-1} which are originated from C—H stretching of alkanes were not detected on the SCWG chars (Nanda et al. 2013). Compared to fresh CM, the SCWG char contains much lower content of moisture, also, most of the unreacted alkanes were removed by the separation procedure. Secondly, the peaks in the range of 1500 -1743 cm^{-1} were not found on SCWG chars.

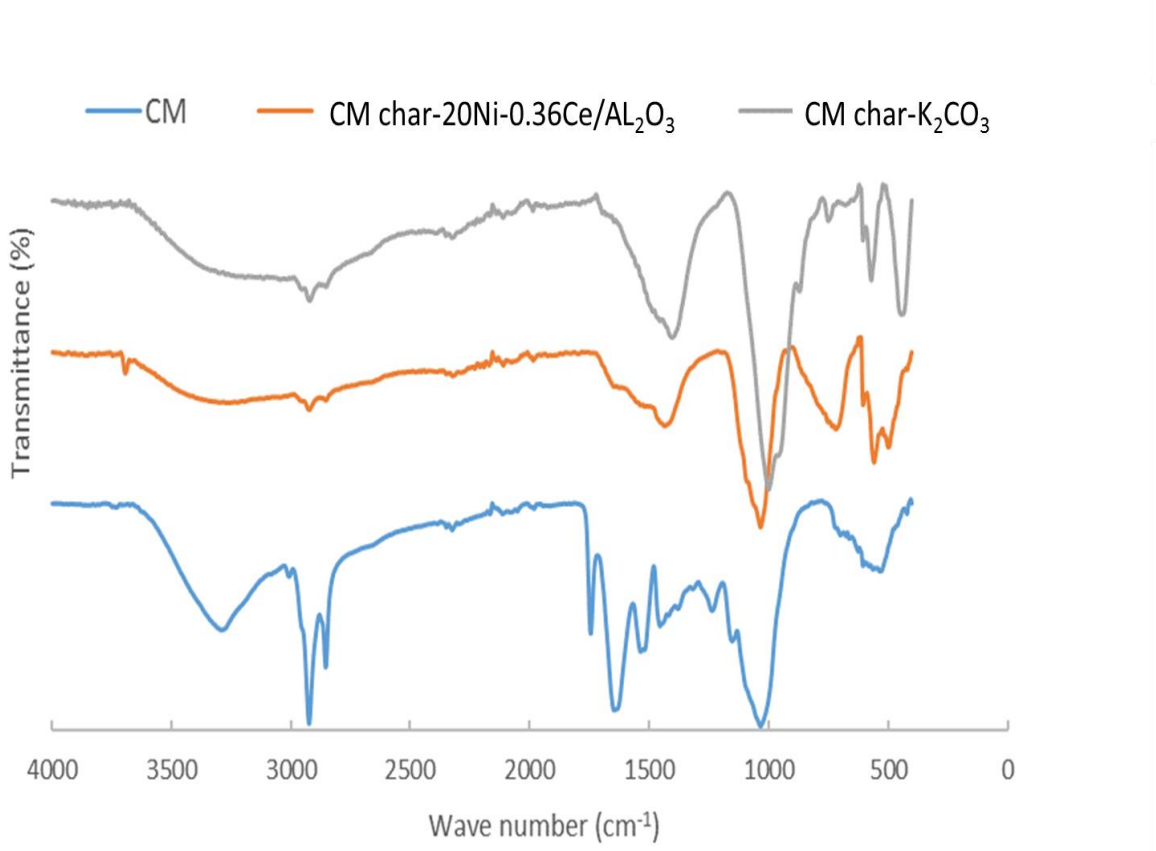

Figure 6.6 FT-IR spectra of CM and SCWG char from CM using best homo/heterogeneous catalysts

Based on the literature, these are characteristic peaks of stretching of C—C bond in aromatic rings (1521 cm^{-1} and 1631 cm^{-1}), and stretches of C=O bond in aldehydes, esters, ketones, carboxylic acids (1745 cm^{-1}) (Nanda et al. 2013). Also, the difference between K_2CO_3 and 20Ni-0.36Ce/Al_2O_3 can be identified by the spectra. Specifically, as compared to 20Ni-Ce/Al_2O_3, for K_2CO_3 FT-IR spectrum: peak at 1396 cm^{-1} becomes more detectable, which is assigned to the CH_2 bending (Sun et al. 2004). What's more, intensities of peaks are different on these two spectra, indicating that catalyst type will affect the functional composition of the SCWG chars.

6.5.4.2 Effect of temperature

The predominant effect of temperature on hydrogen production via SCWG was confirmed by Taguchi approach here and is also reported in the literature (Lu et al. 2012b). As the result given in Table 6.7, the average hydrogen yield increased from 0.32 mmol/g to 1.85 mmol/g with an increase of temperature from 450 °C to 650 °C. However, as is shown in Figure 6.4, at a

temperature higher than 550 °C, the trend of increase in average hydrogen yield with an increase in temperature slows down. This indicates that the optimum temperature for hydrogen production from SCWG of biomass is still higher than 650 °C but might be close. This observation is in coherence with the previous result that for effective SCWG of biomass with high loading, the temperature of 750 °C or higher is necessary (Lu et al. 2012b).

6.5.4.3 Effect of biomass type

As is shown in Figure 6.4, using different biomass, the average hydrogen yield was in the order of CM > WS > TG. This result is reasonable based on biomass characterization. Specifically, the analysis results shown in Table 8 indicate that CM has the highest HHV, which is 21.3 MJ/Kg. What's more, another reason might be that the lignin content of different biomass is in the order of TG (18.1 wt%) > WS (16.3 wt%) > CM (12.0 wt%) (Nanda et al. 2013, Tilay et al. 2014). As lignin is more stable under hydrothermal condition than other components. In addition, what should be mentioned here is that the ash content of different biomass is in the order of CM > WS > TG. The higher ash content may also play a role in the better performance of CM.

6.5.4.4 Effect of catalyst loading

Figure 6.4 and data in Table 6.7 show that for both K_2CO_3 and 20NI-0.36Ce/Al_2O_3, the hydrogen yield could be increased by an increase in catalyst loading from 25% to 100%. In the case of K_2CO_3, this trend could be explained by the fact that consumption of K_2CO_3 occurs in the SCWG process. As K_2CO_3 will act as a reactant to form an intermediate (KOOCH) which is then reacted with water to generate hydrogen following the reaction pathway mentioned in the literature (Onsager, Brownrigg, and Lødeng 1996). In the case of the 20Ni-0.36Ce/Al_2O_3 catalyst, the increase in hydrogen yield with an increase in catalyst loading could be explained by the presence of more nickel as an active phase of the SCWG process.

6.5.5 Further discussion on biomass properties and its effect on SCWG process

6.5.5.1 Effect of Cellulose and Lignin as model biomass for hydrogen production

As an interesting observation of this study, as shown in Table 2, from both K_2CO_3 and 20Ni-0.36Ce-Al_2O_3 catalysts, lower hydrogen yield was produced from cellulose than lignin. However, the gas yield from cellulose is significantly higher than that of lignin. A clearer idea could be obtained from the comparison of the gas phase composition. As is shown in Figure 6.5, the product gas from lignin always contains a higher content of hydrogen than that from cellulose.

Several factors might contribute to this observation. Firstly, as reported in Table 6.8, the ash content in lignin sample (13.9 wt%) is significantly higher than that of the cellulose (0.1 wt%). The high ash content present in the lignin sample might be introduced by the preparation method. To be more specific, the lignin sample used in this study was Alkali lignin, which was produced by Kraft pulping process. Kraft pulping process involves degradation of wood chips in sodium hydroxide and sodium sulfide aqueous solution from approximately 70 °C to 170 °C, and lignin was obtained after removal of undesirable extractives (Gierer 1980). So there is a possibility for the alkali metals to be introduced to the sample via the pulping process, which stays as impurities.

Table 6.8 Result of elemental analysis and heating value of biomass samples

Biomass	Cellulose sample	Lignin sample	Canola meal	Wheat straw	Timothy grass
Moisture (wt%)	5.7	5.3	5.4	3.9	3.5
Ash (wt%)	0.1	13.9	6.6	4.0	3.9
N (wt%)	0.0	0.1	6.3	0.4	0.9
C (wt%)	42.3	48.2	46.7	42.0	42.0
S (wt%)	0.0	4.6	0.9	0.1	0.1
H (wt%)	6.7	4.7	6.7	6.3	6.3
O (wt%)	51.0	28.5	32.9	47.2	46.9
Heating value (MJ/Kg)	16.1	19.2	21.3	16.2	16.6

The alkali metals, such as potassium and sodium in the ash could catalyze the tar cracking reactions as well as water-gas shift reaction, which in turn lead to increase in hydrogen yield (Afif, Azadi, and Farnood 2011). Secondly, correlation curves of hydrogen yield versus strong acid content for 20Ni-Ce/AL_2O_3 catalyst group (Figure 6.7) showed that for hydrogen production, the demand of catalyst acidity is different for different biomass. In SCWG process, acidic sites on the catalyst are active for C—O and C—C bond cleavage, thus can promote the decomposition of feedstock (Ma, Troussard, and van Bokhoven 2012). However, it might also lead to the formation of tarry compounds by catalyzing the polymerization reactions (Azadi, Afif, et al. 2012). In addition, the

interaction of lignin and cellulose in high-temperature wood pyrolysis was observed (Hosoya, Kawamoto, and Saka 2007). Therefore, as a recommendation for future study on hydrogen production from biomass via SCWG, catalyst screening/comparison using different types of model biomass rather than single types provide a better evaluation.

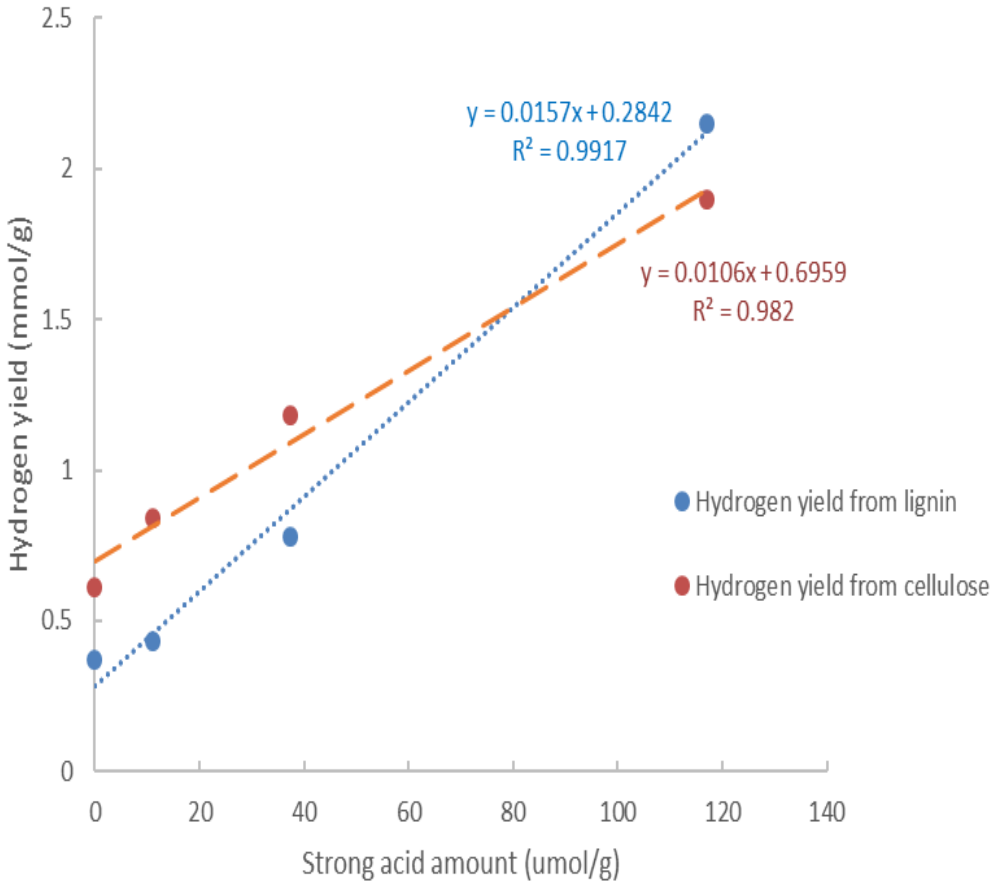

Figure 6.7 Correlation curve of hydrogen yield versus strong acid amount for 20Ni-Ce/Al_2O_3 catalyst group

6.5.5.2 Overview of the SCWG process for hydrogen production from different biomass precursors

A better understanding of the fuel properties of biomass samples could be obtained from the *van Krevelen diagram* (Figure 6.8), where the atomic O/C and H/C ratios were plotted. Generally, biomass ingredients such as cellulose, hemicelluloses and lignin have a significantly higher atomic ratio of H/C and O/C than fossil fuel (Basu 2010). The lignin sample showed lower H/C and O/C ratios than other samples and was more close to fossil fuel in terms of elemental composition. Also,

in terms of waste biomass, CM is significantly lower in O/C atomic ratio than WS and TG, which indicates that CM have more potential as a fuel precursor than others.

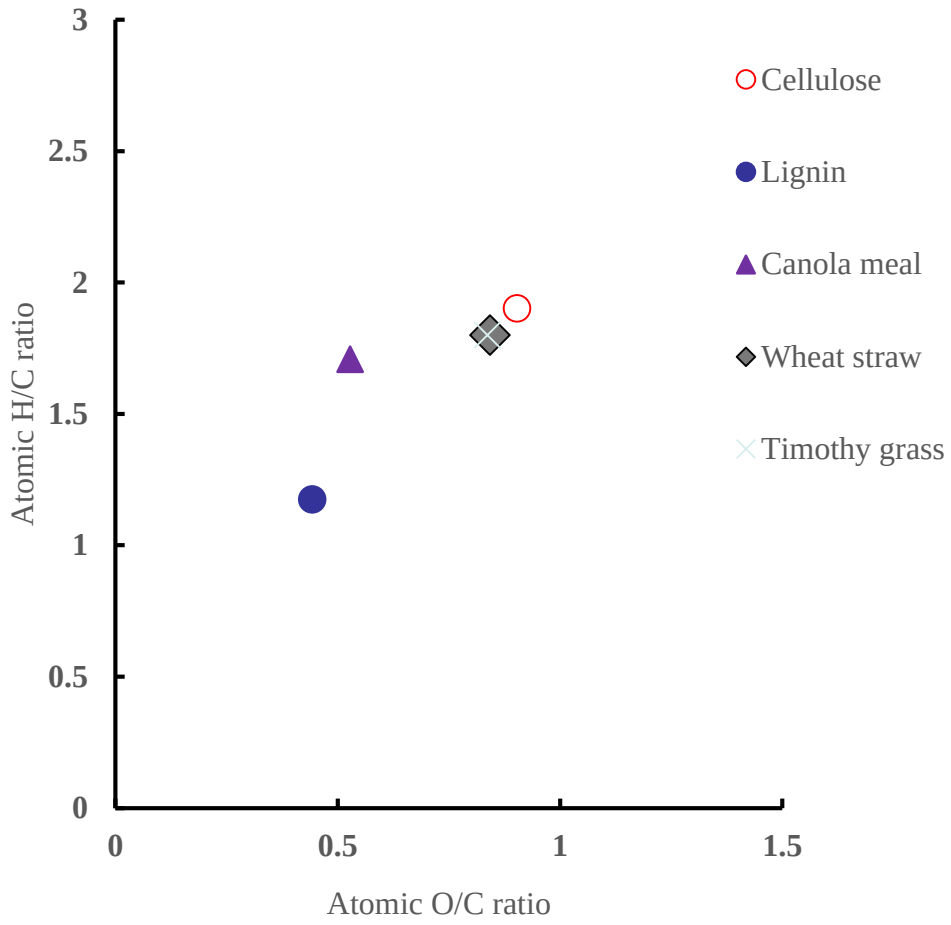

Figure 6.8 Fuel classification curve for biomass samples and gas/char from lignin SCWG

The C—H—O ternary diagram (Figure 6.9) is plotted to better depict the SCWG process. Briefly, three corners of the diagram represent carbon, oxygen, and hydrogen at 100% concentrations, whereas points within the triangle represent the ternary composition of these three elements (Basu 2010). As the figure shows, SCWG of lignin pushes the gas phase product toward the oxygen-hydrogen border with decreased carbon content and increased oxygen content, while the SCWG char was pushed down to the oxygen-carbon border with decreased hydrogen content and increased oxygen content.

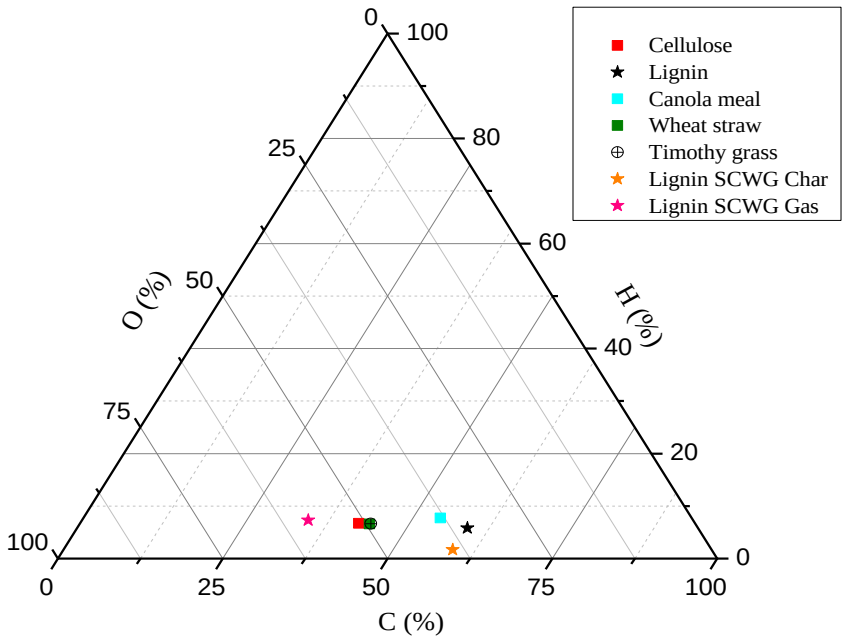

Figure 6.9 C-H-O ternary diagram of biomass samples and lignin SCWG products

6.6 Conclusions

In this research, results of hydrogen production via catalytic SCWG of various biomass samples were presented. K_2CO_3 and 20Ni-0.36Ce/Al_2O_3 were identified as promising homo/heterogeneous catalysts for this process. As confirmed by optimization study based on Taguchi approach, the relative importance of parameters used in this study for hydrogen production was in the order of temperature > catalyst loading > catalyst type > biomass type. The average hydrogen yield using different waste biomass follows the order of canola meal > wheat straw > timothy grass.

Chapter 7 Conclusions and Recommendations

7.1 Conclusions

The core objective of this project was to maximize the hydrogen yield from SCWG process. Lignin was used to study the effects of different reaction parameters without the presence of a catalyst, and these parameters were optimized for hydrogen production using CCD method. Lignin was also used as a biomass model compound for the evaluation of the performance of various catalysts. Promising catalysts were modified to improve their performance in terms of hydrogen yield. Many catalysts have been screened to identify the best performer, including Ni/Ru-based catalyst with different supports and promoters, and Ni-Co bimetallic catalysts supported by the Mg-Al support. To understand the properties of the catalysts, various characterizations have been performed. Also, to facilitate the understanding of the role of different catalysts/catalyst compounds in lignin catalytic SCWG process, the possible reaction mechanism has been proposed. In the last phase of this work, lignin, as well as cellulose, were used as biomass model compounds to evaluate the performance of different catalysts. Wherein, the best heterogeneous catalyst was compared to various homogenous catalysts including K_2CO_3 and Na_2CO_3. A further optimization study of the catalytic SCWG was conducted using Taguchi experimental design. In this phase, three types of real biomass were used in the optimization study including wheat straw, canola meal, and timothy grass. Also, the role of different feedstock in SCWG and the effects of their properties were discussed based on characterizations. Important conclusions of this research are provided below:

For non-catalytic SCWG of lignin:

- For hydrogen production by non-catalytic SCWG, use of high temperature (~650 °C) is crucial.
- At certain temperature, there is a specific value of water to biomass ratio for highest hydrogen yield (e.g., the optimum conditions predicted by the model are Temperature = 651 °C, Pressure = 25 MPa, and Water to biomass mass ratio = 3.9, where the hydrogen yield = 1.60 mmol/g.)

For the screening and modification of the Ni based catalysts:

- Activity of Ni catalyst with different supports was in the order of: Al_2O_3 > TiO_2 > AC > ZrO_2 > MgO.
- The activity of Ni catalyst using different promoters was in the order of Ce > Co > Cu.

- Better performance of Ni-Ce/Al_2O_3 catalyst can be attributed to better Ni dispersion, reducibility as well as coke resistance.

For the screening and modification of the novel catalysts:

- For Ni/TiO_2 catalysts, 5 wt% Ni loading is suitable for hydrogen production.
- For Ni-Co/Mg-Al bimetallic catalysts, higher hydrogen yield could be correlated to strong acidic sites in the range of 400-600 °C, coprecipitation is better than impregnation for preparation.

For the optimization of the catalytic SCWG process using real biomass:

- K_2CO_3 and 20Ni-0.36Ce/Al_2O_3 are promising catalysts for hydrogen production from biomass.
- High temperature and high catalyst loading are desirable for high hydrogen yield.
- The average hydrogen yield using different biomass residues follows the order of canola meal > wheat straw > timothy grass.

Above all, K_2CO_3 and 20Ni-0.36Ce/Al_2O_3 were identified as promising homo/heterogeneous catalysts for hydrogen production from lignin as well as other biomass via SCWG process. The Ce promoter improved the hydrogen selectivity by promoting the Ni dispersion and weakening the Ni-Al_2O_3 interaction. Ni-Ce/Al_2O_3 was the best performer in terms of hydrogen yield. The better performance of this catalyst is caused by its improved metal dispersion, coke resistance, and increased reducibility. Higher temperature up to 650 °C and higher catalyst loading up to 100% is desirable for hydrogen production. Canola meal, which has higher ash content, as well as lower lignin content is more suitable for hydrogen production via SCWG.

7.2 Recommendations

- The product separation and collection procedure used in this study caused inevitable loss of some products, which made the quantification of the product difficult and caused poor mass balance calculation. To improve this, a better method could be found or a larger reactor could be built, in which more reactant could be loaded.
- In this study, the hydrogen yield from SCWG was optimized for a batch SCWG reactor. Optimization study using a continuous flow reactor is recommended as the results may provide more insight into the effect of variation in process parameters.

- In order to eliminate the mass transfer resistance in the reactor, agitation apparatus should be added to the batch reactor for further investigations.
- The lignin sample tested in this study was commercial lignin sample, and different types of lignin are available in the market. Hence, the effect of different types of lignin as feedstock on hydrogen yield from SCWG could be studied.
- The effects of lignin/cellulose ratio in the feedstock, and the potential interaction between lignin and cellulose were not studied. Therefore, it is recommended to study this effect in future.
- The focus of this study was to maximize the hydrogen yield. Therefore, no detailed characterization was performed for the liquid phase products. The characterization of these products could be helpful to understand the reaction mechanism, and therefore, is recommended for future work.
- The small dimensions of the reactor make the collection of spent catalyst difficult, so no recycling study of the catalysts was performed. This can be explored by using larger reactors.
- The compressed helium gas should be used to pressurising the reactor instead of nitrogen to avoid potential overlap of the peak with hydrogen in GC analysis.
- The Ni-Ce/Al_2O_3 catalyst should be further evaluated in terms of reusability and stability under the SCWG operating conditions.
- In-situ characterization of the Ni-Ce/Al_2O_3 catalyst should be considered to investigate the possible phase change of catalyst supports, active metals and promoters during the supercritical gasification reactions.
- Economic and technological analysis are recommended to evaluate the SCWG process for its application for hydrogen production from biomass.

References

Afif, E., Azadi, P., and Farnood, R. 2011. "Catalytic hydrothermal gasification of activated sludge." *Applied Catalysis B: Environmental* 105 (1–2):136-143. doi: http://dx.doi.org/10.1016/j.apcatb.2011.04.003.

AKSOYLU, E.A., AKIN, A.N., Gönenç, S.S., and ÖNSAN, Z.İ. 1996. "The effect of metal loading on the adsorption parameters of carbon dioxide on coprecipitated nickel-alumina catalysts." *Turkish Journal of Chemistry* 20 (1):88-94.

Antal, M.J., Stephen, G.A., Deborah, S., Xu, X.D, and Divilio, R.J. 2000. "Biomass Gasification in Supercritical Water†." *Industrial & Engineering Chemistry Research* 39 (11):4040-4053. doi: 10.1021/ie0003436.

Azadi, P., Afif E., Azadi, F., and Farnood, R. 2012. "Screening of nickel catalysts for selective hydrogen production using supercritical water gasification of glucose." *Green Chemistry* 14 (6):1766-1777. doi: 10.1039/C2GC16378K.

Azadi, P., and Farnood, R., 2011. "Review of heterogeneous catalysts for sub-and supercritical water gasification of biomass and wastes." *International Journal of Hydrogen Energy* 36 (16):9529-9541. doi: http://dx.doi.org/10.1016/j.ijhydene.2011.05.081.

Azadi, P., Oliver R. Inderwildi, Farnood R., and David A. K. 2013. "Liquid fuels, hydrogen and chemicals from lignin: A critical review." *Renewable and Sustainable Energy Reviews* 21:506-523. doi: http://dx.doi.org/10.1016/j.rser.2012.12.022.

Azadi, P., Sami, K., Friederike, S., Azadi, F., and Farnood, R. 2012. "Hydrogen production from cellulose, lignin, bark and model carbohydrates in supercritical water using nickel and ruthenium catalysts." *Applied Catalysis B: Environmental* 117–118 (0):330-338. doi: http://dx.doi.org/10.1016/j.apcatb.2012.01.035.

Azargohar, R., and Dalai, A.K. 2008. "Steam and KOH activation of biochar: Experimental and modeling studies." *Microporous and Mesoporous Materials* 110 (2):413-421.

Azargohar, R., and Dalai, A.K. 2005. "Production of activated carbon from Luscar char: Experimental and modeling studies." *Microporous and Mesoporous Materials* 85 (3):219-225. doi: http://dx.doi.org/10.1016/j.micromeso.2005.06.018.

Azargohar, R., Sonil, N., Rao, B.V.S.K., and Dalai, A.K. 2013. "Slow Pyrolysis of Deoiled Canola Meal: Product Yields and Characterization." *Energy & Fuels* 27 (9):5268-5279. doi: 10.1021/ef400941a.

Badoga, S., Mouli K.C., Kapil, K.S., Dalai, A. K., and J. Adjaye. 2012. "Beneficial influence of EDTA on the structure and catalytic properties of sulfided NiMo/SBA-15 catalysts for hydrotreating of light gas oil." *Applied Catalysis B: Environmental* 125 (0):67-84. doi: http://dx.doi.org/10.1016/j.apcatb.2012.05.015.

Bao, Z.W., Yang, F.S., Wu, Z., Nyamsi, S.N., and Zhang, Z.X. 2013. "Optimal design of metal hydride reactors based on CFD–Taguchi combined method." *Energy Conversion and Management* 65:322-330. doi: http://dx.doi.org/10.1016/j.enconman.2012.07.027.

Basu, P. 2010. *Biomass gasification and pyrolysis: practical design and theory*: Academic press.

Basu, P., and Vichuda, M. 2009. "Biomass Gasification in Supercritical Water--A Review." *International Journal of Chemical Reactor Engineering* 7 (1).

Bengaard, H. S., Nørskov, J. K., Sehested, J., Clausen, B. S., Nielsen, L. P., Molenbroek, A. M., and Rostrup-Nielsen, J. R.. 2002. "Steam Reforming and Graphite Formation on Ni Catalysts." *Journal of Catalysis* 209 (2):365-384. doi: http://dx.doi.org/10.1006/jcat.2002.3579.

Bioenergy, IEA. 2007. "Potential contribution of bioenergy to the world's future energy demand." *IEA Bioenergy: ExCo* 2007:02-12.

Boero, M., Tamio, I., Chee, C.L., Kiyoyuki, T., and Michele, P.. 2004. "Hydrogen Bond Driven Chemical Reactions: Beckmann Rearrangement of Cyclohexanone Oxime into ε-Caprolactam in Supercritical Water." *Journal of the American Chemical Society* 126 (20):6280-6286. doi: 10.1021/ja049363f.

Boukis, N., Diem, V., Habicht, W., and Dinjus E. 2003. *Ind. Eng. Chem. Res.* 4:728.

Bulushev, D.A., and Julian, R.H.R. 2011. "Catalysis for conversion of biomass to fuels via pyrolysis and gasification: A review." *Catalysis Today* 171 (1):1-13. doi: http://dx.doi.org/10.1016/j.cattod.2011.02.005.

Byrd, A.J., Pant, K.K., and Ram, B.G. 2008. "Hydrogen production from glycerol by reforming in supercritical water over Ru/Al_2O_3 catalyst." *Fuel* 87 (13–14):2956-2960. doi: http://dx.doi.org/10.1016/j.fuel.2008.04.024.

Castello, D., and Luca, F. 2011. "Supercritical water gasification of biomass: Thermodynamic constraints." *Bioresource Technology* 102 (16):7574-7582. doi: http://dx.doi.org/10.1016/j.biortech.2011.05.017.

Chakar, F.S., and Arthur, J.R. 2004. "Review of current and future softwood kraft lignin process chemistry." *Industrial Crops and Products* 20 (2):131-141. doi: http://dx.doi.org/10.1016/j.indcrop.2004.04.016.

Chaubey, R., Satanand, S., Olusola, O.J., and Sudip, M. 2013. "A review on development of industrial processes and emerging techniques for production of hydrogen from renewable and sustainable sources." *Renewable and Sustainable Energy Reviews* 23 (0):443-462. doi: http://dx.doi.org/10.1016/j.rser.2013.02.019.

Chen, D.H., Huang, F.Z., Cheng, Y.B., and Rachel, A.C. 2009. "Mesoporous Anatase TiO_2 Beads with High Surface Areas and Controllable Pore Sizes: A Superior Candidate for High-Performance Dye-Sensitized Solar Cells." *Advanced Materials* 21 (21):2206-2210.

Chen, W.H., Chen C.J., and Hung, C.I. 2013. "Taguchi approach for co-gasification optimization of torrefied biomass and coal." *Bioresource Technology* 144:615-622. doi: http://dx.doi.org/10.1016/j.biortech.2013.07.016.

Chen, Y.G., and Ren, J. 1994. "Conversion of methane and carbon dioxide into synthesis gas over alumina-supported nickel catalysts. Effect of Ni-Al_2O_3 interactions." *Catalysis Letters* 29 (1-2):39-48. doi: 10.1007/BF00814250.

Cortright, R.D., Davda, R.R., and Dumesic, J.A. 2002. "Hydrogen from catalytic reforming of biomass-derived hydrocarbons in liquid water." *Nature* 418 (6901):964-967.

Crouch, S.R., and Douglas, A.S. 2007. "Principles of instrumental analysis." *Brooks/Cole Cengage Learning: Belmont, CA* 6:498-542.

Dahmen, N., Dinjus, E., and Kruse, A. 2009. "FUELS – HYDROGEN PRODUCTION| Biomass: Thermochemical Processes." In *Encyclopedia of Electrochemical Power Sources*, edited by Garche Editor-in-Chief: Jürgen, 259-267. Amsterdam: Elsevier.

Demirbas, A. 2004. "Hydrogen-rich gas from fruit shells via supercritical water extraction." *International Journal of Hydrogen Energy* 29 (12):1237-1243. doi: http://dx.doi.org/10.1016/j.ijhydene.2003.11.012.

Deniz, I., Fazilet, V.S., Mithat, Y., Mehmet, S., Levent, B., and Ozlem, Y.C. 2015. "Hydrogen production from marine biomass by hydrothermal gasification." *Energy Conversion and Management* 96:124-130. doi: http://dx.doi.org/10.1016/j.enconman.2015.02.048.

Designation, ASTM. 1996. "D 3173–87." *Standard Test Method for Moisture in the Analysis Sample of Coal and Coke, Annual Book of ASTM Standards* 5:295-296.

Ding, N., Azargohar, R., Dalai, A.K. and Kozinski, J.A. 2014. "Catalytic gasification of cellulose and pinewood to H2 in supercritical water." *Fuel* 118 (0):416-425. doi: http://dx.doi.org/10.1016/j.fuel.2013.11.021.

Dixit, M., Manish, M., Joshi, P.A., and Shah, D.O. 2013. "Physico-chemical and catalytic properties of Mg–Al hydrotalcite and Mg–Al mixed oxide supported copper catalysts." *Journal of Industrial and Engineering Chemistry* 19 (2):458-468. doi: http://dx.doi.org/10.1016/j.jiec.2012.08.028.

Djinović, P., Ilja, G.O.Č., Boštjan, E., and Albin, P. 2012. "Influence of active metal loading and oxygen mobility on coke-free dry reforming of Ni–Co bimetallic catalysts." *Applied Catalysis B: Environmental* 125 (0):259-270. doi: http://dx.doi.org/10.1016/j.apcatb.2012.05.049.

Dong, W.S., Hyun, S.R., Ki, W.J., Sang E.P., and Young, S.O. 2002. "Methane reforming over Ni/Ce-ZrO2 catalysts: effect of nickel content." *Applied Catalysis A: General* 226 (1–2):63-72. doi: http://dx.doi.org/10.1016/S0926-860X(01)00883-3.

Dunn, S. 2002. "Hydrogen futures: toward a sustainable energy system." *International Journal of Hydrogen Energy* 27 (3):235-264. doi: http://dx.doi.org/10.1016/S0360-3199(01)00131-8.

Elliott, D.C., John S.L., and Eddie, G.B. 1993. "Chemical processing in high-pressure aqueous environments. 2. Development of catalysts for gasification." *Industrial & Engineering Chemistry Research* 32 (8):1542-1548.

Elliott, D.C. 2008. "Catalytic hydrothermal gasification of biomass." *Biofuels, Bioproducts and Biorefining* 2 (3):254-265. doi: 10.1002/bbb.74.

Fang, Z. 2014. "Near-critical and supercritical water and their applications for biorefineries." Springer.

Fang, Z., Takafumi, S., Richard, L.S., Hiroshi, I., Kunio, A., and Kozinski, J.A. 2008. "Reaction chemistry and phase behavior of lignin in high-temperature and supercritical water." *Bioresource Technology* 99 (9):3424-3430. doi: http://dx.doi.org/10.1016/j.biortech.2007.08.008.

Furusawa, T., Takafumi, S., Hirokazu, S., Yasutomo, M., Yasuyoshi, I., Masahide S., Naotsugu, I., and Noboru, S. 2007. "Hydrogen production from the gasification of lignin with nickel

catalysts in supercritical water." *International Journal of Hydrogen Energy* 32 (6):699-704. doi: http://dx.doi.org/10.1016/j.ijhydene.2006.08.001.

Gellerstedt, G., Lindfors, E.L., Lapierre, C., and Monties, B. 1984. "Structural-changes in lignin during kraft cooking. 2. Characterization by acidolysis." *Svensk Papperstidning-Nordisk Cellulosa* 87 (9):R61-R67.

Gellerstedt, G., and Kristina, G. 1987. "Structural changes in lignin during kraft cooking. Part 5. Analysis of dissolved lignin by oxidative degradation." *Journal of wood chemistry and technology* 7 (1):65-80.

Gellerstedt, G., and Eva-Lisa, L. 1984a. "Structural changes in lignin during kraft pulping." *Holzforschung-International Journal of the Biology, Chemistry, Physics and Technology of Wood* 38 (3):151-158.

Gellerstedt, G., and Eva-Lisa, L. 1984b. "Structural changes in lignin during kraft cooking. Part 4. Phenolic hydroxyl groups in wood and kraft pulps." *Svensk Papperstidn* 87 (15):R115-R118.

Gierer, J. 1980. "Chemical aspects of kraft pulping." *Wood Science and Technology* 14 (4):241-266. doi: 10.1007/BF00383453.

Goyal, H.B., Diptendu, S., and Saxena, R.C. 2008. "Bio-fuels from thermochemical conversion of renewable resources: A review." *Renewable and Sustainable Energy Reviews* 12 (2):504-517. doi: http://dx.doi.org/10.1016/j.rser.2006.07.014.

Guo, L.J., Lu, Y. J., Zhang, X.M., Ji, C.M., Guan, Y., and Pei, A.X. 2007. "Hydrogen production by biomass gasification in supercritical water: A systematic experimental and analytical study." *Catalysis Today* 129 (3–4):275-286. doi: http://dx.doi.org/10.1016/j.cattod.2007.05.027.

Guo, Y., Wang, S.Z., Xu D.H., Gong, Y.M., Ma, H.H., and Tang, X.Y. 2010. "Review of catalytic supercritical water gasification for hydrogen production from biomass." *Renewable and Sustainable Energy Reviews* 14 (1):334-343. doi: http://dx.doi.org/10.1016/j.rser.2009.08.012.

Guo, Y., Wang, S.Z., Thomas, Y., and Savage, P.E. 2015. "Catalytic gasification of indole in supercritical water." *Applied Catalysis B: Environmental* 166–167:202-210. doi: http://dx.doi.org/10.1016/j.apcatb.2014.11.033.

Hao, X.H., Guo, L.J., Zhang, X.M., and Guan, Y. 2005. "Hydrogen production from catalytic gasification of cellulose in supercritical water." *Chemical Engineering Journal* 110 (1–3):57-65. doi: http://dx.doi.org/10.1016/j.cej.2005.05.002.

Heinze, T., and Andreas, K. 2005. "Solvents applied in the field of cellulose chemistry: a mini review." *Polímeros* 15:84-90.

Hosoya, T., Kawamoto, H., and Saka, S. 2007. "Cellulose–hemicellulose and cellulose–lignin interactions in wood pyrolysis at gasification temperature." *Journal of Analytical and Applied Pyrolysis* 80 (1):118-125. doi: http://dx.doi.org/10.1016/j.jaap.2007.01.006.

Hosseini, S.E., Mazlan, A.W., and Ganjehkaviri, A. 2015. "An overview of renewable hydrogen production from thermochemical process of oil palm solid waste in Malaysia." *Energy Conversion and Management* 94:415-429. doi: http://dx.doi.org/10.1016/j.enconman.2015.02.012.

Huber, G.W., Shabaker, J.W., and Dumesic, J.A. 2003. "Raney Ni-Sn Catalyst for H2 Production from Biomass-Derived Hydrocarbons." *Science* 300 (5628):2075-2077. doi: 10.1126/science.1085597.

Ibrahim, H.M., Wan, M., Yusoff, Aidil, A.H., Rosli, M.I., Othman, H., and Othman, O. 2005. "Optimization of medium for the production of β-cyclodextrin glucanotransferase using Central Composite Design (CCD)." *Process Biochemistry* 40 (2):753-758. doi: http://dx.doi.org/10.1016/j.procbio.2004.01.042.

Jakab, E., Faix, O., and Till, F. 1997. "Thermal decomposition of milled wood lignins studied by thermogravimetry/mass spectrometry." *Journal of Analytical and Applied Pyrolysis* 40–41:171-186. doi: http://dx.doi.org/10.1016/S0165-2370(97)00046-6.

Kalinci, Y., Arif, H., and Ibrahim, D. 2009. "Biomass-based hydrogen production: A review and analysis." *International Journal of Hydrogen Energy* 34 (21):8799-8817. doi: http://dx.doi.org/10.1016/j.ijhydene.2009.08.078.

Kang, K., Azargohar, R., Dalai A.K., and Wang, H. 2015. "Noncatalytic Gasification of Lignin in Supercritical Water Using a Batch Reactor for Hydrogen Production: An Experimental and Modeling Study." *Energy & Fuels* 29 (3):1776-1784. doi: 10.1021/ef5027345.

Kang, K., Azargohar R., Dalai, A.K., and Wang, H. 2016. "Systematic screening and modification of Ni based catalysts for hydrogen generation from supercritical water

gasification of lignin." *Chemical Engineering Journal* 283:1019-1032. doi: http://dx.doi.org/10.1016/j.cej.2015.08.032.

Kang, S.M., Li, X.L., Fan, J., and Chang, J. 2013. "Hydrothermal conversion of lignin: A review." *Renewable and Sustainable Energy Reviews* 27 (0):546-558. doi: http://dx.doi.org/10.1016/j.rser.2013.07.013.

Kopetz, H. 2013. "Renewable resources: Build a biomass energy market." *Nature* 494 (7435):29-31.

Kritzer, P. 2004. "Corrosion in high-temperature and supercritical water and aqueous solutions: a review." *The Journal of Supercritical Fluids* 29 (1–2):1-29. doi: http://dx.doi.org/10.1016/S0896-8446(03)00031-7.

Kruse, A. 2009. "Hydrothermal biomass gasification." *The Journal of Supercritical Fluids* 47 (3):391-399. doi: http://dx.doi.org/10.1016/j.supflu.2008.10.009.

Kruse, A., and Gawlik, A. 2002. "Biomass Conversion in Water at 330−410 °C and 30−50 MPa. Identification of Key Compounds for Indicating Different Chemical Reaction Pathways." *Industrial & Engineering Chemistry Research* 42 (2):267-279. doi: 10.1021/ie0202773.

Kruse, A., Henningsen, T., Sınağ, A., and Pfeiffer, J. 2003. "Biomass Gasification in Supercritical Water: Influence of the Dry Matter Content and the Formation of Phenols." *Industrial & Engineering Chemistry Research* 42 (16):3711-3717. doi: 10.1021/ie0209430.

Kumar, A., David, J., and Milford, H. 2009. "Thermochemical Biomass Gasification: A Review of the Current Status of the Technology." *Energies* 2 (3):556-581.

Kumar, M., Aberuagba, F., Gupta, J.K., Rawat K.S., Sharma L.D, and Dhar, G.M. 2004. "Temperature-programmed reduction and acidic properties of molybdenum supported on MgO–Al_2O_3 and their correlation with catalytic activity." *Journal of Molecular Catalysis A: Chemical* 213 (2):217-223.

Kumar, P., Sun, Y.P., and Raphael, O.I. 2008. "Comparative study of Ni-based mixed oxide catalyst for carbon dioxide reforming of methane." *Energy & Fuels* 22 (6):3575-3582.

Lawoko, M., Gunnar, H., and Göran, G. 2005. "Structural Differences between the Lignin−Carbohydrate Complexes Present in Wood and in Chemical Pulps." *Biomacromolecules* 6 (6):3467-3473. doi: 10.1021/bm058014q.

Lazic, Z.R. 2004. *Design of Experiments in Chemical Engineering: A Practical Guide*: Wiley.

Lee, I.G. 2011. "Effect of metal addition to Ni/activated charcoal catalyst on gasification of glucose in supercritical water." *International Journal of Hydrogen Energy* 36 (15):8869-8877. doi: http://dx.doi.org/10.1016/j.ijhydene.2011.05.008.

Lee, I.G., and Son K.I. 2008. "Catalytic Gasification of Glucose over Ni/Activated Charcoal in Supercritical Water." *Industrial & Engineering Chemistry Research* 48 (3):1435-1442. doi: 10.1021/ie8012456.

Lee, J.W., Bon W.K., Joon W.C., Don H.C., and In G.C. 2008. "Evaluation of waste mushroom logs as a potential biomass resource for the production of bioethanol." *Bioresource Technology* 99 (8):2736-2741. doi: http://dx.doi.org/10.1016/j.biortech.2007.07.003.

Lee, S.H, Thomas V.D., Robert J.L., and Jonathan S.D. 2009. "Ionic liquid-mediated selective extraction of lignin from wood leading to enhanced enzymatic cellulose hydrolysis." *Biotechnology and Bioengineering* 102 (5):1368-1376.

Leonardo, C.S., Leonardo, S.P.S.C, Venkatesh, B., and Bruce, E.D. 2009. "'Cradle-to-grave' assessment of existing lignocellulose pretreatment technologies." *Current Opinion in Biotechnology* 20 (3):339-347. doi: http://dx.doi.org/10.1016/j.copbio.2009.05.003.

Levin, D.B., and Richard, C. 2010. "Challenges for renewable hydrogen production from biomass." *International Journal of Hydrogen Energy* 35 (10):4962-4969. doi: http://dx.doi.org/10.1016/j.ijhydene.2009.08.067.

Levin, D.B., Lawrence, P., and Murray, L. 2004. "Biohydrogen production: prospects and limitations to practical application." *International Journal of Hydrogen Energy* 29 (2):173-185. doi: http://dx.doi.org/10.1016/S0360-3199(03)00094-6.

Li, G.H., Hu, L.J., and Josephine, M.H. 2006. "Comparison of reducibility and stability of alumina-supported Ni catalysts prepared by impregnation and co-precipitation." *Applied Catalysis A: General* 301 (1):16-24. doi: http://dx.doi.org/10.1016/j.apcata.2005.11.013.

Li, S., Guo, L.J., Zhu, C., and Lu, Y.J. 2013. "Co-precipitated Ni–Mg–Al catalysts for hydrogen production by supercritical water gasification of glucose." *International Journal of Hydrogen Energy* 38 (23):9688-9700. doi: http://dx.doi.org/10.1016/j.ijhydene.2013.05.002.

Li, S., Lu, Y.J., Guo, L.J., and Zhang, X.M. 2011. "Hydrogen production by biomass gasification in supercritical water with bimetallic Ni–M/γAl_2O_3 catalysts (M = Cu, Co and

Sn)." *International Journal of Hydrogen Energy* 36 (22):14391-14400. doi: http://dx.doi.org/10.1016/j.ijhydene.2011.07.144.

Liao, C.N., and Hsing P.K. 2010. "Supplier selection model using Taguchi loss function, analytical hierarchy process and multi-choice goal programming." *Computers & Industrial Engineering* 58 (4):571-577. doi: http://dx.doi.org/10.1016/j.cie.2009.12.004.

Liu, Q., Wang, S.R., Zheng, Y., Luo Z.Y., and Kefa, C. 2008. "Mechanism study of wood lignin pyrolysis by using TG–FTIR analysis." *Journal of Analytical and Applied Pyrolysis* 82 (1):170-177.

Lu, Y.J., Guo, L.J., Ji, C.M., Zhang, X.M., Hao, X.H., and Yan, Q.H. 2006. "Hydrogen production by biomass gasification in supercritical water: A parametric study." *International Journal of Hydrogen Energy* 31 (7):822-831. doi: http://dx.doi.org/10.1016/j.ijhydene.2005.08.011.

Lu, Y.J., Guo, L.J., Zhang, X.M., and Ji. C.M. 2012. "Hydrogen production by supercritical water gasification of biomass: Explore the way to maximum hydrogen yield and high carbon gasification efficiency." *International Journal of Hydrogen Energy* 37 (4):3177-3185. doi: http://dx.doi.org/10.1016/j.ijhydene.2011.11.064.

Lu, Y.J., Li, S., and Guo, L.J. 2014. "Catalysis in Supercritical Water Gasification of Biomass: Status and Prospects." In *Near-critical and Supercritical Water and Their Applications for Biorefineries*, edited by Fang, Z. and Xu, C.B., 343-371. Springer Netherlands.

Lu, Y.J., Li, S., Guo, L.J., and Zhang, X.M. 2010. "Hydrogen production by biomass gasification in supercritical water over Ni/γAl_2O_3 and Ni/CeO_2-γAl_2O_3 catalysts." *International Journal of Hydrogen Energy* 35 (13):7161-7168. doi: http://dx.doi.org/10.1016/j.ijhydene.2009.12.047.

Lu, Y.J., Zhu, Y.M., Li, S., Zhang, X.M., and Guo L.J. 2014. "Behavior of nickel catalysts in supercritical water gasification of glucose: Influence of support." *Biomass and Bioenergy* 67 (0):125-136. doi: http://dx.doi.org/10.1016/j.biombioe.2014.04.038.

Ma, Z.Q., Ekaterina, T., and Jeroen, A.B. 2012. "Controlling the selectivity to chemicals from lignin via catalytic fast pyrolysis." *Applied Catalysis A: General* 423–424 (0):130-136. doi: http://dx.doi.org/10.1016/j.apcata.2012.02.027.

Mansouri, N.E., and Joan, S. 2006. "Structural characterization of technical lignins for the production of adhesives: Application to lignosulfonate, kraft, soda-anthraquinone,

organosolv and ethanol process lignins." *Industrial Crops and Products* 24 (1):8-16. doi: http://dx.doi.org/10.1016/j.indcrop.2005.10.002.

Matsumura, Y., Masaki, H., Kyoko, N., and Yoshihiro, K. 2006. "Effect of heating rate of biomass feedstock on carbon gasification efficiency in supercritical water gasification." *Chemical Engineering Communications* 193 (5):649-659. doi: 10.1080/00986440500440157.

Minitab. 2006. "StatGuide, Version 15." In: Minitab Inc., State College, Pa, USA.

Montgomery, D.C., George C.R., and Norma, F.H. 2009. *Engineering statistics*: John Wiley & Sons.

Morterra, C., Vera B., and Giuliana, M. 1996. "Surface characterization of modified aluminas. Part 4.-Surface hydration and Lewis acidity of CeO_2-Al_2O_3 systems." *Journal of the Chemical Society, Faraday Transactions* 92 (11):1991-1999. doi: 10.1039/FT9969201991.

Muangrat, R., Jude, A.O., and Paul, T.W. 2010. "Influence of alkali catalysts on the production of hydrogen-rich gas from the hydrothermal gasification of food processing waste." *Applied Catalysis B: Environmental* 100 (3–4):440-449. doi: http://dx.doi.org/10.1016/j.apcatb.2010.08.019.

Nanda, S., Jamie, I., Dalai, A.K., and Kozinski, J.A. 2016. "Gasification of fruit wastes and agro-food residues in supercritical water." *Energy Conversion and Management* 110:296-306. doi: http://dx.doi.org/10.1016/j.enconman.2015.11.060.

Nanda, S., Pravakar, M., KamalK, P., Satyanarayan, N., Kozinski, J.A., and Dalai A.K. 2013. "Characterization of North American Lignocellulosic Biomass and Biochars in Terms of their Candidacy for Alternate Renewable Fuels." *BioEnergy Research* 6 (2):663-677. doi: 10.1007/s12155-012-9281-4.

Nanda, S., Sivamohan, N.R., Howard, N.H., Dalai, A.K., and Kozinski, J.A. 2015. "Supercritical water gasification of fructose as a model compound for waste fruits and vegetables." *The Journal of Supercritical Fluids* 104:112-121. doi: http://dx.doi.org/10.1016/j.supflu.2015.05.009.

Natesakhawat, S., Rick, B.W., Wang, X.Q., and Umit, S.O. 2005. "Deactivation characteristics of lanthanide-promoted sol–gel Ni/Al_2O_3 catalysts in propane steam reforming." *Journal of Catalysis* 234 (2):496-508. doi: http://dx.doi.org/10.1016/j.jcat.2005.07.014.

Navarro, R.M., Peña, M.A., and Fierro, J.L.G. 2007. "Hydrogen Production Reactions from Carbon Feedstocks: Fossil Fuels and Biomass." *Chemical Reviews* 107 (10):3952-3991. doi: 10.1021/cr0501994.

Navarro, R.M., Sanchez-Sanchez, M.C., Alvarez-Galvan, M.C., Valle, F., and Fierro J.L.G. 2009. "Hydrogen production from renewable sources: biomass and photocatalytic opportunities." *Energy & Environmental Science* 2 (1):35-54. doi: 10.1039/B808138G.

Onsager, O.T., Marit S., Brownrigg, A., and Rune, L. 1996. "Hydrogen production from water and CO via alkali metal formate salts." *International Journal of Hydrogen Energy* 21 (10):883-885. doi: http://dx.doi.org/10.1016/0360-3199(96)00031-6.

Onwudili, J.A., and Paul, T.W. 2016. "Catalytic conversion of bio-oil in supercritical water: Influence of RuO_2/γ-Al_2O_3 catalysts on gasification efficiencies and bio-methane production." *Applied Catalysis B: Environmental* 180:559-568. doi: http://dx.doi.org/10.1016/j.apcatb.2015.06.058.

Osada, M., Norihito, H., Osamu, S., Kunio, A., and Masayuki, S. 2007. "Effect of Sulfur on Catalytic Gasification of Lignin in Supercritical Water." *Energy & Fuels* 21 (3):1400-1405. doi: 10.1021/ef060636x.

Osada, M., Osamu, S., Kunio, A., and Masayuki, S. 2006. "Stability of Supported Ruthenium Catalysts for Lignin Gasification in Supercritical Water." *Energy & Fuels* 20 (6):2337-2343. doi: 10.1021/ef060356h.

Osada, M., Osamu, S., Masaru, W., Kunio, A., and Masayuki, S. 2006. "Water Density Effect on Lignin Gasification over Supported Noble Metal Catalysts in Supercritical Water." *Energy & Fuels* 20 (3):930-935. doi: 10.1021/ef050398q.

Pandey, M.P., and Kim, C.S. 2011. "Lignin Depolymerization and Conversion: A Review of Thermochemical Methods." *Chemical Engineering & Technology* 34 (1):29-41. doi: 10.1002/ceat.201000270.

Park, K.C., and Hiroshi, T. 2003. "Gasification reaction of organic compounds catalyzed by RuO_2 in supercritical water." *Chemical Communications* 0 (6):694-695. doi: 10.1039/B211800A.

Parsell, T.H., Benjamin, C.O., Ian, K., Tiffany, M.J., Christopher, L.M., Laura, J.H., Lucas, M. A., Hilkka, I.K., Fabio, R., Jeffrey, T.M., and Mahdi, M.A.O. 2013. "Cleavage and

hydrodeoxygenation (HDO) of C-O bonds relevant to lignin conversion using Pd/Zn synergistic catalysis." *Chemical Science* 4 (2):806-813. doi: 10.1039/C2SC21657D.

Pauly, M., Sascha, G., Liu, L.F., Nasim, M., Amancio, S., Alex, S., and Xiong, G.Y. 2013. "Hemicellulose biosynthesis." *Planta* 238 (4):627-642. doi: 10.1007/s00425-013-1921-1.

Peterson, A.A., Frederic, V., Russell, P.L., Morgan, F., Michael, J.A., and Jefferson, W.T. 2008. "Thermochemical biofuel production in hydrothermal media: A review of sub- and supercritical water technologies." *Energy & Environmental Science* 1 (1):32-65.

Pu, Y.Q, Nan, J., and. Ragauskas, A.J. 2007. "Ionic liquid as a green solvent for lignin." *Journal of Wood Chemistry and Technology* 27 (1):23-33.

Ragauskas, A.J., Gregg, T.B., Mary, J.B., Richard, C., Fang, C., Mark, F.D., Brian, H.D., Richard, A.D., Paul, G., and Martin, K. 2014. "Lignin valorization: improving lignin processing in the biorefinery." *Science* 344 (6185):1246843.

Ragauskas, A.J., Gregg, T.B., Mary, J.B., and Richard, C. 2014. "Lignin Valorization: Improving Lignin Processing in the Biorefinery." *Science* 344 (6185). doi: 10.1126/science.1246843.

Ragupathi, C., Judith, V.J., and John, K.L. "Preparation, characterization and catalytic properties of nickel aluminate nanoparticles: A comparison between conventional and microwave method." *Journal of Saudi Chemical Society* (0). doi: http://dx.doi.org/10.1016/j.jscs.2014.01.006.

Reddy, S.N., Nanda, S., Dalai, A.K., and Kozinski, J.A. 2014. "Supercritical water gasification of biomass for hydrogen production." *International Journal of Hydrogen Energy* 39 (13):6912-6926. doi: http://dx.doi.org/10.1016/j.ijhydene.2014.02.125.

Resende, F.L.P., Stephanie, A.F., Michael J. Berger, and Phillip E. Savage. 2008. "Noncatalytic Gasification of Lignin in Supercritical Water." *Energy & Fuels* 22 (2):1328-1334. doi: 10.1021/ef700574k.

Resende, F.L.P., and Phillip, E.S. 2010. "Effect of metals on supercritical water gasification of cellulose and lignin." *Industrial & Engineering Chemistry Research* 49 (6):2694-2700.

Reyero, I., Velasco, I., Sanz, O., Montes, M., Arzamendi, G., and Gandía, L.M. 2013. "Structured catalysts based on Mg–Al hydrotalcite for the synthesis of biodiesel." *Catalysis today* 216:211-219.

Richardson, J.T. 1989. *Principles of catalyst development*: Plenum Press: New York.

Robert, D.R., Michel B., Göran, G., and Eva, L.L. 1984. "Structural changes in lignin during kraft cooking part 3. On the structure of dissolved lignins." *Journal of wood chemistry and technology* 4 (3):239-263.

Roh, H.S., Ki, W.J., Wen, S.D., Jong, S.C., Sang, E.P., and Yung, I.J. 2002. "Highly active and stable Ni/Ce–ZrO_2 catalyst for H_2 production from methane." *Journal of Molecular Catalysis A: Chemical* 181 (1–2):137-142. doi: http://dx.doi.org/10.1016/S1381-1169(01)00358-2.

Rynkowski, J.M., Paryjczak, T., and Lenik, M. 1993. "On the nature of oxidic nickel phases in NiO/γ-Al_2O_3 catalysts." *Applied Catalysis A: General* 106 (1):73-82.

Sahoo, S., Seydibeyoğlu, M.Ö, Mohanty, A.K., and Misra, M. 2011. "Characterization of industrial lignins for their utilization in future value added applications." *Biomass and Bioenergy* 35 (10):4230-4237. doi: http://dx.doi.org/10.1016/j.biombioe.2011.07.009.

Saisu, M., Takafumi, S., Masaru, W., Tadafumi, A., and Kunio, A. 2003. "Conversion of Lignin with Supercritical Water−Phenol Mixtures." *Energy & Fuels* 17 (4):922-928. doi: 10.1021/ef0202844.

Sajjadi, S., Mohammad, H., AliAlizadeh E., and Farhad, R.. 2013. "Hydrogen production via CO_2-reforming of methane over Cu and Co doped Ni/Al_2O_3 nanocatalyst: impregnation versus sol–gel method and effect of process conditions and promoter." *Journal of Sol-Gel Science and Technology* 67 (3):601-617. doi: 10.1007/s10971-013-3120-8.

San-José-Alonso, D., Juan J.J., M. J. Illán-Gómez, and M. C. Román-Martínez. 2009. "Ni, Co and bimetallic Ni–Co catalysts for the dry reforming of methane." *Applied Catalysis A: General* 371 (1–2):54-59. doi: http://dx.doi.org/10.1016/j.apcata.2009.09.026.

Sánchez-Sánchez, M.C., Navarro, R.M., and Fierro, J.L.G. 2007. "Ethanol steam reforming over – (La, Zr and Mg) catalysts: Influence of support on the hydrogen production." *International Journal of Hydrogen Energy* 32 (10–11):1462-1471. doi: http://dx.doi.org/10.1016/j.ijhydene.2006.10.025.

Singh, R., Singh, K.D., Trimukhe, K.V., Pandare, K.B., Bastawade, D.V., Gokhale, and Varma, A.J. 2005. "Lignin–carbohydrate complexes from sugarcane bagasse: Preparation, purification, and characterization." *Carbohydrate Polymers* 62 (1):57-66. doi: http://dx.doi.org/10.1016/j.carbpol.2005.07.011.

Siró, I., and David, P. 2010. "Microfibrillated cellulose and new nanocomposite materials: a review." *Cellulose* 17 (3):459-494. doi: 10.1007/s10570-010-9405-y.

Sricharoenchaikul, V. 2009. "Assessment of black liquor gasification in supercritical water." *Bioresource Technology* 100 (2):638-643. doi: http://dx.doi.org/10.1016/j.biortech.2008.07.011.

Standard, ASTM. D3174-04 in Standard Test Method for Ash in the Analysis Sample ofCoal and Coke from Coal. ASTM International, West Conshohocken, PA.

Standard, ASTM. 2007. A standard test method for gross calorific value of coal and coke. In *ASTM D5865*: ASTM International, West Conshohocken, PA.

Sun, J.X., Sun, X.F., Zhao, H., and Sun, R.C. 2004. "Isolation and characterization of cellulose from sugarcane bagasse." *Polymer Degradation and Stability* 84 (2):331-339. doi: http://dx.doi.org/10.1016/j.polymdegradstab.2004.02.008.

Taguchi, G. 1986. *Introduction to quality engineering: designing quality into products and processes*.

Taguchi, G. 1987. Systems of experimental design. UNIPUB. Kraus International Publications, New York.

Takehira, K., Tomonori, K., Tetsuya, S., Kazuhiro, M., Takenori, O., Daisuke, S., Masahide, H., and Ken, T. 2005. "Mechanism of reconstitution of hydrotalcite leading to eggshell-type Ni loading on MgAl mixed oxide." *Journal of Catalysis* 231 (1):92-104. doi: http://dx.doi.org/10.1016/j.jcat.2005.01.025.

Takehira, K., Tetsuya, S., Wang, P., Tokuhisa, K., and Ken, T. 2004. "Autothermal reforming of CH_4 over supported Ni catalysts prepared from Mg–Al hydrotalcite-like anionic clay." *Journal of Catalysis* 221 (1):43-54. doi: http://dx.doi.org/10.1016/j.jcat.2003.07.001.

Teichmann, D., Wolfgang, A., Peter, W., and Raymond, F. 2011. "A future energy supply based on liquid organic hydrogen carriers (LOHC)." *Energy & Environmental Science* 4 (8):2767-2773.

Tejado, A., Peña C., Labidi J., Echeverria J.M., and Mondragon, I. 2007. "Physico-chemical characterization of lignins from different sources for use in phenol–formaldehyde resin synthesis." *Bioresource Technology* 98 (8):1655-1663. doi: http://dx.doi.org/10.1016/j.biortech.2006.05.042.

Thomas, L.H., Trevor, F.V., Adriana, Š., Craig J.K., Roland, P.M., Clemens M.A., David C. A., Timothy J.W., and Michael C.J. 2013. "Structure of cellulose microfibrils in primary cell walls from collenchyma." *Plant physiology* 161 (1):465-476.

Tilay, A., Azargohar, R., Regan, G., Dalai, A.K., and Kozinski, J.A. 2014. "Gasification of Canola Meal and Factors Affecting Gasification Process." *BioEnergy Research* 7 (4):1131-1143. doi: 10.1007/s12155-014-9437-5.

Venkata, M.S., and Venkateswar, R.M. 2013. "Optimization of critical factors to enhance polyhydroxyalkanoates (PHA) synthesis by mixed culture using Taguchi design of experimental methodology." *Bioresource Technology* 128:409-416. doi: http://dx.doi.org/10.1016/j.biortech.2012.10.037.

Wang, G,G., and Shan, S. 2007. "Review of metamodeling techniques in support of engineering design optimization." *Journal of Mechanical Design* 129 (4):370-380.

Wang, H., Jeffrey, T.M., Mohsen, S., Xi, C.Y., Wu, T.P., Zhao H.Y., and Cem A.M. 2013. "XANES and EXAFS studies on metal nanoparticle growth and bimetallic interaction of Ni-based catalysts for CO_2 reforming of CH_4." *Catalysis Today* 207:3-12. doi: http://dx.doi.org/10.1016/j.cattod.2012.09.015.

Wang, S.B., and Lu, G.Q. 1998a. "Role of CeO_2 in Ni/CeO_2–Al_2O_3 catalysts for carbon dioxide reforming of methane." *Applied Catalysis B: Environmental* 19 (3–4):267-277. doi: http://dx.doi.org/10.1016/S0926-3373(98)00081-2.

Wang, S.B., and Lu, G.Q. 1998b. "CO_2 reforming of methane on Ni catalysts: Effects of the support phase and preparation technique." *Applied Catalysis B: Environmental* 16 (3):269-277. doi: http://dx.doi.org/10.1016/S0926-3373(97)00083-0.

Williams, P.T., and Jude, O. 2006. "Subcritical and Supercritical Water Gasification of Cellulose, Starch, Glucose, and Biomass Waste." *Energy & Fuels* 20 (3):1259-1265. doi: 10.1021/ef0503055.

Xu, X.D., Yukihiko, M., Jonny, S., and Michael, J.A. 1996. "Carbon-Catalyzed Gasification of Organic Feedstocks in Supercritical Water†." *Industrial & Engineering Chemistry Research* 35 (8):2522-2530. doi: 10.1021/ie950672b.

Yamaguchi, A., Norihito, H., Osamu, S., Mitsumasa, O., and Masayuki, S. 2008. "Lignin Gasification over Supported Ruthenium Trivalent Salts in Supercritical Water." *Energy & Fuels* 22 (3):1485-1492. doi: 10.1021/ef8001263.

Yong, Tau, L.K., and Y, Matsumura. 2012. "Reaction Kinetics of the Lignin Conversion in Supercritical Water." *Industrial & Engineering Chemistry Research* 51 (37):11975-11988. doi: 10.1021/ie300921d.

Yung, Matthew, M., Whitney, S.J., and Kimberly, A.M. 2009. "Review of catalytic conditioning of biomass-derived syngas." *Energy & Fuels* 23 (4):1874-1887.

Zakzeski, J., Pieter, B., Anna, L.J., and Bert, M.W. 2010. "The catalytic valorization of lignin for the production of renewable chemicals." *Chemical reviews* 110 (6):3552-3599.

Zein, S.H.S., and Abdul, R.M. 2004. "Mn/Ni/TiO_2 Catalyst for the Production of Hydrogen and Carbon Nanotubes from Methane Decomposition." *Energy & Fuels* 18 (5):1336-1345. doi: 10.1021/ef0340864.

Zhang, J.G., Wang, H., and Dalai, A.K. 2007. "Development of stable bimetallic catalysts for carbon dioxide reforming of methane." *Journal of Catalysis* 249 (2):300-310. doi: http://dx.doi.org/10.1016/j.jcat.2007.05.004.

Zhang, J.G., Wang, H., and Dalai, A.K. 2008. "Effects of metal content on activity and stability of Ni-Co bimetallic catalysts for CO_2 reforming of CH_4." *Applied Catalysis A: General* 339 (2):121-129. doi: http://dx.doi.org/10.1016/j.apcata.2008.01.027.

Zhang, L.H., Champagne, P., and Xu, C.B. 2011. "Screening of supported transition metal catalysts for hydrogen production from glucose via catalytic supercritical water gasification." *International Journal of Hydrogen Energy* 36 (16):9591-9601. doi: http://dx.doi.org/10.1016/j.ijhydene.2011.05.077.

Zieliński, J. 1993. "Morphology of coprecipitated nickel/alumina catalysts with low alumina content." *Applied Catalysis A: General* 94 (2):107-115. doi: http://dx.doi.org/10.1016/0926-860X(93)85001-6.

Appendix (A): Calibrations for GC, reactor temperature and calcination furnace

A.1 Calibration for GC

Table A.1 Calibration data for GC

#	Residence time (Min)	Signal	Compound	Level	Amount [mol%]	Peak area	Rsp..Factor
1	1.00	FID1 A	Methane	1	7.41	10692	6.93E-04
				2	15.00	22121	6.78E-04
2	1.11	TCD3 C	Hydrogen	1	35.54	11051	3.22E-03
				2	38.29	12864	2.98E-03
3	1.27	FID1 A	Ethane	1	3.44	9354.4	3.68E-04
				2	7.02	19269	3.64E-04
4	1.25	FID1 A	Ethylene	1	8.68	10154	3.62E-04
				2	7.50	20979	3.57E-04
5	1.67	FID1 A	Propane	1	3.94	16335	2.41E-04
				2	8.04	30225	2.66E-04
6	2.59	FID1 A	Propylene	1	3.05	11507	2.65E-04
				2	4.48	18087	2.48E-04
7	3.40	TCD2 B	CO_2	1	3.01	1746.6	1.72E-03
				2	6.10	3407.6	1.79E-03
8	3.72	FID1 A	Acetylene	1	1.00	3259.3	3.07E-04
				2	1.96	6399.3	3.06E-04
9	4.20	FID1 A	I-butane	1	2.04	8235.8	2.48E-04
				2	4.96	27370	1.81E-04
10	4.77	TCD2 B	O_2	1	99.50	40597	2.45E-03
				2	66.32	27501	2.41E-03
11	5.24	TCD2 B	N_2	1	3.96	1873.2	2.11E-03
				2	3.97	2005.6	1.98E-03
				3	99.99	44121	2.66E-03
12	7.01	TCD2 B	CO	1	2.01	844.35	2.38E-03
				2	3.92	1699.6	2.31E-03

a. Methane

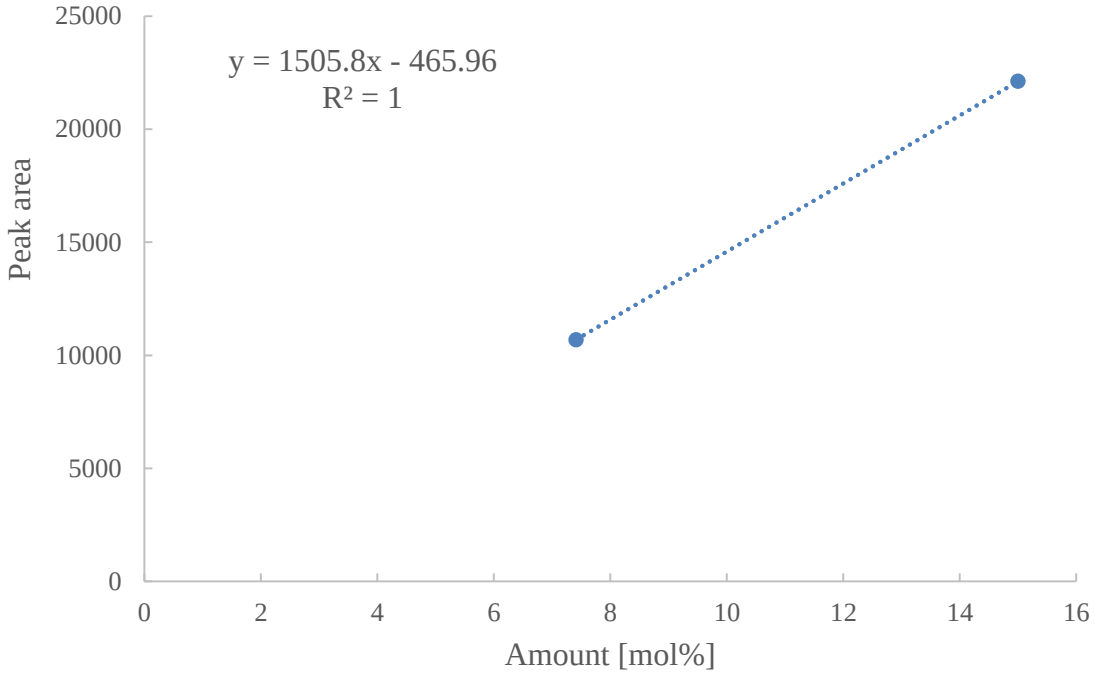

b. Hydrohen

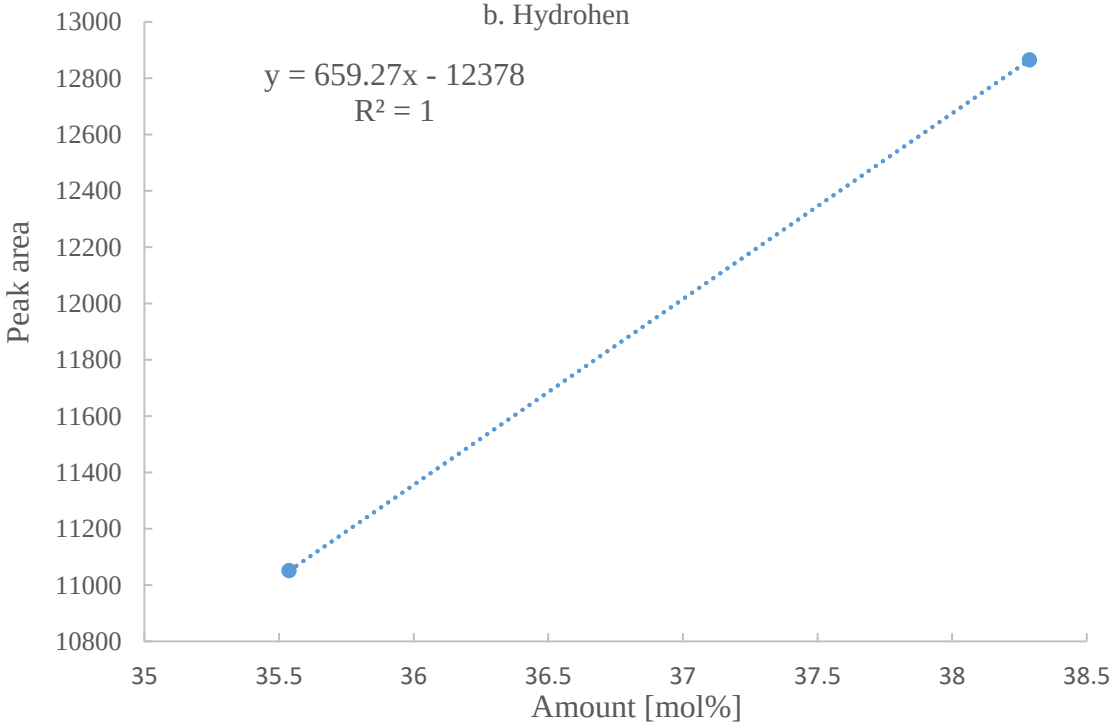

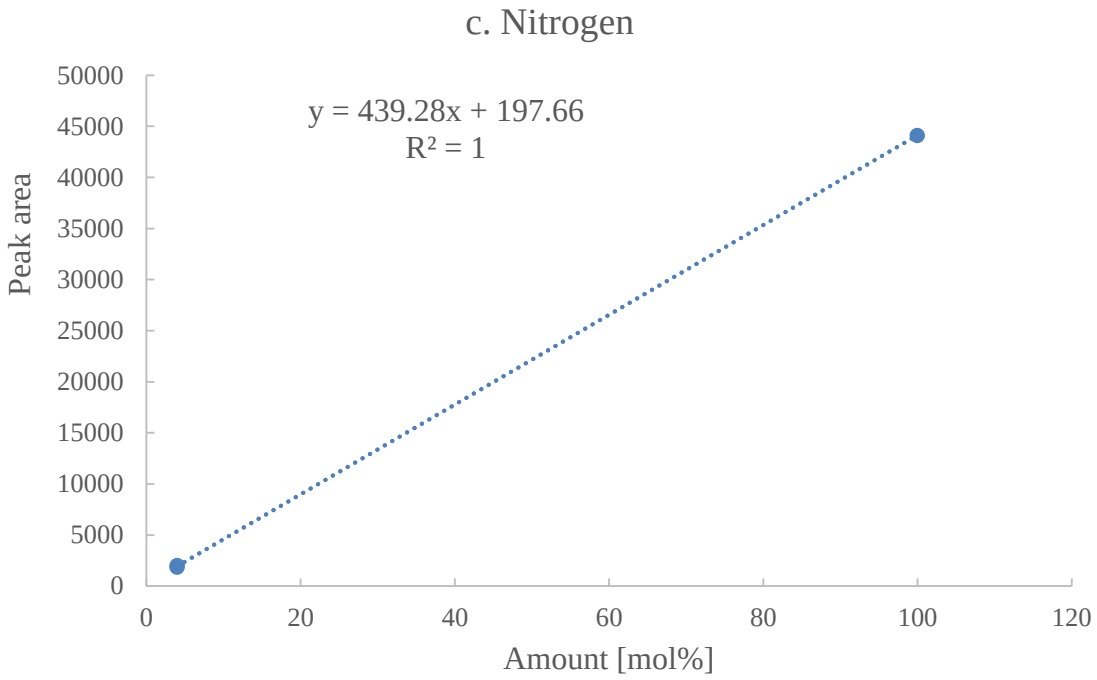

Figure A.1 calibration curves for GC for selected gases

A.2 Calibration for reactor temperature controller and calcination furnace

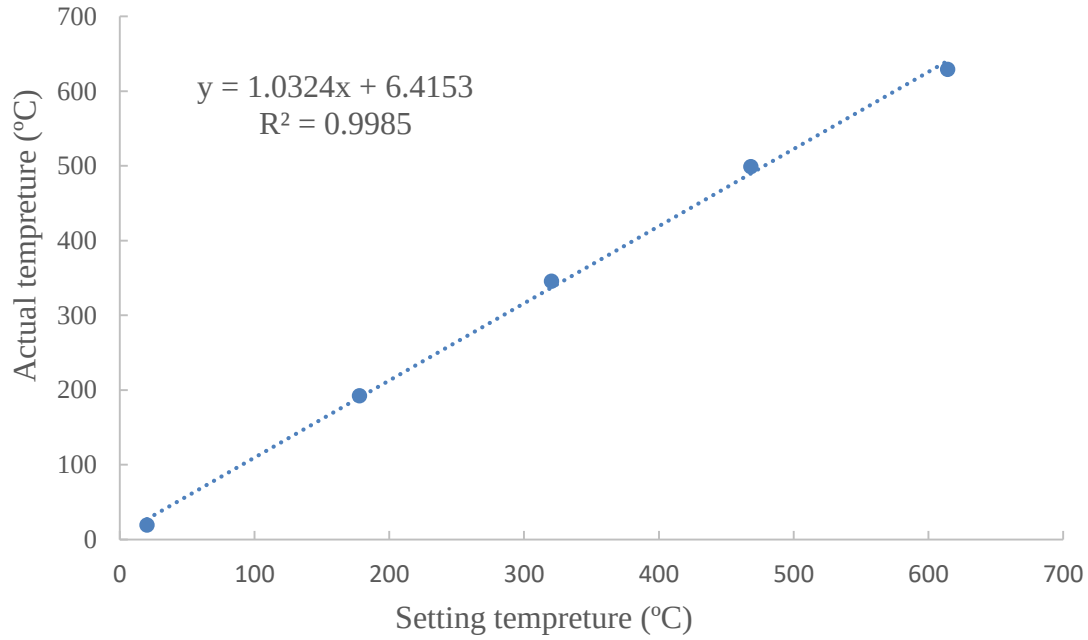

Figure A.2 Calibration curve for reactor temperature controller

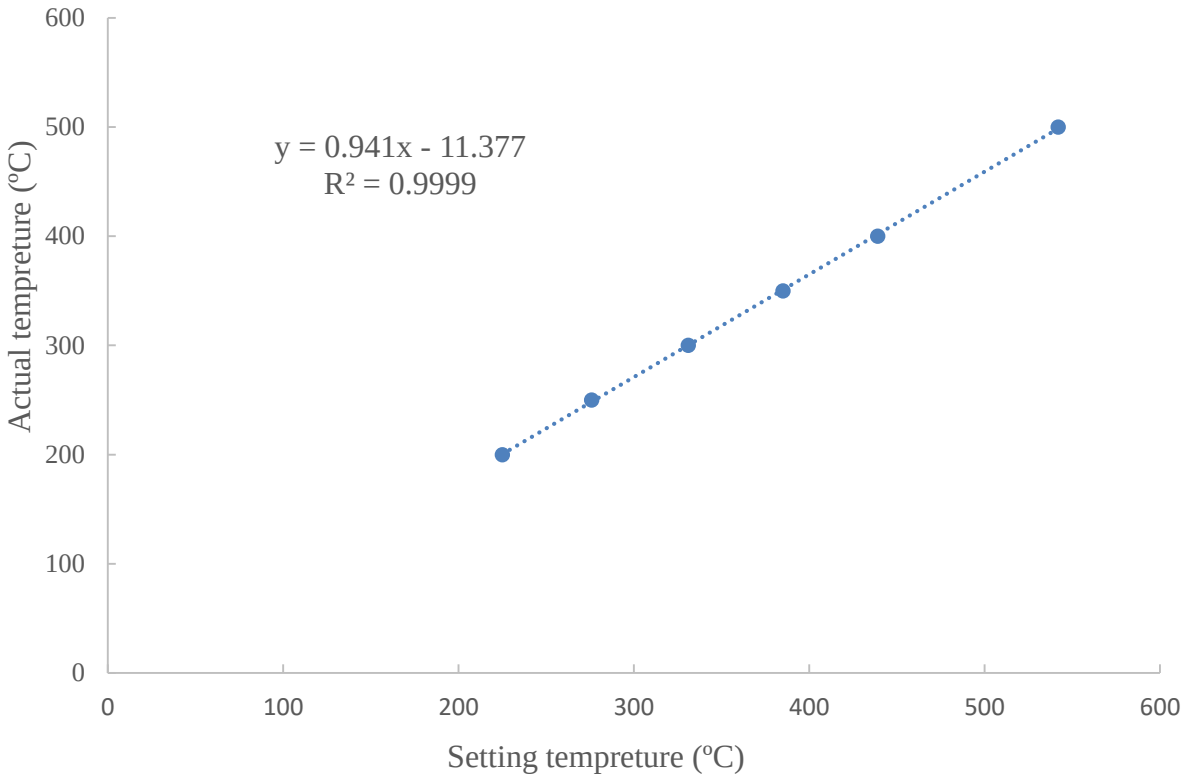

Figure A.3 Calibration curve for calcination furnace

Appendix (B): Calculations for catalyst preparation, SCWG test results, and mass balance

B.1 Calculations for catalyst preparation

B.1.1 Calculation for the weight of metal precursor.

For a specific catalyst metal loading L_{metal} (wt%), the amount of precursor $mM_{precursor}$ (g) required for catalyst synthesis is calculated by the equation:

$$mM_{precursor} = \frac{m_{cat} \times L_{metal}}{M_{metal}} \times \frac{MM_{precusor}}{P_{purity}} \quad \text{.....(B.1)}$$

where m_{cat} (g) is the mass of catalyst to be prepared,

M_{metal} (g/mol) is the atomic weight of the metal,

$MM_{precursor}$ (g/mol) is the molecular weight of the metal precursor,

MP_{purity} (wt%) is the purity of the metal precursor.

B.1.2 Calculation for weight of promoter precursor

For a specific promoter atom to metal atom molar ratio $R_{P/M}$ (mol/mol), the amount of promoter precursor $mP_{precursor}$ (g) required for catalyst synthesis is calculated by the following equation:

$$mP_{precusor} = \left(\frac{m_{cat} \times L_{metal}}{M_{metal}} \times R_{P/M}\right) \times \frac{MP_{precusor}}{PP_{purity}} \quad \text{.....(B.2)}$$

where $MP_{precursor}$ (g/mol) is the molecular weight of the promoter precursor,

PP_{purity} (wt%) is the purity of the promoter precursor.

B.1.3 Calculation for weight of catalyst support

$$m_{support} = m_{cat} \times \left(1 - \frac{L_{metal}}{100} - \left(\frac{mP_{precusor} \times PP_{purity}}{MP_{precusor}} \times \frac{M_{promoter}}{m_{cat}}\right)\right) \quad \text{.....(B.3)}$$

where $M_{promoter}$ (g/mol) is the atomic weight of the promoter.

B.1.4 Sample calculation for catalyst preparation

Based on the calculation mentioned above, take 20Ni-0.36Ce/Al_2O_3 catalyst as an example, if 10g of catalyst need to be prepared. We need to use $Ni(NO_3)_2 \cdot 6H_2O$ as the metal precursor for Ni metal,

$Ce(NO_3)_3 \cdot 6H_2O$ as promoter precursor for Ce promoter, and Al_2O_3 as the catalyst support. Then the input information for catalyst preparation could be read from Table B.1.

Table B.1 Input information for catalyst preparation

Catalyst name	L_{metal} (wt%)	$R_{M/P}$	Ative metal	Metal precursor	Promoter	Promoter precursor	Support
20Ni-0.36Ce/Al_2O_3	20	0.36	Ni	$Ni(NO_3)_2 \cdot 6H_2O$	Ce	$Ce(NO_3)_3 \cdot 6H_2O$	Al_2O_3
Atomic/Molecular weight (g/mol)	NA	NA	58.69	290.79	140	434.22	101.96
Purity of precusor (wt%)	NA	NA	NA	98	NA	98	100

Use the data in Table B.1, the weight of precursor, as well as support, could be determined, and the results are given in Table B.2. The amount of water used for make impregnation solution was determined by the total pore volume and the weight of the support been used. The amount of chemicals used for the preparation of other catalysts were determined following similar calculations.

Table B.2 Usage and calculated amount of chemicals for preparation of 10g catalyst

Chemical name	$Ni(NO_3)_2 \cdot 6H_2O$	$Ce(NO_3)_3 \cdot 6H_2O$	Al_2O_3
Usage of chemical in catalyst preparation	the precursor for Ni	the precursor for Ce	catalyst support
Amount needed (g/10g catalyst)	10.11	5.44	6.28

B.2 Calculation for GC results: Hydrogen yield, Gas yield, hydrogen Selectivity

B.2.1 Calculation of sealed reaction space volume

In order to calculate the moles of N_2 used for the SCWG tests, the volume of sealed reaction space (V_{sealed}) should be firstly specified. Figure B.1 shows the schematic of the batch type SCW reactor which has been used throughout the program. The reactor was made from 316 stainless steel tubing, with an outside diameter (OD) of 0.95 cm and wall thickness (T_{wall}) of 0.17 cm. And the length ($L_{reactor}$) of the reactor is 21 cm.

As is described in the figure, two main parts of the sealed reactor space including $V_{reactor,}$ which is the volume of the reactor itself. And $V_{parts+tubing}$, which is the volume of the tubing sealed when the

reaction is going on (indicated by the green dash lines in the figure). The volume of the reactor could be calculated as:

$$V_{reactor} = \pi \times [(OD-2 \times T_{wall})/2]^2 \times L_{reactor} = 6.13\ cm^3 \quad \text{(B.4)}$$

The rest of the sealed reactor space V_{tubing} consists of space inside different parts including tubing unions, reducers, filter, relief valve, and gauges which are connected by tubing with 0.635 cm ID. This volume of this part is calculated by careful calculation based on dimensions provided by of Swagelok website, and the value is calculated to be 4.62 cm^3. So the sealed reaction volume could be calculated as:

$$V_{sealed} = V_{reactor} + V_{parts+tubing} = 10.75\ cm^3 \quad \text{(B.5)}$$

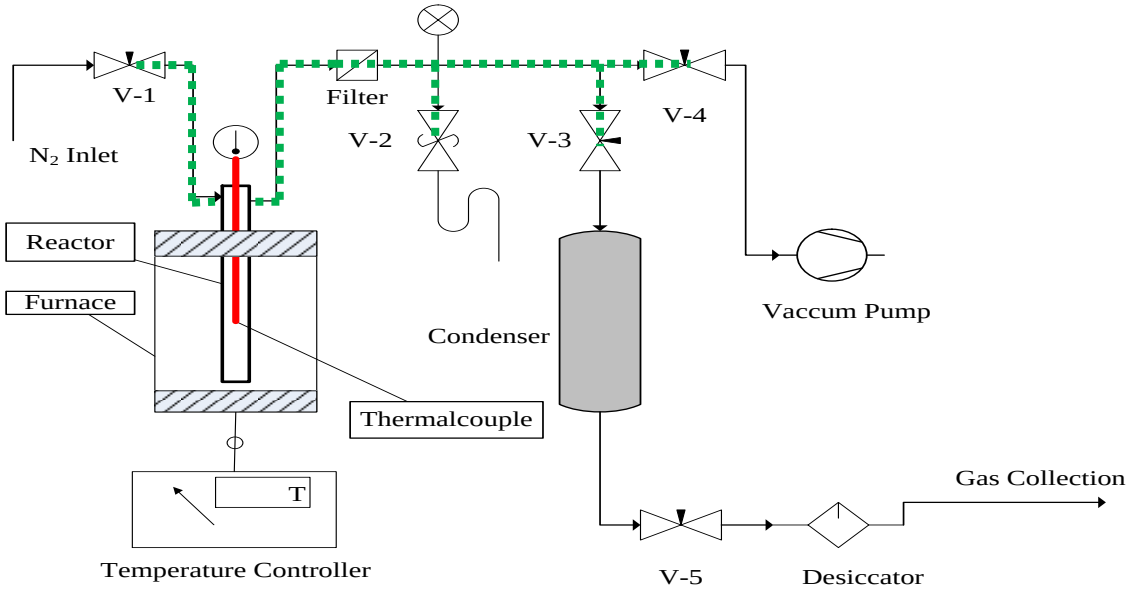

Figure B.1 Structure of supercritical water reactor for sealed reaction for calculations

B.2.2 Calculation of amount of nitrogen used in SCWG tests

Before the reaction, the air in the reactor was removed by a vacuum pump, and then N_2 was used to pressurize the reactor to a desired initial pressure. Therefore, it was assumed that the initial pressure of the sealed volume, which could be read from the pressure gauge (Figure B.1), could be assigned to the pressure of nitrogen gas. According to the ideal gas law, which is:

$$P_{N_2} \times V_{sealed} = n_{N_2} \times R \times T_0 \quad \text{(B.6)}$$

The moles of N_2 (n_{N_2}) present in the SCWG test could be calculated as:

$$n_{N_2} = \frac{P_{N_2} \times V_{sealed}}{R \times T_0} \quad \text{(B.7)}$$

where P_{N_2} is the initial pressure of the N_2 (atm), R is the gas constant (0.082 L·atm/(mol·K)), and T_0 (K) is the initial reactor temperature.

For example, for a catalytic SCWG experiment performed at following reaction conditions (Table B.3):

Table B.3 Reaction conditions used for a lignin SCWG test using 20Ni-0.36Ce/Al_2O_3 catalyst

Temperature (ºC)	P_{N2} (psi)	Residence Time (Min)	H_2O loading (g)	Biomass Loading (g/run)	Water to biomass ratio （g/g）
650	1800	50	3.25	0.65	5

The moles of N_2 (nN_2) present in the specific test could be calculated as:

$$n_{N_2} = \frac{P_{N_2} \times V_{sealed}}{R \times T_0} = \frac{122.48 \text{ atm} \times 0.01075 \text{ L}}{0.082 \text{ L·atm·mol}^{-1}\text{·k}^{-1} \times 293 \text{ K}} = 0.054 \text{ mol} \quad \text{(B.8)}$$

B.3 Calculation for different species of product presents in the gas phase

Since the N_2 gas was not consumed by any reactions in SCWG process, the amount of N_2 present in the reactor is considered constant and used as a reference for calculation of other gas species. The concentration of each gas was directly given in the GC report for the test results, therefore, the amount of each gas phase product could be calculated using the following equation:

$$n_i = \frac{n_{N_2} \times C_i}{C_{N_2}} \quad \text{(B.9)}$$

where n_i (mol) is the number of gas species i, and C_i (mol%) is the concentration of gas species i. Then the mass - m_i (g) and yield- Yg_i (mmol/g) of the i^{th} gas phase product could be calculated using the following equations:

$$m_i = n_i \times Mi \quad \text{(B.10)}$$

$$Yg_i = \frac{n_i}{\text{Biomass loading}} \quad \text{(B.11)}$$

where Mi (g/mol) is the molecular weight of species i in gas phase product.

Further, the gas yield-Y_{Gas} (wt%) and hydrogen selectivity η_{H_2} (%) from the SCWG test could be calculated as:

$$Y_{Gas} = \frac{\sum_1^n m_i}{\text{Biomass loading}} \quad \text{(B.12)}$$

$$\eta_{H_2} = \frac{Y_{H_2}}{2 \times Y_{CH_4}} \quad \text{(B.13)}$$

A sample of calculation for different gas phase products is given in Table B.4, with the run performed at the conditions mentioned in Table B.3. Different columns in the table present the concentration obtained from GC, normalization on the concentration, and the yield of different gas species. Based on these results the gas yield of this experiments were calculated to be 13.31 wt%, and the hydrogen selectivity was calculated to be 117 %, respectively.

Table B.4 Calculation of different gas phase production for a lignin SCWG test using 20Ni-0.36Ce/Al_2O_3 catalyst

Gas name	Concentration from GC (mol%)	Normalized concentration (mol%)	Y_i (mmol/g)
Methane	1.13E+00	1.02E+00	9.27E-01
Hydrogen	2.65E+00	2.39E+00	2.17E+00
Ethane	9.06E-02	8.19E-02	7.43E-02
Ethylene	6.26E-03	5.66E-03	5.14E-03
Propane	1.94E-02	1.75E-02	1.59E-02
Propylene	5.94E-03	5.37E-03	4.88E-03
CO_2	3.06E+00	2.76E+00	2.51E+00
Acetylene	2.71E-03	2.45E-03	2.23E-03
I-butane	2.86E-03	2.58E-03	2.35E-03
O_2	8.97E-01	8.11E-01	7.36E-01
N_2	1.03E+02	9.29E+01	8.43E+01
CO	0.00E+00	0.00E+00	0.00E+00
Total	1.11E+02	1.00E+02	

B.4 Calculations for mass balance

The product separation and collection procedure used in this program were given in Figure B.2. As is indicated in the figure, for the calculation of the mass balance, water phase, solid phase, and

acetone phase products were all collected and justified by weighting. And the gas phase products are quantified by the calculations mentioned above.

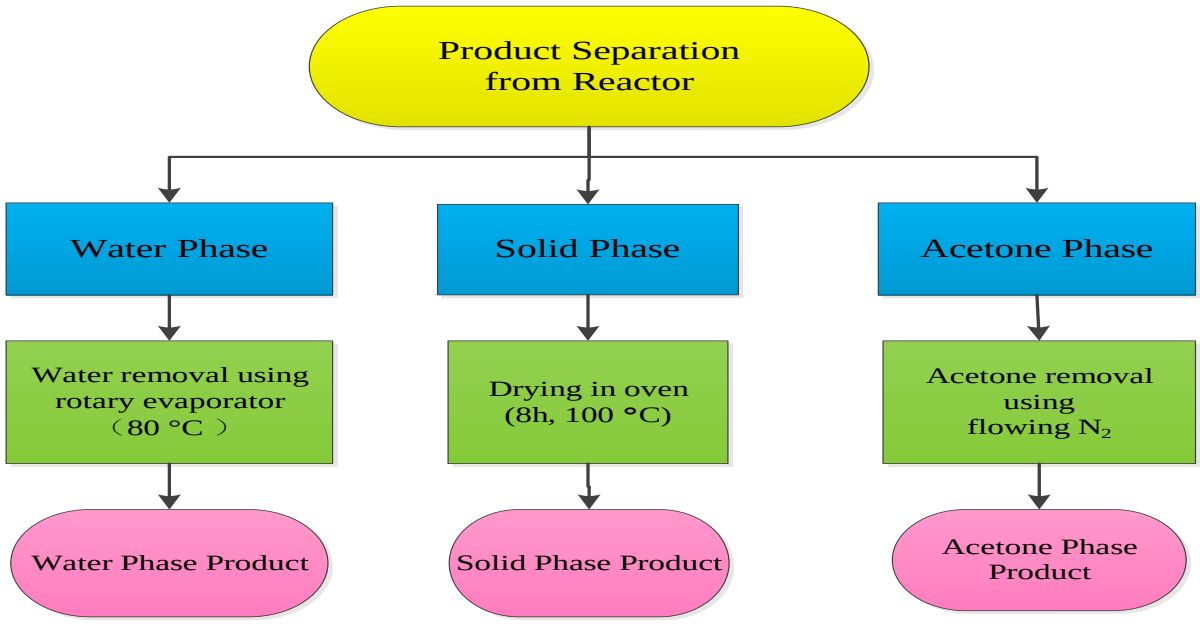

Figure B.2 Procedures for product separation and analysis

Based on the above, the total mass of reactant- m_{Total} (g) and yield of each product phase-Y_i (wt%) during the reaction could be calculated as follow:

$$m_{Total} = m_{Biomass} \times (1+R_{W/B}) \quad \text{(B.14)}$$

$$Y_i = \frac{mp_i}{m_{Biomass}} \quad \text{(B.15)}$$

where mp_i is the weight of product phase i, and $R_{W/B}$ (g/g) is the ratio of water to biomass. Then the total yield Y_{total} of the SCWG could be calculated as:

$$Y_{Total} = \sum_1^n Y_i = Y_{Gas} + Y_{Water} + Y_{Acetone} + Y_{Solid} \quad \text{(B.16)}$$

Then, the total mass balance MB_{total} (%) could be calculated as:

$$MB_{Total} = \left(1 - \frac{\text{Weight loss}}{\text{Total weight of reactants}}\right) \times 100 = \left(1 - \frac{1 - Y_{Total/100}}{1+R_{W/B}}\right) \times 100 \quad \text{(B.17)}$$

A sample of calculation for mass balance for the SCWG of lignin without the catalyst is given below in Table B.5. As is provided in the table, the total mass balance is calculated to be from 86% to 96%.

Table B.5 Calculation data for mass balance of lignin SCWG at different conditions

Experiment Number	Biomass loading (g)	Water to biomass ratio (g/g)	Gas phase yield (wt%)	Water phase yield (wt%)	Actone phase yield (wt%)	Solid phase yield (wt%)	Total mass balance (%)
1	0.65	3.00	12.98	13.69	1.23	32.15	90.01
2	0.65	3.00	7.99	18.00	1.23	18.77	86.50
3	0.65	7.00	3.14	10.92	1.38	26.92	92.80
4	0.65	5.00	3.48	26.15	2.92	43.54	96.02
5	0.65	5.00	16.10	14.31	2.77	34.02	94.53
6	0.65	5.00	7.64	10.77	1.08	32.92	92.07
7	0.65	5.00	9.86	10.77	1.85	31.38	92.31
8	0.65	5.00	8.63	12.00	1.69	32.00	92.39
9	0.65	7.00	10.17	21.85	0.77	5.69	92.31
10	0.65	5.00	10.34	12.62	1.23	32.62	92.80
11	0.65	5.00	8.15	12.62	1.23	33.23	92.54
12	0.65	1.60	4.80	22.54	0.77	38.92	81.32
13	0.65	3.00	11.15	17.38	0.62	26.00	88.79
14	0.65	7.00	2.87	11.85	1.38	22.15	92.28
15	0.65	5.00	1.16	2.31	0.62	29.85	88.99
16	0.65	5.00	6.67	17.85	1.85	28.77	92.52
17	0.65	3.00	7.18	12.31	2.31	22.15	85.99
18	0.65	8.30	2.43	10.77	0.62	17.54	92.62
19	0.65	7.00	4.51	16.92	2.31	24.46	93.53
20	0.65	5.00	8.13	12.92	1.23	32.62	92.48

Appendix (C): Samples of raw data and lab data sheet

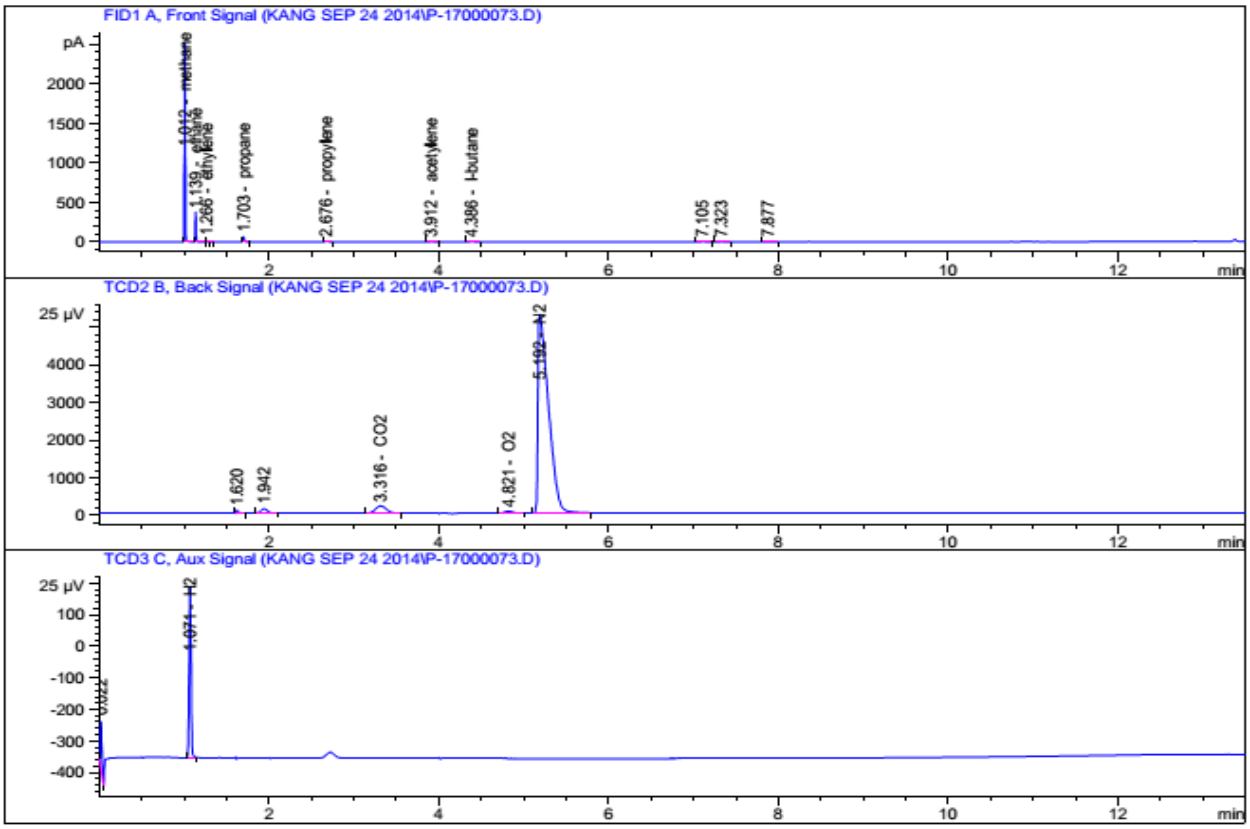

RetTime [min]	Sig	Type	Area	Amt/Area	Amount [mol %]	Grp	Name
1.012	1	BB S	1659.27258	6.80966e-4	1.12991		methane
1.071	3	BB	858.82410	3.08247e-3	2.64730		H2
1.139	1	BV T	248.22754	3.64971e-4	9.05957e-2		ethane
1.266	1	VB T	17.47614	3.58439e-4	6.26413e-3		ethylene
1.703	1	BB	74.20738	2.60811e-4	1.93541e-2		propane
2.676	1	BB	23.50047	2.52944e-4	5.94431e-3		propylene
3.316	2	BB	1721.52466	1.77663e-3	3.05852		CO2
3.912	1	BB	8.85662	3.06393e-4	2.71361e-3		acetylene
4.386	1	BB	15.16463	1.88542e-4	2.85916e-3		I-butane
4.821	2	BB	366.05020	2.45090e-3	8.97152e-1		O2
5.192	2	BB S	4.53598e4	2.26549e-3	102.76185		N2
7.016	2		-	-	-		CO
Totals :					110.62245		

Figure C.1 Sample GC report for lignin SCWG test

Table C.1 Sample of data collection sheet used for the program

Data collection and record for research phase 3									
Run Date	Catalyst	Temperature (ºC)	Biomass loading (g)	Water loading (g)	Water to biomass ratio (g/g)	Gas yield (wt%)	Total mass balance (%)	Hydrogen yield (mmol/)	Hydrogen selectivity (%)

Appendix (D): Permissions to use papers in thesis

Permissions to use following papers in thesis are listed as follows:

[1] Kang, K., Azargohar R., Dalai, A.K., and Wang, H. Noncatalytic Gasification of Lignin in Supercritical Water Using a Batch Reactor for Hydrogen Production: An Experimental and Modeling Study. Energy & Fuels. 29 (2015) 1776-84.

Copyright Clearance Center RightsLink®

Home | Account Info | Help

ACS Publications Most Trusted. Most Cited. Most Read.

Title: Noncatalytic Gasification of Lignin in Supercritical Water Using a Batch Reactor for Hydrogen Production: An Experimental and Modeling Study

Author: Kang Kang, Ramin Azargohar, Ajay K. Dalai, et al

Publication: Energy & Fuels

Publisher: American Chemical Society

Date: Mar 1, 2015

Copyright © 2015, American Chemical Society

Logged in as: KANG KANG
Account #: 3000991791
LOGOUT

PERMISSION/LICENSE IS GRANTED FOR YOUR ORDER AT NO CHARGE

This type of permission/license, instead of the standard Terms & Conditions, is sent to you because no fee is being charged for your order. Please note the following:

- Permission is granted for your request in both print and electronic formats, and translations.
- If figures and/or tables were requested, they may be adapted or used in part.
- Please print this page for your records and send a copy of it to your publisher/graduate school.
- Appropriate credit for the requested material should be given as follows: "Reprinted (adapted) with permission from (COMPLETE REFERENCE CITATION). Copyright (YEAR) American Chemical Society." Insert appropriate information in place of the capitalized words.
- One-time permission is granted only for the use specified in your request. No additional uses are granted (such as derivative works or other editions). For any other uses, please submit a new request.

BACK | CLOSE WINDOW

Copyright © 2016 Copyright Clearance Center, Inc. All Rights Reserved. Privacy statement. Terms and Conditions.
Comments? We would like to hear from you. E-mail us at customercare@copyright.com

[2] Kang, K., Azargohar R., Dalai, A.K., and Wang, H. Systematic screening and modification of Ni based catalysts for hydrogen generation from supercritical water gasification of lignin. Chemical Engineering Journal. 283 (2016) 1019-32.

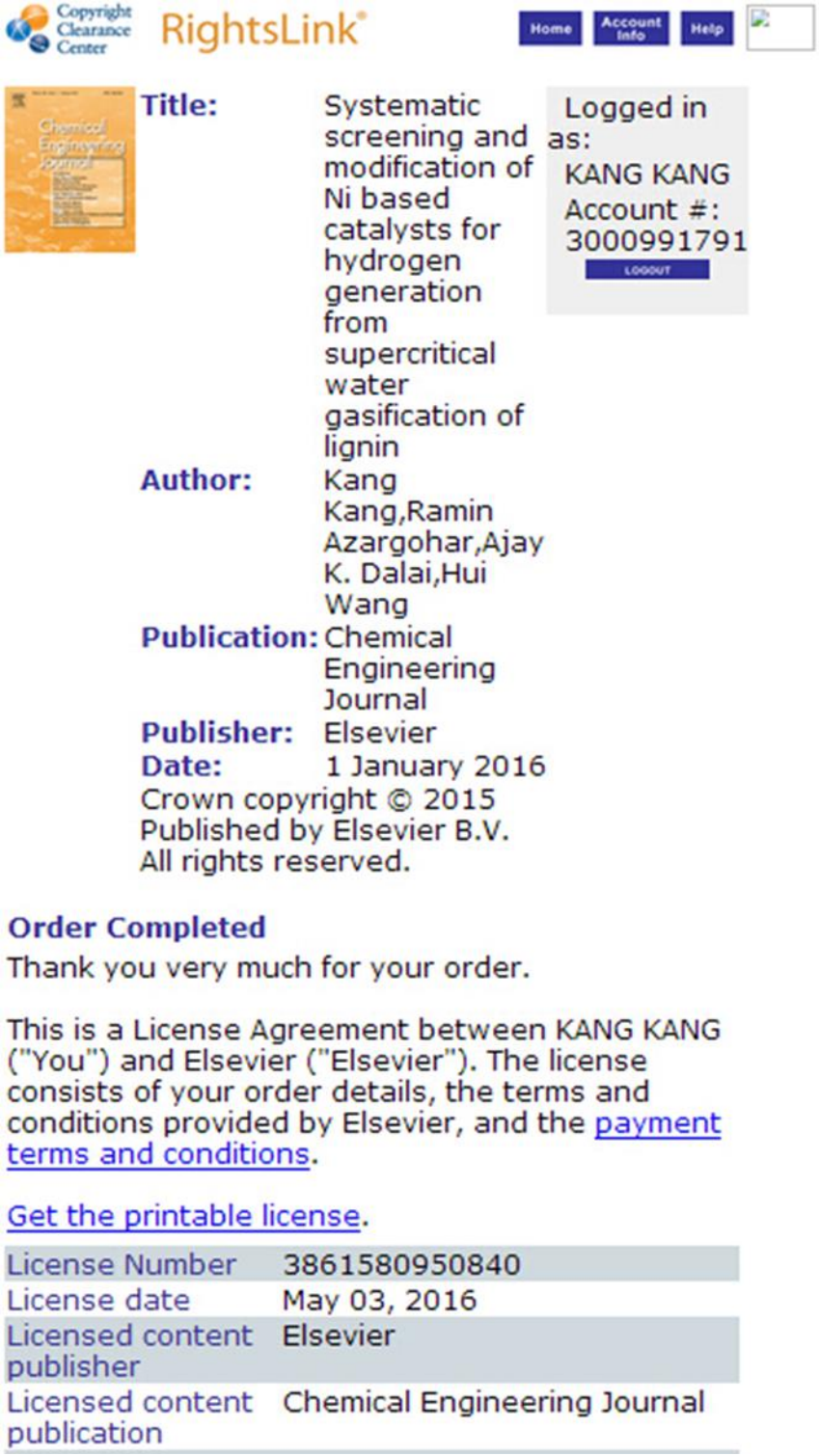

Copyright Clearance Center RightsLink®

Home | Account Info | Help

Title: Systematic screening and modification of Ni based catalysts for hydrogen generation from supercritical water gasification of lignin

Logged in as:
KANG KANG
Account #:
3000991791
LOGOUT

Author: Kang Kang,Ramin Azargohar,Ajay K. Dalai,Hui Wang

Publication: Chemical Engineering Journal

Publisher: Elsevier

Date: 1 January 2016

Crown copyright © 2015
Published by Elsevier B.V.
All rights reserved.

Order Completed

Thank you very much for your order.

This is a License Agreement between KANG KANG ("You") and Elsevier ("Elsevier"). The license consists of your order details, the terms and conditions provided by Elsevier, and the payment terms and conditions.

Get the printable license.

License Number	3861580950840
License date	May 03, 2016
Licensed content publisher	Elsevier
Licensed content publication	Chemical Engineering Journal

Licensed content title	Systematic screening and modification of Ni based catalysts for hydrogen generation from supercritical water gasification of lignin
Licensed content author	Kang Kang,Ramin Azargohar,Ajay K. Dalai,Hui Wang
Licensed content date	1 January 2016
Licensed content volume number	283
Licensed content issue number	n/a
Number of pages	14
Type of Use	reuse in a thesis/dissertation
Portion	full article
Format	both print and electronic
Are you the author of this Elsevier article?	Yes
Will you be translating?	No
Title of your thesis/dissertation	Hydrogen Production from Supercritical Water Gasification of Lignin, Cellulose and Lignocellulosic Biomass Residues
Expected completion date	Jun 2016
Estimated size (number of pages)	200
Elsevier VAT number	GB 494 6272 12
Permissions price	0.00 CAD
VAT/Local Sales Tax	0.00 CAD / 0.00 GBP
Total	0.00 CAD

ORDER MORE... CLOSE WINDOW

[3] Kang, K., Azargohar R., Dalai, A.K., and Wang, H. Hydrogen production from lignin, cellulose and waste biomass via supercritical water gasification: Catalyst activity and process optimization study. Energy Conversion and Management. 117 (2016) 528-37.

Copyright Clearance Center RightsLink®

Home | Account Info | Help | Live Chat

Title: Hydrogen production from lignin, cellulose and waste biomass via supercritical water gasification: Catalyst activity and process optimization study

Author: Kang Kang,Ramin Azargohar,Ajay K. Dalai,Hui Wang

Publication: Energy Conversion and Management

Publisher: Elsevier

Date: 1 June 2016

Crown copyright © 2016 Published by Elsevier Ltd. All rights reserved.

Logged in as: KANG KANG
Account #: 3000991791
LOGOUT

Review Order

Please review the order details and the associated terms and conditions. To edit billing or contact information please click on 'account info' at the top of this page.

Licensed content publisher	Elsevier
Licensed content publication	Energy Conversion and Management
Licensed content title	Hydrogen production from lignin, cellulose and waste biomass via supercritical water gasification: Catalyst activity and process optimization study
Licensed content author	Kang Kang,Ramin Azargohar,Ajay K. Dalai,Hui Wang
Licensed content date	1 June 2016